

**MULTISCALE MODELLING OF MOLECULES AND CONTINUUM  
MECHANICS USING BRIDGING SCALE METHOD**

BY

Banafsheh Hashemi Pour

A DISSERTATION SUBMITTED TO THE FACULTY OF GRADUATE STUDIES IN  
PARTIAL FULFILMENT OF THE REQUIREMENTS FOR THE DEGREE OF  
DOCTOR OF PHILOSOPHY

GRADUATE PROGRAM IN PHYSICS & ASTORONOMY

YORK UNIVERSITY  
TORONTO, ONTARIO

May 2016

© Banafsheh Hashemi Pour, 2016

## **Abstract**

This PhD dissertation is about developing a multiscale methodology for coupling two different time/length scales in order to improve properties of new space materials. Since the traditional continuum mechanics models cannot describe the influence of the nanostructured upon the mechanical properties of materials and full atomistic description is still computationally too expensive, millions of degrees of freedom are needed just for modeling few hundred cubic nanometers, this leads to a coupled system of equations of finite element (FE) in continuum and molecular dynamics (MD) in atomistic domain. Coupling efficiently and accurately two dissimilar domains presents challenges especially in handshaking area where the two domains interact and transfer information. The objective of this study is (i) develop a novel nodal position FE method that can couple with the MD easily, (ii) develop a proper methodology to couple the FE with MD for FE/MD multi-scale modeling and let the information transfer in a seamless manner between the two domains, and (iii) implement complicated cases to confirm accuracy and validity of the proposed model.

## **Acknowledgements**

First of all, I would like to thank Professor Zheng Hong Zhu for his enduring patience and effort in being my supervisor, instructing me in Solid Mechanics and FEM techniques as well as molecular dynamic and coupling the two molecules and continuum domain successfully and carefully reviewing all my papers and drafts, and giving me this opportunity to work with him and his other graduate students at York University to develop a new multiscale method in order to accomplish my PhD. Professor Zhu has provided a wealth of experience and knowledge in the field of science and engineering. I would also like to thank Professor A. Kumarakrishnanand and Professor Jinjun Shan, members of my supervisory committee, for their support and help in reviewing my research and documentation throughout this work.

In addition, I want to extend my gratitude to my family and friends for believing in me, supporting me through a lot of difficult times.

Finally, I want to thank Faculty of Graduate Studies at York University for providing the financial support to carry out the study.

# CONTENTS

Abstract	ii
Acknowledgements	iii
List of Symbols	vii
List of Abbreviations	x
List of Tables	xii
List of Figures	xiii
Chapter 1      Introduction and Justification	1
1.1    Multiscale Modeling and Its Applications	1
1.2    Justification of the Research	8
1.3    Limitations of the Existing Finite Element Method	8
1.4    Limitations of Existing Multiscale Methods	10
1.5    Objectives of the Research	13
1.6    Methodology	13
1.6.1    Continuum Domain	13
1.6.2    Atomic Domain	14
1.6.3    Handshaking Zone	15
1.7    Layout of Thesis Document	18
Chapter 2      Literature Review of Multiscale Modeling	19
2.1    Introduction of Concurrent Coupling Methods	19
2.2    Finite element-atomistic method (FEAt)	22
2.3    Material Point Method	24

2.4	Coarse Grained Molecular Dynamic Method	28
2.5	Coupled Atomistic Dislocation Dynamic Method	30
2.6	Atomic-scale Finite Element Method	33
2.7	Quasi-Continuum Method	34
2.7.1	Local Quasi-Continuum Method	36
2.7.2	Non-Local Quasi-Continuum Method	38
2.7.3	Coupled Local/Non-Local Quasi-Continuum Method	42
2.8	Bridging Scale Method	44
Chapter 3	Theoretical Development and Formulation	48
3.1	Introduction	48
3.2	Nodal Position Finite Element Method	49
3.2.1	Potential Energy and Stiffness Matrix	49
3.2.2	Kinetic Energy and Mass Matrix	56
3.2.3	Equation of Motion of NPFEM	57
3.3	Molecular Dynamics	59
3.4	Coupling of FEM/MD	62
3.5	Numerical Integration Scheme	63
Chapter 4	Implementation of NPFEM, MD and Multiscale method	67
4.1	Program Layout	67
4.2	Evaluation Modules for Stiffness Matrices	75
4.2.1	NPFEM for Continuum Domain	75
4.2.2	MD for Atomic Domain	77
4.3	Evaluation Module for Mass Matrices	79

4.3.1	NPFEM for Continuum Domain	79
4.3.2	MD for Atomic Domain	80
Chapter 5	Results and Discussion	82
5.1	Modeling with One Element	82
5.2	Modeling with Three Elements	89
5.3	Modeling with Five by Five Mesh/Lattice	96
Chapter 6	Conclusions and Future Work	109
6.1	General Conclusions	109
6.2	Thesis Accomplishments	109
6.2.1	Development of Nodal Position Finite Element Method	110
6.2.2	Implementation and Validation of NPFEM	111
6.2.3	Molecular Dynamic Simulation in Atomic Domain	111
6.2.4	Implementation and Validation of Molecular Dynamic	112
6.2.5	Development of Multiscale Method Coupling NPFEM and MD	112
6.2.6	Implementation and Validation of Multiscale Method	113
6.3	Contributions of Thesis Work	114
6.4	Future Work	115
Bibliography		116

## List of Symbols

$a$	Length of the element
$a_0 - a_7$	Newmark integration constants
$b$	Width of the element
$\mathbf{B}_L$	Linear strain matrix
$\mathbf{B}_N$	Non-linear strain matrix
$\mathbf{D}$	2D elastic vector
$\mathbf{F}$	External force vector
$f(r_{ij})$	Lennard-Jones force
$f_i^{ext}$	External force in atomic region
$\mathbf{F}_{ke}$	Equivalent nodal force vector
$\mathbf{K}$	Stiffness matrix
$\mathbf{K}_e$	Effective stiffness matrix
$\mathbf{K}_L$	Linear stiffness matrix
$\mathbf{K}_{MD}$	Stiffness matrix analog to FEM
$\mathbf{K}_{N1}$	Non linear stiffness matrix first component
$\mathbf{K}_{N2}$	Non linear Stiffness matrix second component
$\mathbf{M}$	Mass matrix
$m_i$	Mass of each particle
$\mathbf{M}_{MD}$	Mass matrix in atomic region

$\mathbf{N}$	Element shape function matrix
$\tilde{r}$	Position vector of an arbitrary point P after deformation
$r$	Position vector of an arbitrary point P before deformation
$\ddot{r}$	Acceleration vector of an arbitrary point P before deformation
$\dot{r}$	Velocity vector of an arbitrary point P before deformation
$r_{ij}$	The distance between two particles
$T$	Kinetic energy
$t$	Thickness
$T^M$	Kinetic energy in the atomic region
$u$	Displacement in x direction
$\mathbf{u}$	Displacement matrix
$U$	Strain energy
$U^M$	Potential energy in the atomic region
$U_{ij}^M$	Lennard-Jones potential
$v$	Displacement in y direction
$W^{\text{ext}}$	Work done by external force in atomic region
$\tilde{x}_e$	Local deformed element coordinate vector
$x_e$	Local original element coordinate vector
$\tilde{X}_i, \tilde{Y}_i$	Global new nodal coordinated (for deformed element)
$X_i, Y_i$	Global original nodal coordinates (for undeformed element)
$\tilde{x}_i, \tilde{y}_i$	Local new nodal coordinated (for deformed element)
$x_i, y_i$	Local original nodal coordinates (for undeformed element)
$\ddot{\tilde{x}}_e$	Nodal acceleration vector



$\dot{\tilde{x}}e$	Nodal velocity vector
$\alpha, \beta$	Newmark integration parameter
$\alpha$	Weight function
$\Delta t$	Newmark integration time step
$\varepsilon$	Depth of potential well in atomic region
$\varepsilon$	Total strain
$\varepsilon_{ij}$	Green-Lagrangian strain of the element
$\Pi^C$	Total energy of the continuum region
$\Pi^{CM}$	Total energy of the transition region
$\Pi^M$	Total energy of the atomic region
$\rho$	Density
$\sigma$	Stress vector
$\sigma$	Finite distance at which the inter particle potential is zero
$\{\varepsilon_L\}$	Linear strain vector
$\{\varepsilon_N\}$	Non-linear strain

## List of Abbreviations

All units are given in SI derived units, time in seconds (s), distance in metres (m), velocity in metres per second (m/s), except where otherwise noted.

AFEM	the Atomic-scale Finite Element Method
CADD	Coupled Atomistic Dislocation Dynamics Method
CB	Cauchy-Born
CGMD	Coarse Grained Molecular Dynamic
DFT	Density Function Theory
EAM	Embedded Atom Method
FEAt	Finite Element Atomistic methods
FE	Finite Element
FEM	Finite Element Method
FLIP	Fluid Implicit Particle
LAMMPS	Large-scale Atomic/Molecular Massively Parallel Simulator
LJ	Lennard-Jones potential
MD	Molecular Dynamic
MPM	Material Point Method
NPFEM	Nodal Position Finite Element Method
ODE	Ordinary Differential Equation

PDE Partial Differential Equation

PIC Particle in Cell

QC Quasicontinuum

## List of Tables

Table 4.1 Description of master routine.

68

## List of Figures

Figure 1.1 Coupling of continuum and atomistic domains in coupling zone .....	7
Figure 1.2 Outline of approach methodology .....	17
Figure 2.1 Finite element-atomistic method .....	24
Figure 2.2 Combining MD and MPM region scheme .....	28
Figure 2.3 Representative atom selection based on deformation gradient with corresponding FE mesh in Quasicontinuum method .....	36
Figure 2.4 Continuum Scale Deformation and Corresponding Atomic Scale Deformation with Cauchy-Born Rule .....	37
Figure 2.5 Bridging scale model .....	45
Figure 3.1 Element before and after displacement .....	50
Figure 3.2 Transition region from molecules domain (M) to continuum domain (C).....	62
Figure 4.1 Flow chart of master routine for NPFEM.....	69
Figure 4.2 Flow chart of master routine for MD. ....	71
Figure 4.3 Flow chart of master routine for multiscale method. ....	73
Figure 4.4 Evaluation modules for NPFEM global stiffness matrix. ....	76
Figure 4.5 Evaluation modules for MD equivalent global stiffness matrix.....	78
Figure 4.6 Evaluation module for NPFEM global mass matrix. ....	80
Figure 4.7 Evaluation module for MD global mass matrix. ....	81
Figure 5.1 (a) four-node element in two dimensional plane scheme (b) four pair molecule interacting two by two .....	83
Figure 5.2 Time history of displacement in y direction of one element using NPFEM. ..	84

Figure 5.3 Time history of velocity in y direction of one element using NPFEM. ....	84
Figure 5.4 Time history of Hamiltonian of one element using NPFEM. ....	85
Figure 5.5 Time history of displacement in y direction of four particles using MD. ....	86
Figure 5.6 Time history of velocity in y direction of four particles using MD. ....	86
Figure 5.7 Time history of Hamiltonian of four particles using MD.....	87
Figure 5.8 Time history of displacement in y direction using coupled NPFEM/MD.....	88
Figure 5.9 Time history of velocity in y direction using coupled NPFEM/MD.....	88
Figure 5.10 Time history of Hamiltonian using coupled NPFEM/MD.....	89
Figure 5.11 Three-element model.....	90
Figure 5.12 Time history of displacement of top nodes in Y direction by NPFEM – 3 element model.....	91
Figure 5.13 Time history of velocity of top nodes in Y direction by NPFEM – 3 elements model.....	92
Figure 5.14 Time history of system Hamiltonian by NPFEM – 3 element model. ....	92
Figure 5.15 Time history of displacement of top nodes in Y direction by MD – 3 element model.....	93
Figure 5.16 Time history of velocity of top nodes in Y direction by MD – 3 element model .....	93
Figure 5.17 Time history of system Hamiltonian by MD – 3 element model.....	94
Figure 5.18 Time history of displacement of top nodes in Y direction by NPFEM/MD – 3 element model.....	95
Figure 5.19 Time history of velocity of top nodes in Y direction by NPFEM/MD – 3 element model.....	95

Figure 5.20 Time history of system Hamiltonian by NPFEM/MD – 3 element model....	96
Figure 5.21 5 by 5 lattice. ....	99
Figure 5.22 Time history of displacement of top nodes in Y direction by NPFEM.....	100
Figure 5.23 Time history of velocity of top nodes in Y direction by NPFEM.....	100
Figure 5.24 Time history of system Hamiltonian by NPFEM – 25 element model .....	101
Figure 5.25 Time history of displacement of top nodes in Y direction by MD.....	101
Figure 5.26 Time history of velocity of top nodes in Y direction by MD.....	102
Figure 5.27 Time history of system Hamiltonian by MD – 25 element model .....	102
Figure 5.28 Time history of displacement of top nodes in Y direction by MD/NPFEM 25 element model.....	103
Figure 5.29 Time history of velocity of top nodes in Y direction by MD/NPFEM 25 element model.....	103
Figure 5.30 Time history of system Hamiltonian by MD/NPFEM – 25 element model	104
Figure 5.31 Time history of displacement indifferent layers in Y direction by MD/NPFEM 25 element model.....	106
Figure 5.32 Magnified time history of displacement of top nodes in Y direction by MD/NPFEM 25 element model.....	106
Figure 5.33 Magnified time history of velocity of top nodes in Y direction by MD/NPFEM 25 element model.....	107
Figure 5.34 Magnified time history of system Hamiltonian by MD/NPFEM 25 element model.....	107
Figure 5.35 Magnified time history of displacement in different layers in Y direction by MD/NPFEM 25 element model.....	108

# **Chapter 1 INTRODUCTION AND JUSTIFICATION**

## **1.1 Multiscale Modeling and Its Applications**

Over the past decades the advances in nanotechnology, nanomaterials and nanomechanics provide numerous potential applications in science and engineering. With the fast development of nanotechnology, more attention has been devoted to enhance the existing materials or synthesis of new materials at the nanoscale using nanoparticles as building blocks to achieve desirable macroscale properties. An emphasis on nanoscale entities will make the manufacturing technologies and infrastructure more sustainable in terms of reduced energy usage and environmental pollution [1]. Therefore, new methods and techniques are required both experimentally and computationally for modeling, synthesizing and characterization of materials at nanoscale to learn more about their fascinating properties and characteristics, such as silica aerogels which are very well-known for their low density and low thermal conductivity [2]. Traditionally, computational solid mechanics is widely used for this task. Solid mechanics is based on the continuum principle and studies the deformation, force balancing and kinematics of materials. As the research focus shifts from macroscale into the microscale and nanoscale details, the materials can no longer be treated as the continuum and molecular dynamics (MD) has



been considered as one of the most successful tools for characterizing physical properties of materials. Therefore, the approach of simulations from continuum mechanics turned to atomistic models which involve billions of molecules that are connected by chemical bonds. However, applying MD or full atomistic description is unrealistic in engineering applications, since even the use of state-of-the-art parallel supercomputers can only handle a limited number of atoms ( $\sim 10^9$ ), corresponding to less than one cubic micron of material [3]. On the other hand, traditional solid mechanics approaches such as finite element method (FEM) cannot accurately describe the influence of nanostructure upon material properties [4-6]. For the study of this type of problems related to nanomechanics and nanomaterials, new approaches are required. This leads us to a coupled system of equations of FEM in continuum and MD in atomistic/molecular domain [7]. However, efficient and accurate coupling of two dissimilar domains with wide range of time and length scales presents challenges, especially in the handshaking area where the atoms meet the continuum to transfer information.

Many efforts have been devoted to the challenges in dealing with the multiscale materials modeling and simulation. The multiscale modeling combines existing and emerging methods from diverse scientific disciplines to bridge the dramatically different time and length scales reflecting essential phenomena of materials at different domains. With the fast advance of computing ability, more realistic and detailed descriptions of material responses, more efficient computational methodologies, and more accurate numerical solutions of initial and boundary value problems have been developed and grown in the research of computational solid mechanics for a long time [8, 9]. A more detailed description and concepts as well as strength and limitations of most popular coupling

methods are presented in Chapter 2 of this dissertation.

Molecular dynamics was initially developed as a computational method used for physical chemistry and thermodynamics to determine the average thermo-chemical properties of physical systems such as; solids, liquids and gases. However, nowadays the MD method is widely used for simulations of atomic behaviour of materials. There are two fundamental assumptions in MD simulations. First, particles or molecules are considered as material points that interact with each other through force field or interatomic/ intermolecular potential that is a set of functional parameters that calculates potential energy of the system of molecules/particles. In order to calculate a trajectory, only initial positions of the atoms are sufficient with an initial distribution of velocities and the acceleration, which is determined by the gradient of the potential energy function. The molecular motion is described with time dependent vectors of position and velocity. Second, the number of particles in the system remains the same or the mass of the system does not change in simulation. In standard MD simulation, the system is defined to be isolated, leading to the energy conservation of the system [10-13]. The method generates the trajectories of each particle and expresses them in terms of position, velocity and acceleration in the time domain. The information further can be used for determining other properties of the system such as; energy, pressure and temperature. In other words, molecular dynamics is a step-by-step numerical simulation for solving the equations of motion for an atomic system. First, forces acting on the atoms should be calculated and these are derived from the potential energy [14]. Therefore, in the most MD simulations, the initial positions and velocities as well as proper interatomic potential functions will be provided and the model conducts the simulation. Choosing a proper interatomic potential

energy function based on material characteristics and numerical integration algorithm are two critical decisions. There are many different potential functions due to various types of materials. The desired accuracy as well as the material bonds with consideration of computational costs affects the choice of potential. Rafiee-Tabar has an excellent review paper published in 2000 [15] about modeling the nanoscale phenomena in condensed matter and a full section about different types of interatomic potentials based on various bonds and material. Perhaps one of the most popular interatomic potentials in molecular dynamic is the Lennard-Jones (LJ) potential [16]. This potential was defined as the total interaction potential between the carbon atoms in two  $C_{60}$  molecules. Moreover, LJ potential is well-known as the best fit for the van der Waals forces among molecules.

The Lennard-Jones potential function is

$$U_{ij}^M = 4\varepsilon \left[ \left( \frac{\sigma}{r_{ij}} \right)^{12} - \left( \frac{\sigma}{r_{ij}} \right)^6 \right] \quad (1.1)$$

where  $\varepsilon$  is the depth of potential well,  $\sigma$  is the finite distance at which the inter particle potential is zero and  $r_{ij}$  is the distance between atom  $i$  and  $j$ . Therefore, the LJ potential has been widely applied in large-scale simulations to save computational costs, where the focus is on fundamental studies in MD methodology and the type of specific material is not an issue. After choosing the inter-atomic potential function of the material, numerical integration algorithm should be chosen for solving the equation of motion. In MD simulation there is no analytical solution to the equation of motion because of the complexity of the model. One of the most popular numerical methods used in MD simulation is the Verlet algorithm [17]. This method originally was proposed for solving

of equation of motion of a system consisting of 864 particles interacting through Lennard-Jones. Later, two other methods called Verlet leapfrog [18] and velocity Verlet [19] have been proposed. These two methods are from Symplectic integrators' category which is subclass of geometric integrators. This class of numerical integrators is designed for Hamiltonian systems such as molecular dynamic simulations. The Symplectic structure of the algorithm ensures the energy and momentum conservation of the numerical model over the long-term time integration, which is critical in MD simulation due to extremely small time step and as a result error accumulation. However, in this thesis our focus is on the coupling characteristics of MD and FE methods, where the accuracy over the long simulation time is not the concern. This is due to the fact that in molecular dynamics simulations the behaviour of molecules is studied usually in a longer period of time. However, in this study the idea is to ensure that the information transfers from one domain to the other smoothly and seamlessly. Thus, the energy conserving Newmark numerical [20] method, which is commonly used in the continuum domain, has been applied for numerical integration.

Continuum domain equations are often in the form of partial differential equations (PDE's) and many numerical methods have been proposed to solve the PDE's. The FEM is one of the most popular and successful numerical methods for solving PEDs. In the FEM, the PDEs are converted into a set of ODEs by discretizing the continuum domain into elements. The conventional FEM has some advantages like flexible geometry, ease of including multiple materials, and refinement for convergence. In other words, there is no limitation with regards to geometry, physical composition of domain and the elements can get smaller and smaller. The smaller the element gets in the body; the more accurate the numerical

solution becomes unless the computational costs become prohibitive. Since in FEM a complex PDE of the main is approximated with a set of ODEs within the element, this method is considered local and the deformation of the material is only dependent on the local effects such as stress within the element. Accordingly, the energy in the entire element only depends on displacement of nodes. Furthermore, one of the features of conventional FEM is that its formulation is based on nodal displacement that is a relative movement with respect to its previous position. In this research, both static and dynamic of the system have been studied. In dynamic system, in continuum and molecular domain, two variables are known as state variables; nodal positions and velocities. These state variables are enough to describe the behaviour of the dynamic system. Therefore, while displacement is very convenient in dealing with solid mechanics problems, it is not a state variable used in the MD simulation where the nodal position is a state variable. To couple the FEM and MD is a united formation; a new method of coupling molecular dynamic and finite element method will be developed in this thesis. Generally, there are four length scales used in the simulation. First, angstrom level for atomic studies as well as electrons and nuclei and the corresponding model is quantum mechanics. Second is the nanometer level where molecular dynamic method explains this length scale. Third is the micrometer level where micromechanics techniques are applicable for this scale. Last is the macroscale where the continuum mechanics principles are accurate enough for this length scale. Challenges arise when a model involves different scale. For instance, let us consider a one-dimensional sample for simplicity.

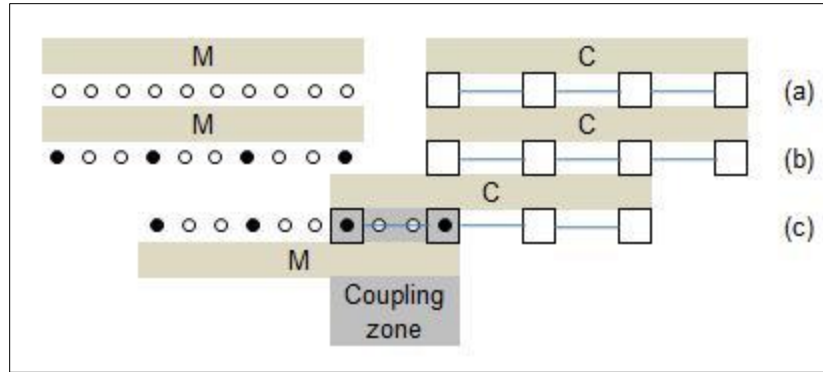


Figure 1.1 Coupling of continuum and atomistic domains in coupling zone

Figure 1.1 illustrates the concepts of coupling molecular and continuum in a simple way. On the left hand side, atomistic domain exists with the finer scale shown a number of circles illustrate atoms/molecules and on the right hand side, continuum domain exists with coarser scale which the squares show the FE nodes as shown in Figure 1.1(a). In order to be able to combine the two regions first we choose some representative or rep atoms in such a way that the distance between two rep atoms matches the distance between two nodes as shown in Figure 1.1(b). Finally, the two domains interact and part of continuum overlap part of molecular and the coupling zone or handshaking area forms as shown in Figure 1.1(c). This dissertation is to investigate on how to couple the two different domains based on energy conservation law. First, the total Hamiltonian of the system should be constant or the energy should be conserved. Second, the information passes through one region to the other smoothly. Detailed information about the methodology and results are presented in Chapters 3 and 4.

## **1.2 Justification of the Research**

Material science along with the traditional continuum mechanics and molecular physics play an important role in developing desired innovative materials applicable for constructing economical spacecraft, satellites, space products and other science and engineering applications. To reduce empirical, time-consuming and costly prototype testing, modeling of new nanostructured materials can be introduced as a significant approach. Multiple-scale modeling methods have become very popular because of the following reasons; Firstly, this class of simulation methods has important and useful applications in nanotechnology research and developing nanoscale materials. Secondly, the existence of connection between microscale physics and macroscale deformation is confirmed by experiments, and finally, the ongoing explosion in computational power has made the linking of disparate length scales feasible.

## **1.3 Limitations of the Existing Finite Element Method**

Many mechanical systems experience large rigid-body motions coupled with small elastic deformations. For this type of mechanical systems, the current nodal positions in the systems are usually more meaningful than the displacements, the difference between the current and original positions, for the designers and analysts. Unfortunately, the existing finite element methods are displacement based solution procedures. They solve for the displacements of the systems relative to their previous positions in order to obtain the current positions of the systems. However, this approach suffers from the accumulated errors arising from each step, which will eventually lead to erroneous and unstable solutions over a long period due to the violation of energy conservation. The existing

approach to this challenge is to improve the numerical integration algorithm by introducing the Symplectic type of numerical integrators. Symplectic integrators are numerical integration schemes for Hamiltonian systems. Therefore, the Symplectic integrators are very well-known schemes for solving molecular dynamic simulations. This research studies the Hamiltonian of the system and proposes a model based on energy conservation. Three models in three domains are studied, continuum, molecular and coupled continuum and molecular. The aim is to satisfy the energy conservation in all three models. In this thesis, we propose an alternative approach from the FEM - a new nodal position finite element method (NPFEM). The newly developed NPFEM uses the nodal positions as state variables instead of the nodal displacements used in the existing FEM. As a result, the strain energy of the deformed element is calculated with respect to the undeformed element directly from current and original nodal positions as opposed to the conventional FEM where the strain energy is calculated based on approximated displacement. In NPFEM, the approximation errors in strain evaluation in the existing FEM have been eliminated to avoid the accumulated errors over a long period. Furthermore, the new NPFEM formulation will be consistent with the MD where the positions are the state variables. Thus, the new NPFEM has the potential to provide a convenient way in the proposed multiscale MD/FE scheme to link the solution in the atomistic zero using molecule dynamics to the solution in the continuum region using finite element method [21]. The NPFEM can use the existing finite elements to solve for the nodal positions directly and thus can be integrated into existing FE codes easily. The numerical examples such as cantilever beam subjected to a pulse load presented in details in the published paper [21], show that the NPFEM is robust and gives the same results as the existing FEM. The new NPFEM will provide a useful tool



in dynamic modeling of mechanical systems where the positions, instead of displacements, of the systems are of interest.

#### **1.4 Limitations of Existing Multiscale Methods**

The concurrent method belongs to a major category of multiscale models, which couples a region described with full atomistic details (including all atomic scale's information) interacting with another region using continuum mechanics. Concurrent methods, simultaneously and continually transfers information from one domain to another smoothly and seamlessly. Since this category of multiscale models are able to pass information from one length scale to the other length scale continuously and ensure consistency among variables between two simulation methods, it is suitable for models which the two length scale are highly depends on one another. A critical segment of the model is the transition area where the two domains overlap and should interact and transfer boundary conditions in a smooth and seamless fashion. In the last two decades, many concurrent methods have been developed to couple molecular level simulations such as molecular dynamics and continuum level of simulations such as finite element method [22, 23]. Local and non-local Quasi-continuum (QC) are among of the most well-known methods [24], which have been developed and applied to a large number of applications [25-28]. The highlights of local methods are first the implementation of representative atoms in order to decrease the number of degrees of freedom and second the use of Cauchy-Born (CB) rule which means the deformation gradient will be uniform in the entire element. The deformation gradient is a fundamental measure of deformation in continuum mechanics which maps line elements in the original configuration into line elements in deformed configuration. When

the deformation of a unit cell within a body follows the deformation of the whole body, the deformation gradient is called uniform. These approximations of the local QC method are valid within the element. However, in interfaces between two elements and the free surfaces the deformation gradient is not uniform thus the Cauchy-Born rule is not valid. Therefore, non-local quasi-continuum for more accurate energy calculation is introduced which a representative atom in the interface between two elements will be subject to a deformation gradient that is different in each element [29, 30]. The full description about Quasi-Continuum method is presented in chapter 2.

Bridging scale is another successful method. The main idea behind that is to combine both MD and FEM in one unified system [22]. Both MD and FEM simulations run simultaneously and exchange information. This method decomposes the total displacement field into coarse and fine scales. The coarse displacement is a function of initial positions of the atoms. However, it is a continuous field and can be interpolated between atoms by finite element shape functions. The fine scale is only at atomic positions. In Bridging scale method the fine scale is defined to be the projection of the coarse scale subtracted from total displacement which is obtained by MD simulations. In this method, the FE domain is everywhere; whereas the MD domain will exist in the area of interest where higher accuracy is required and can be determined by specific problems. An impedance force should be introduced to compensate the effects of the removed atoms [31]. This force contains time history kernel and acts to dissipate fine scale energy from MD simulation into the surrounding continuum. Note that the time history kernel functions are the time-delayed response to a delta function input, reflecting the underlying lattice structure, accurate and efficient calculations of the kernel functions are crucial for the overall

accuracy of the multi-scale algorithm. For more information please refer to time history kernel functions for square lattice by Pang et al. in 2011 [32]. A full description and formulation of most important concurrent methods including the quasi-continuum and the bridging scale methods is presented in Chapter 2. This research has employed both quasi-continuum and bridging scale concepts to develop a new multiscale method for modeling nanostructured materials and addressing existing limitations such as the wave reflection and the ghost force. The wave reflection is a phenomenon that happens in multiscale modeling. When the wave from the fine region propagates to the interface of fine and coarse region, it may not pass through because the wavelength of the atomistic region or MD is much smaller than what can be captured by the coarse region or FEM. Therefore, it partially reflects back to the MD region and causes oscillations. The ghost force on the other hand, is a phenomenon that arises from local and nonlocal mismatch formulation of FEM and MD respectively. FEM formulation in continuum domain is local because the definition of energy depends only on the nodal displacements of that element. However, MD formulation is nonlocal due to the fact that energy of each atom depends on not only the adjacent atoms but also others in cut off distance. When nodal and atomic forces are determined by minimizing the total potential energy, usually inaccurate values are obtained in the transition region. Therefore, the underlying problem of the ghost force is that some force contributions are missing in the transition between the fine and coarse domains because overlap atom energies are not included in the calculations. In this dissertation a multiscale formulation is proposed to avoid these two phenomena in the transition region. In this method, the concept of choosing representative atoms adapted from quasi-continuum method to decrease the number of degrees of freedom and also the scaling

parameter has been adapted from the bridging scale decomposition method for transmitting data between the two regions smoothly and efficiently. However, due to the presence of representative atoms and the interface region structure there is no need for applying impedance force.

## **1.5 Objectives of the Research**

The objectives of the current research are to:

- (i) develop a new FE method both static and dynamic capable of coupling with MD,
- (ii) study and choose proper inter-atomic potential among existing potential functions,
- (iii) study and choose proper numerical method for solving both MD and NPFEM,
- (iv) develop MD formulation with chosen potential function and numerical method,
- (v) develop new coupling method formulation for combining FEM and MD,
- (vi) implement all above formulations in FORTRAN code,
- (vii) validate the result by examining energy conservation.

## **1.6 Methodology**

The proposed study will involve both the continuum and molecule domains and the coupling area, called handshaking zone, between them. Detailed approaches are described in the followings.

### **1.6.1 Continuum Domain**

In the continuum domain, a new nodal position finite element method (NPFEM) as an alternative to the existing finite element method (FEM) for a plane or 2D elastic problem has been proposed, where the stress or strain in the third direction is zero depending on if

it is plane stress and plane strain assumption. The newly developed method addresses the complications of the existing FEM in dealing with dynamic problems experiencing large rigid-body motion coupled with small elastic deformation. Unlike the existing FEM that is based on nodal displacements, the new NPFEM uses nodal positions as basic variables to eliminate the need to decouple the elastic deformation from the rigid-body motion. Full description, formulation and validation can be found in the published paper (21) as well as chapter 3 of this thesis. In addition, since the new NPFEM is position based it can be easily coupled with the position based molecular dynamics (MD) compare to the displacement based finite element (FE) modeling in the multiscale MD/FE analysis. Thus, the NPFEM can provide a unified description in multiscale MD/FE modeling.

### **1.6.2 Atomic Domain**

In order to model the atomic region, the Molecular Dynamics approach was selected. The MD simulations calculate the interaction energies among particles that resolve into forces acting on particles, which caused the changes in their accelerations, velocities and positions. Therefore, the MD is a suitable method for being coupled with the continuum mechanics. The first critical decision in MD simulations is choosing potential function which can be determined by factors such as material being modeled, the bond type, desired accuracy and so on. Different interatomic potentials and their applications have been studied and Lennard-Jones potential is found to be the most suitable for this research. Although in most nanostructured materials atoms are bonded covalently, the bond between two molecules would be the van der Waals type [33]. The second crucial aspect of this class of simulations is choosing the numerical integration method. Since the total potential

energy of the system is a function of the molecular positions of all molecules and due to the complexity of such a function, the resulting equations of motions should be integrated numerically. The Newmark integration method has been chosen as the best match for this model. This method is a numerical integrator for solving differential equations mostly used in dynamic systems of solids such as finite element method to determine the dynamic responses. The method is described in details in chapter 4 of this dissertation. This method was implemented in FORTRAN code, the results for velocities, displacements perfectly matched with analytical estimation, and most importantly, the energy was conserved.

### **1.6.3 Handshaking Zone**

The handshaking zone connects the continuum and molecule domains. It is constructed by overlapping quadrilateral elements with its four nodes with four representative atoms or particles - a simple handshaking region where representative atoms overlap the FE nodes. In finite element method the first step is dividing the body into a set of finite elements with a simple geometry such as; triangles, rectangles or quadrilateral. In this study the rectangle elements are chosen because it is good balance between the simplicity in element formulation and accuracy of solution. In addition, in MD which calculating pair potential is highly dependent on reatoms positions. For consistency, the initial positions between reatoms considered being equal and the diagonal effects neglected in this model. Therefore, quadrilateral elements were chosen for this multiscale model. Moreover, the transition from one domain to another domain is realized in terms of energy conservation, where the total energy of the handshaking zone is the weighted sum of continuum and molecule domain so that the total energy is the same. In summary, the methodology

adopted to achieve the above stated objectives is outlined Figure 1.1. Chapter 4 of this dissertation explains thoroughly the static and dynamic part of continuum region formulated with NPFEM as well as derivation of equivalent stiffness matrix and mass matrix in molecular region with MD model.

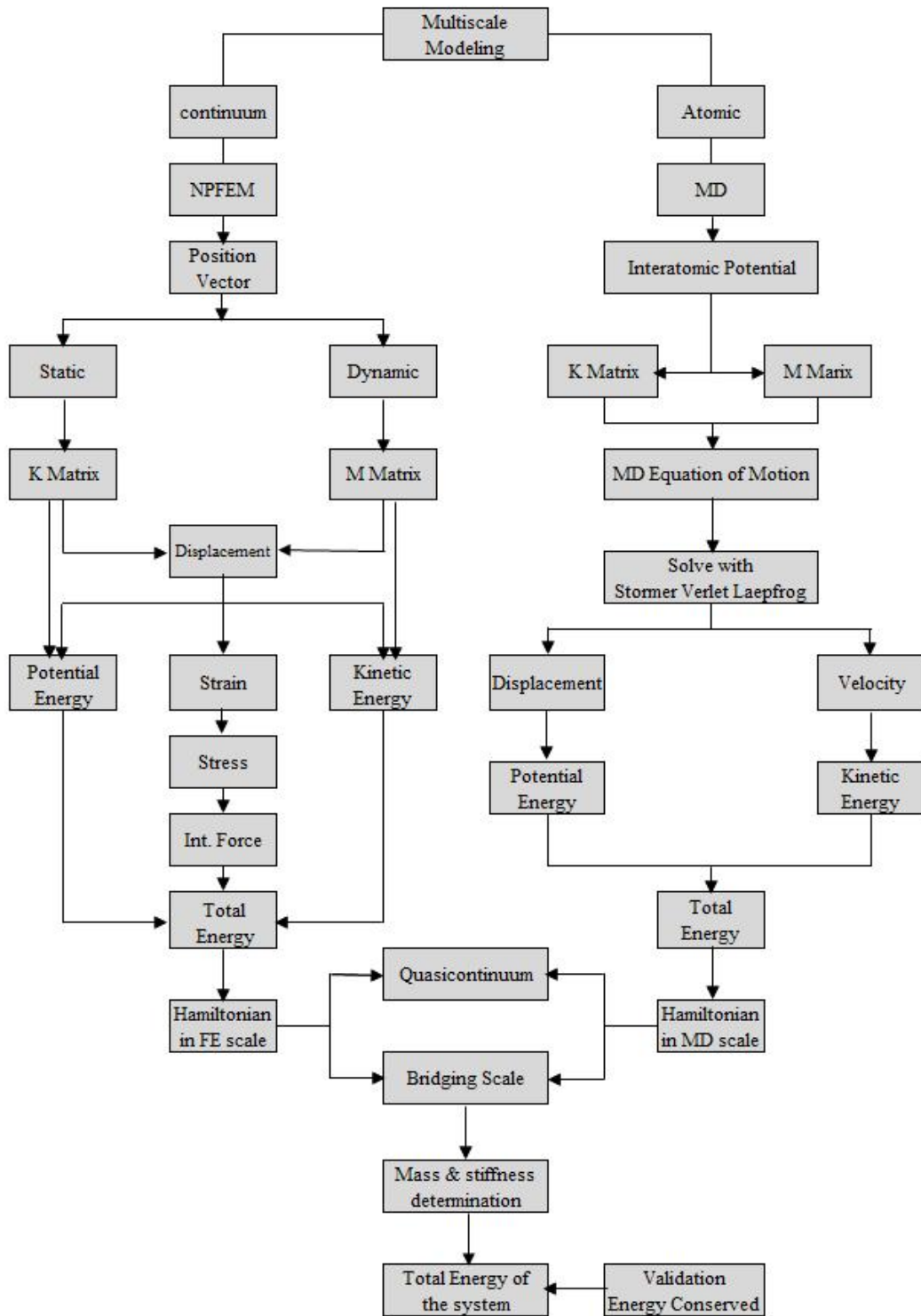


Figure 1.2 Outline of approach methodology



## **1.7 Layout of Thesis Document**

This thesis contains six chapters. Following the current Introduction and Justification Chapter, Chapter 2 provides the literature review in the field. It mainly discusses different existing multiscale methods in nanomechanics. The focus of this chapter is on the concurrent approaches. Finite element atomistic methods (FEAt), material point method (MPM), coupled atomistic dislocation dynamics method (CADD), the atomic-scale finite element method (AFEM), coarse grained molecular dynamic (CGMD), the quasi-continuum both local and non-local formulations, and the bridging scale methods are fully discussed. In Chapter 3, the detailed derivation and formulation of a newly proposed Nodal Position Finite Element Method (NPFEM), detailed formulation of Molecular Dynamic (MD) including determination of inter-atomic potential and force as well as coupling NPFEM and MD applicable in the handshaking zone are discussed. Attention has been devoted to the calculation of the total Hamiltonian of the system. In Chapter 4, the implementations of the NPFEM as well as MD and handshaking zone are discussed in details including the flowcharts of the programs. At the end of this chapter the Newmark time integration has been adopted for this research and a detailed procedure has been discussed. Chapter 5 presents results of two separate models NPFEM and MD as well as the combination of these two methods in the newly proposed multiscale approach. Results start from simple cases and followed by modeling and comparison of more complicated lattice. Finally, Chapter 6 concludes the work, identifies the original contributions of the thesis, and outlines the directions for future work.

# **Chapter 2 LITERATURE REVIEW OF MULTISCALE MODELING**

## **2.1 Introduction of Concurrent Coupling Methods**

Researchers currently employ different multiscale methods not only to predict the behaviour of various new materials but also to improve materials' properties in order to obtain the most desirable characteristics. In physics the length scales vary from very fine or atomistic scale to the much coarser scale, which is the continuum scale. In general, there are four fundamental theory or modeling methods corresponding to each length scale: quantum mechanics, molecular dynamics, micromechanics and continuum mechanics. Behaviour of atoms or the interaction of electrons and nuclei, which happens on the Angstrom level, can be described by quantum mechanics. Molecular dynamic method is a computational method to address problems on nanometer level. Micromechanics modeling method applies continuum mechanics techniques in micrometer level where solids contain inhomogeneities and defects. Finally, the continuum mechanics is accurate enough for describing material behaviour from micrometer scale up to macroscale. Each of the above mentioned methods are accurate in the corresponding length scale. Inaccuracies may arise when a suitable technique for a specific scale applies for a different length scale. Therefore, multiscale modeling computational approaches that aim at developing systematic techniques for bridging scales concurrently, have been developed to treat different scale problems in order to increase the speed of, or enable dynamic calculations. The coupling

length/time scale methods in nanomechanics include sequential and concurrent coupling. In sequential coupling methods, the simulation in each time/length scale is performed independently and the outputs of one scale will be the boundary condition of another scale. The boundary conditions can be displacement or force field. The disadvantage of these category of coupling methods are; first, two totally separate simulations may cause some loss of information transfer between two scales. Second, these methods are more suitable for weak coupling rather than stronger coupling. One time transferring boundary conditions might be insufficient for a desired accuracy. In order to have more accurate and realistic results it is necessary to pass information between scales iteratively and concurrently in a unified system and this is the definition of another category of coupling methods called concurrent coupling.

Due to the accuracy and efficiency of concurrent coupling methods, this category of multiscale models is the most successful method in order to join two domains usually atomistic and continuum to develop a unified and concurrent model of the physical properties of the system. Among concurrent methods, coupling between the continuum domain often modeled by continuum mechanics such as finite element method and the atomistic domain usually modeled by molecular dynamics is the most successful. In this approach, there is a transition region or handshaking zone, already introduced in section 1.5.3, that has atomic region in one side and continuum region of the other side. Continuum and atomistic domains interact and transfer information within the handshaking area. The challenging part of concurrent coupling methods is dealing with this handshaking zone because not only all the approximation happens in this transition region but also two incompatible formulations meet in this area and should transfer information. The

incompatibility arises from the fact that on one hand the formulation of the finite element method is local and the formulation of the molecular dynamic is non-local. On the other hand, the finite element method is displacement based compare to the molecular dynamics that is position based. This issue has already been discussed in Chapter 1, section 1.2.1 when the limitations of conventional FEM are mentioned. In order to have a smooth and seamless transition, the atoms and nodes within this handshaking zone share the positions. As we move away from the transition zone into the continuum zone, the nodes become sparse and the mesh becomes larger to reduce the computational cost. Depending on the desired accuracy and considering computational costs, different types of elements can be chosen for the continuum part. Usually, weighting functions are introduced in the handshaking zone to ensure consistency and smooth transition from one domain to another while the total energy of the material is kept the same across the handshaking zone.

In this chapter, some of the most popular methods will be reviewed, such as, finite element-atomistic method, material point method, coupled atomistic dislocation method, atomic-scale finite element method, coarse grained molecular dynamic, local quasi-continuum method, non-local quasi-continuum method, and bridging scale method. Several review papers already published about coupling atomic to continuum region in solids, for instance, Rudd and Broughton 2000 [34], Miller and Tadmor 2002 [27], Miller 2003 [35], Curtin and Miller 2003 [36], Chung and Narnburu 2003 [37], Ghoniem 2003 [38], Liu et al. 2004 [39], Vvedensky 2004 [40], Miller and Tadmor 2007 [41], Wernik and Meguid 2008 [42], Kalweit and Drikakis 2008 [43], Bernstein 2009 [44], Liu et. al.2010 [45]. All of the above mentioned papers reviewed existing coupling methods which are summarized in this chapter.

## 2.2 Finite element-atomistic method (FEAt)

The Finite element-atomistic method, FEAt, is one of the earliest methods in coupling atomistic to continuum proposed by Kohlhoff et al. 1991 [7], and Gumbsch and Beltz 1995 [46]. They used this method for studying the crack propagation on cleavage and non-cleavage planes in b.c.c. (body-centered cubic) crystals as well as brittle fracture. There is a good review paper about atomistic simulation method and its application with focus on this method by Eidelet. al. 2010 [47]. In this method, the body is divided into three distinguished regions: region I is a lattice modeled fully atomistic using interatomic potential, region IV is a discretized continuum by finite element (FE) method using local nonlinear constitutive law of Kröner's nonlocal elasticity theory [48], and region II-III, which is a transition region between the nonlocal lattice and local continuum, see Figure 2.1. In this method, the transition region is divided into two zones where each zone provides the displacement boundary condition to the other zone. In the zone adjacent to the atomistic domain which can be reduced to a layer of FE, nodes overlap with atoms and move with them. Similarly, the atoms from the transition zone adjacent to the continuum overlap the FE nodes and move with them. The width of this zone at least must be equal to the cut off distance of the potentials that are used in the atomic zone. Cut off distance is the maximum length which paired atoms interact and beyond that interatomic potential may be ignored. This method is suitable for 2D static and dynamic problems with addressing nonlocal/local mismatch between continuum and atomistic regions using nonlocal continuum formulation. Therefore, this method can correct the ghost force phenomenon, already discussed in Chapter 1, in the handshaking area automatically. This model ensures equality of two parameters. One is the equality of displacements in the MD

and FE domains throughout the handshaking zone and as a result the equality of strains is ensured at the interface. Note that, strain is the displacement gradient or partial derivatives of displacement. More details are presented in Chapter 3 of this dissertation. The design of this model is in such a way that forces the equilibrium or equality of stress between MD and FE domains. In order to define a consistent coupling condition, the elastic energy expands into a Taylor series as follows:

$$E(\boldsymbol{\varepsilon}) = E(0) + C_{ij}\varepsilon_{ij} + \frac{1}{2}C_{ijkl}\varepsilon_{ij}\varepsilon_{kl} + \frac{1}{6}C_{ijklmn}\varepsilon_{ij}\varepsilon_{kl}\varepsilon_{mn} + \dots \quad (2.1)$$

where  $E$  is the elastic energy,  $\boldsymbol{\varepsilon}$  is the strain and  $C_{ij}$ ,  $C_{ijkl}$ ,  $C_{ijklmn}$  are elastic constant tensors. In the above equation, since strains are assumed to be equal at the interfaces in order to have stresses in equilibrium, the strain and all the coefficients in the above Taylor series should be equal in both MD and FE domain.

$$C_{ij} = \left( \frac{\partial E}{\partial \varepsilon_{ij}} \right)_0, \quad C_{ijkl} = \left( \frac{\partial^2 E}{\partial \varepsilon_{ij} \partial \varepsilon_{kl}} \right)_0, \quad C_{ijklmn} = \left( \frac{\partial^3 E}{\partial \varepsilon_{ij} \partial \varepsilon_{kl} \partial \varepsilon_{mn}} \right)_0$$

There are two approximations in this method. First, the Taylor expansion has to be cut off at a certain point. Second, there is a transition at the discrete interface from interatomic finite-range forces to continuum Cauchy-type stress. Note that for very small separations, the interaction should be finite. Cauchy-type stress is a second order tensor which defines the state of stress at a point inside a material in the deformed state, or configuration completely. In this method the transition between interatomic forces to continuum stress at the interface causes discontinuity.

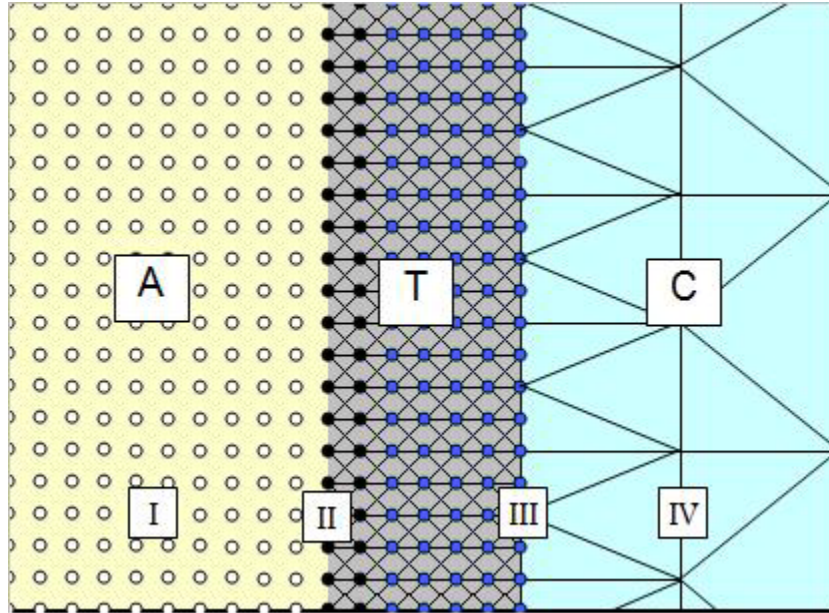


Figure 2.1 Finite element-atomistic method

### 2.3 Material Point Method

The material point method (MPM) is a general numerical tool for the mechanics analysis of continuous media. The idea of MPM is based on particle-in-cell (PIC) method called Fluid Implicit Particle, FLIP, that was originally developed in Los Alamos National Laboratory for solving fluid dynamic problems [49, 50]. This method was further developed into solid mechanics by Sulsky 1995 [51]. FLIP is a Lagrangian particle method in which the material has two discretizations, one is the computational mesh and the other is a collection of material points. Therefore, it uses both Eulerian and Lagrangian advantages and avoids the limitation of each. Note that Lagrangian and Eulerian are two mathematical presentations of fluid motion. The Lagrangian keeps tracks of locations of individual fluid particle and the observer follows the fluid particle as it moves in time and

space. However, in Eulerian approach the coordinates are fixed in space and observer exams the particles passing through a spatial window. The Lagrangian and Eulerian specifications of the fluid motion are also referred as the Lagrangian and Eulerian frame of reference. In fluid implicit particle approach, FLIP, the equations of motions could be solved in a Lagrangian frame using conventional finite difference or finite element method. FLIP can successfully model fluids. Sulsky et al. [52] gave a weak formulation of the FLIP algorithm for solid mechanics and expressed the method in terms of finite element because they believed that the properties of FLIP that made it attractive for fluid dynamics also make it appealing for solid mechanics. Weak formulation in this method is weak formulation of the equation of motion. In general, the ODEs and PDEs can be rewritten in such a way that no derivatives of the solution show up. This helps that the solutions which are not differentiable found. MPM discretizes the body into square grids with a mass on the volume in such a way that it satisfies initial mass density. By means of it, the distribution of the masses on the volumes should be equivalent to the mass per unit volume that in the beginning defined for the model. These masses carry all the corresponding physical properties such as position, velocity, acceleration, stress, strain and constitutive parameters as shown in Figure 2.2. This figure illustrates two distinguished regions MD region on the left and MPM region on the right which substitutes FE region. Therefore, MPM represents the continuum in this model. MPM region has mesh refinement with three levels using quadrilateral elements and the third level as shown in Figure 2.2 is comparable to the MD scale. In transition region both MD and refined MPM exist and transfer information. This method is based on solving momentum conservation on an Eulerian mesh to avoid the mesh lock-up in Lagrangian description. The Lagrangian mesh description is



that it deforms with the body in such a way that both nodes and material points change their positions as the body deforms. In other words, the position of material points remain fixed with respect to the background nodes. However, in Eulerian mesh the nodes remains fixed and the material points move through the mesh. Therefore, the position of material points are not fixed with respect to nodes but varies as body goes under deformation. Each method has its own advantages. The advantage of the Eulerian mesh which made it appealing for this model is that it prevents mesh lock up. This is due to the fact that when body goes under large deformation, since the mesh is fixed in space, there is no mesh distortion. However, the domain should be larger to prevent body to leave the domain. This method has been developed in the past two decades for different applications in engineering, such as, simulations of thin membranes [53], fluid-membrane interaction modeled with material point method [54], material point method simulation of material failure [55], and finally the most recent application of MPM for quasi-static problems. In addition, solving quasi-static equations with MPM [56] is another application of the method. Quasi-static problems are problems in which the sources change slowly enough that the system considered being at equilibrium all the time. These problems become more complicated when several length and time scale get involved. The MPM and its applications in modeling solids and fluids is an alternative to FEM. However, this method could be also combined with other methods such as MD to develop multiscale methods. For the first time, Guo and Yang in 2005 proposed a multiscale method, which seamlessly combined the conventional MD with the continuum mechanics formulated under MPM, and its application in high energy impacts [57]. In this research, they used Lennard-Jones, embedded atom method (EAM) and bonding-angle potential for silicon. These are three

different interatomic potentials popular in molecular dynamics simulations; Lennard-Jones as explained earlier is a pair potential for neutral atoms with a weak or van der Waals bond, embedded is also pair interatomic potential appropriate for metallic bonds. However, bonding angle potential is a potential of three atoms with two chemical bonds where the two bonds forms fixed angle in equilibrium. In 2006, Lu et al proposed a multiscale simulation from atomistic to continuum coupling MD and MPM. They used Tersoff-type, three body potential in MD simulation [58]. This research showed the behaviour of silicon under nanometric tension with increasing elongation in elasticity, dislocation generation and plasticity by slip, void formation and propagation, formation of amorphous structure, necking and final rupture. Chen et al. published a paper in 2011 that extended the usage of handshaking MD and MPM in clarifying the mechanism of nano-processes [59]. In this paper the authors addressed the existing limitations of the existing FEM in the handshaking area by replacing FEM by MPM and with the focus on nano-processes. They further conducted various simulations to validate their method and showed the efficiency of their proposed method. More study was done in 2013 by Liu et al to simulate high velocity impact process with combined MPM and MD [60]. MPM has some advantages compare to FEM. Firstly, it can deal with large deformations in a more natural manner, which avoids FEM mesh lock-up. As explained earlier in this section, since MPM uses Eulerian frame, when body goes under large deformation, mesh does not deform and distort. The second advantage that makes it attractive to multiscale simulations is the fact that it can combine with MD easily. The third advantage is that since this method uses grid structure, it is consistent with parallel computing grids and makes it easier. However, since the discretization of MPM in two dimensions is a square element, in this dissertation referred

to as four-nodded or quadrilateral element, and in three dimensions is a cube element. MPM does not have the flexibility of choosing proper elements such as triangular elements for meshing the body. Therefore, sometimes square mesh is not efficient in the problem and cannot be refined to scale down the size to different levels [61].

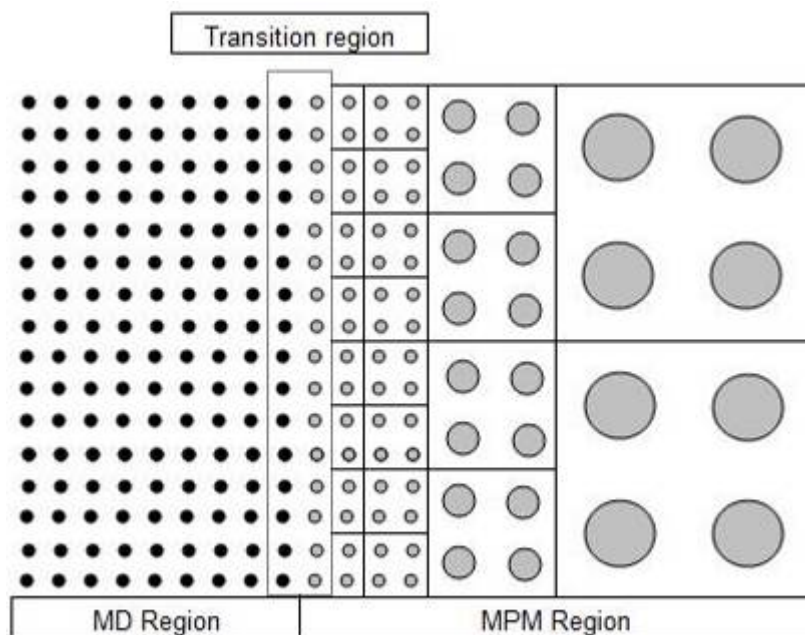


Figure 2.2 Combing MD and MPM region scheme

## 2.4 Coarse Grained Molecular Dynamic Method

The coarse grained molecular dynamic method (CGMD) captures the important atomistic effects without the computational cost of MD in such a way that the important regions of the system may be modeled by MD while the peripheral regions are coarse grained for efficiency. MD simulations usually use large computational resources especially on large systems. However, coarse graining by grouping atoms in a cluster or bead of atoms decreases the number of degrees of freedom and as a result the computational cost. Coarse grain molecular dynamic model was introduced to the field of multiscale modeling in 2005

by Rudd and Broughton [62]. As the interests grew into development of nanoscale mechanical components for applications in Micro-Electro Mechanical Systems (MEMS) and Nano-Electro Mechanical Systems (NEMS), Rudd published another paper that used the CGMD for the design of nanomechanical systems [63]. CGMD is also very popular in computational chemistry for modeling protein structures, lipid bilayers [64] and polymer chains [65]. In the same year, Rudd and Broughton extended the procedure to derive a coarse grained model for nanoparticles. They applied the methodology to C<sub>60</sub> and to carbonaceous nanoparticles produced in combustion environments [66]. They further expanded the multiscale coarse graining to build a mixed all-atom and coarse grained model of the gramicidin A (gA), model membrane protein, ion channel embedded in a lipid bilayer and water environment. In this model, they described gA in full atomistic detail while the lipid and the water molecules were described by coarse grained representation [67]. The authors compared the results of the all-atom coarse-grained AA-CG to all-atom MD for the entire system and concluded that the coarse-grained multiscale method is valid. Ensing et al. also in 2006 found successful application of the hybrid atomistic/coarse grained molecular dynamics in the modeling of polymer melts, bio membranes and proteins [68]. To name just a few, materials that have been modeled by atomic to coarse grained molecular dynamics could be found in literature: Ionic liquids [69], Polyglutamine aggregation [70], single component micelles formed by lysophospholipids of different chain length [71], and sodium dodecyl sulfate micelles [72]. The main idea of the CGMD is to group some atoms or particles into a cluster or bead in order to decrease the number of degrees of freedom in such a way that these beads or clusters carry all the properties of each atom or particle. In this model for coarse graining part, equations can be derived from

an atomistic Hamiltonian. Therefore, all the equations are based on MD principals and are independent of continuum parameters. The only idea that this method adopts from FEM is the idea of meshing. Otherwise there are no other sign of continuum concepts, which appear in FEM. This leads to a seamless coupling between two scales and reduces the errors that arise in other coupling methods. In this method, the stiffness matrix is computed once in the beginning of the simulation and it remains unchanged during the following dynamics and it is valid as long as the vibration of atoms across the cell boundaries is negligible. More details about calculation of the mass and stiffness matrix are presented in Rudd and Broughton [62] publication. The advantages of this method can be summarized as follows. Firstly, this method treats the element stiffness matrix in such a way that the number of degrees of freedom and the computational costs reduce drastically. Secondly, the identical time step can be used for both scales and there is no need to use longer time step for the coarser scale. Note that since short range forces change rapidly with time shorter time scale is more accurate and in general, shorter time scale ensure the numerical method accurately follow the true trajectory. Lastly, like other methods, wherever the high accuracy is desired, the mesh can be refined all the way to position the nodes on atoms in MD region.

## **2.5 Coupled Atomistic Dislocation Dynamic Method**

Coupled atomistic dislocation dynamic method (CADD) was initially presented by Shilkrot et al. [73]. This model couples continuum finite elements to a full atomistic region with two advantages: the ability to accommodate discrete dislocations in the continuum region by an algorithm for automatically detecting dislocations as they move from the atomistic region to the continuum region and the correctly converting the atomistic dislocations to

the continuum dislocations or vice-versa. In this work, the authors discussed the application of this method to nanoindentation atomic scale void growth under tensile stress, and fracture to validate and show the capabilities of the model. Nanoindentation is a technique used for material testing in micro-scales. Nanoindentation is also known as an instrumented indentation test: A high-strength material with a defined shape penetrates the specimen surface by applying a specified load[74]. In this research Shilkrot et al. used CADD mesh to simulate nanoindentation and compared the results with full atomic simulation in a very small region. Four distinguishable components were introduced: the atomistic model, the discrete dislocation framework, the coupling between these regions and the method for detecting and passing dislocations between the two regions. The first two components were adopted from the literature. The atomistic method was adopted from embedded atom method (EAM) developed by Daw and Baskes in 1984 [75] and the discrete dislocation dynamics framework were adopted from Giessen and Needleman 1995 [76]. However, the important part that was developed by the authors is the coupling of the two regions and the automatic detecting and passing dislocations from the atomistic to the continuum and vice versa. CADD is the best match to the problems where dislocations tend to travel over a long distance. These problems usually can be found in ductile metals. Other atomistic to continuum methods connect an atomistic region to a defect-free continuum region. Key and distinguishing features of CADD are that (i) dislocations exist in the continuum region, (ii) they are mechanically coupled to one another and to the atomistic region, and (iii) they can be passed between the atomistic and continuum regions so that the plastic deformation is not confined to the atomistic region [73]. In CADD, the important regions such as crack tips, inclusions or grain boundaries can be modeled fully atomistically to ensure

interatomic forces control of the nucleation. The CADD method was first formulated for 2D problems. However, it has not successfully extended to 3D yet. One of the advantages of this method is that the multiscale treatment of dislocations is independent of the coupling method. Therefore, any of the coupling methods that had been developed previously could be potentially used. This method was primarily designed for zero temperature but Shiari et al in 2005 [77] performed simulations of nanoindentation in single crystals using a finite temperature coupled atomistic/continuum discrete dislocation method both in static and dynamic cases. In 2006, Dewald and Curtin [78] quantified the error in the dislocation driving forces near the atomistic/continuum interface employed in the CADD method and introduced a simple method to modify CADD that permits dislocations to move closer to the atomistic/continuum from either side of the interface while maintain high accuracy on the forces and deformations.. The CADD method still attracts researchers' attention since in engineering materials the deformation and fracture processes often require treatments at different time and length scales. Pavia and Curtin in 2015 [79] presented a high-performance parallel 3D computing framework for executing large multiscale studies, which couples an atomic domain. This model uses MD while the continuum domain is modeled explicitly by FEM. In the same work, they used the robust Coupled Atomistic/Discrete-Dislocation displacement-coupling method, but without the transfer of dislocations between atoms and continuum. The main purpose of the work is to provide a multiscale implementation within an existing large-scale parallel molecular dynamics code (LAMMPS) that enables use of all the tools associated with this popular open-source code, while extending CADD-type coupling to 3D.

## 2.6 Atomic-scale Finite Element Method

The atomic-scale finite element method (AFEM) was introduced by Liu et al in 2004 [80]. They proposed this method as an alternative to MD, which has the same level of accuracy but is much faster than the widely used conjugate gradient method. The Conjugate Gradient Method is the most prominent iterative method for solving sparse systems of linear equations [81]. There are two main advantages for the AFEM compared to the MD. Firstly, this method can handle discrete atoms and is useful for the multi-body interactions among atoms. Since this method is an order- $N$  method, it is much faster than the order- $N^2$  conjugate gradient method that is often used in atomistic simulations. The reason lies in the fact that in order to minimize the energy of the system, the conventional MD method usually uses the order- $N^2$  conjugate gradient numerical method, which uses only the first derivative. As a result, it requires multiple iterations. However, the AFEM uses both first and second order derivatives within one-step for linear systems. Note that this advantage is only valid for the linear systems. For nonlinear systems that involve more complicated interatomic potentials, the second derivative for minimization of energy does not help the speed and simplicity of computation. Secondly, a smooth and seamless link between the AFEM and FEM can be made in order to develop a powerful multiscale method that reduces the number of degrees of freedom drastically because the theory behind both methods is the same and a similar structure can be used to establish a unified system of equations. This method is applicable in 2D and 3D but is limited to static problems. Liu et al in 2005 [82] proposed and studied woven nanostructures of carbon nanotubes using their newly proposed method. This method has attracted researchers' attention in the static study of carbon nanotube deformation and crack propagation [83-85]. In 2009, Morandi and Cecchi



et al. used atomic-scale finite element method for simulation of mechanical behaviour of single-walled carbon nanotubes [86]. In this research, they determined the numerical results for Young's modulus, Poisson ratios, the shear modulus for ground energy configurations, where all of the numerical results agreed with the available experimental values. The above-mentioned are some examples about the application of AFEM in carbon nanotubes. This method also has the potential for solving other optimization problems. One of the most recent papers by Zhang et al in 2012 used this method for simulating evolutions of ferroelectric nanodomains [87].

## **2.7 Quasi-Continuum Method**

The quasi-continuum method (QC) originally conceived and developed by Tadmor, Ortiz and Phillips in 1996 [88] at Brown University. This method is one of the most successful methods in multiscale modeling and a number of researchers developed and applied this method to a number of different applications. The idea behind this method is rather simple. The goal is to model an atomistic system without treating every single atom in the problem. Therefore, they developed a technique that uses a largely continuum mechanics framework that contains enough atomistic information wherever required. In many examples, this means that relatively small fractions of problem require full atomistic detail while the rest can be modeled using the assumptions of continuum mechanics [89].

In other words, in most cases, relatively small part of the problem requires full atomistic information whereas the rest can be modeled by continuum mechanics assumption. There exist many good review papers in this regard by Ortiz and Phillips 1999 [90], Ortiz et al 2001 [91], Miller and Tadmor 2002 [89], and Rodney 2003 [92].

In QC method, the displacements of atoms are determined by finding and minimizing the total energy of the system with respect to the atomic positions. This is valid due to the fact that the atomistic models are based on interatomic potentials which depend on displacements through relative positions of atoms in the configuration and the total energy of the system is the summation over all atoms in the problem. However, in QC the total energy of the system is the sum over rep atoms. Therefore, in this method; first, the number of degrees of freedom and the computer costs are reduced while retaining full atomistic description whenever required. Second, the total energy of the system is approximated accurately without the need to compute the energy of all atoms, as shown in Figure 2.3. This Figure illustrates the selection of rep atoms which is shown with the black filled circles. The density of rep atoms are increased around the dislocation core and decreased when they get further away from the core and meshed by triangular elements. In order to reduce the degrees of freedom in this method, instead of considering all atoms the authors considered only a small fraction of atoms and called them repatoms. Therefore, the displacements of the repatoms can be calculated and the displacements of the remaining atoms can be approximated through interpolation. The density of repatoms may vary to the needs of the problem of interest. For instance, wherever the full atomistic description is desired, the repatoms can be denser or even all the atoms can be chosen as repatoms. Otherwise, the density of repatoms can be reduced. Note that the QC method uses the FEM interpolation functions. Interpolation functions or shape functions in finite element method are a set of equations which show the relations between different nodes and the shape of those functions depend on the form of the mesh. In chapter 4 of this dissertation a set of shape function for quadrilateral mesh will be used. Moreover, the repatoms can act as

atoms in the atomistic domain and can act as nodes in the continuum domain. Therefore, if the position of nodes can be determined by the FEM interpolation functions, the atom positions can be also revealed. When the relative positions of atoms are known, the interatomic potential of atoms can be determined. In addition to reducing the degrees of freedom, an efficient method is required in order to calculate the total energy and force without considering every single atom by either local or non-local quasi-continuum method.

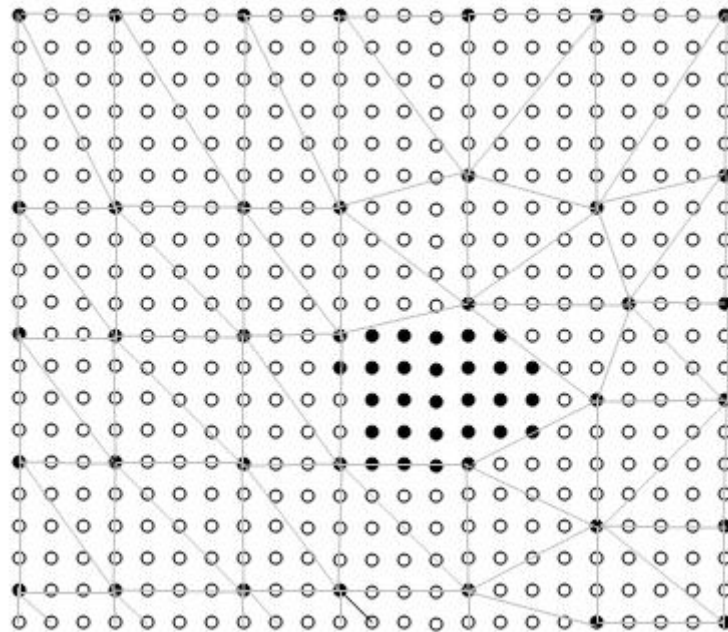


Figure 2.3 Representative atom selection based on deformation gradient with corresponding FE mesh in Quasicontinuum method

### 2.7.1 Local Quasi-Continuum Method

The first approach to calculate the total energy and force without considering every single atom is the local Quasi-Continuum method that uses Cauchy-Born rule, see Figure 2.4. The

Cauchy-Born rule or Cauchy-Born approximation basically is a formulation of solid mechanics. In this approximation the idea is that when a crystalline solid goes under small deformation, the atoms in that crystal follow the same deformation. Therefore, it suggests that the micro-scale deformation gradient is uniform if the deformation gradient is uniform at macro-scale. For instance, in a crystalline solid with a simple structure, all atoms in the same crystal that is subjected to a uniform deformation gradient have the same unit cell energy. Therefore, the energy of all atoms within an element can be determined for one atom and sum over the number of atoms within that element.

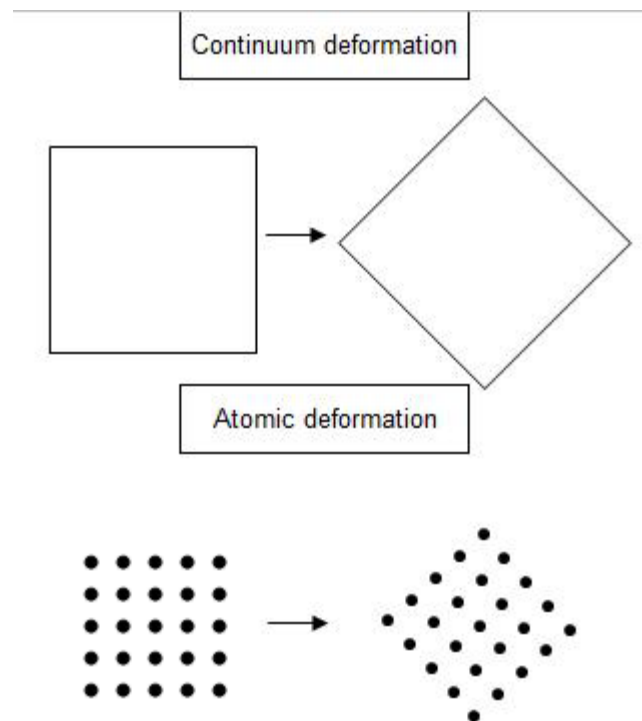


Figure 2.4 Continuum Scale Deformation and Corresponding Atomic Scale Deformation  
with Cauchy-Born Rule

Considering the deformation gradient  $F$ , an element with periodic boundary conditions can

be deformed appropriately and its energy can be calculated. The strain energy density of the element can be calculated as follows:

$$E(F) = \frac{E_0(F)}{\Omega_0} \quad (2.2)$$

where  $E_0$  is the energy of the element and  $\Omega_0$  is the element volume. In addition, the total energy of the system is simply the sum of element's energies:

$$E^{tot} = \sum_{e=1}^N W_e E(F_e) \quad (2.3)$$

Where  $N$  is the total number of elements in the system. As shown in the above equation, a sum over all the atoms in the body is being replaced by the sum over all the elements. Since the number of elements are much smaller than the number of atoms, this method reduces the computational costs drastically. This method is more appropriate for the crystalline solids with a simple lattice structure where every atom in the region subject to uniform deformation gradient has equivalent energy. The limitations of this method are although the deformation gradient is uniform within an element it varies from one element to the other. Moreover, at element boundaries and free surfaces atoms can have different energies and the Cauchy-Born approximation is not accurate anymore.

### 2.7.2 Non-Local Quasi-Continuum Method

In general, the non-local formulation is more accurate but has higher computational costs. When the Cauchy-Born rule is applied in local formulation, it means that only uniform deformation is assumed for the elements. This assumption can be valid throughout the element. However, this is not valid at interfaces and free surfaces. Therefore, in order to

accurately calculate the energy of the system, for instance, the energy of the interfaces between elements as well as free surfaces where the deformation is non-uniform, non-local formulation is suggested [93]. The energy-based and force-based methods are two different approaches for formulating non-locality in the QC method. Both cases start from the fact that the total energy of the system is equal to the total energy of repatoms. In the first approximation (energy-based) of QC, the  $E^{tot}$  can be replaced by the  $E^{tot,h}$ , such that,

$$E^{tot,h} = \sum_{i=1}^N E_i(u^h) \quad (2.4)$$

In the above equation, the atomic displacement can be found from interpolation functions as follows:

$$u^h = \sum_{\alpha=1}^{N_{rep}} N_{\alpha} u_{\alpha} \quad (2.5)$$

where  $N_{\alpha}$  is the interpolation function for repatoms  $\alpha$  and  $N_{rep}$  is the number of repatoms,  $N_{rep} \ll N$ .

The interpolation function contains information that shows the relations between different nodes.

Thus, the energy can be approximated accurately by the total energy of repatoms:

$$E^{tot,h} = \sum_{a=1}^{N_{rep}} n_a E_a(u^h) \quad (2.6)$$

where  $n_{\alpha}$  is the weight function and  $E_{\alpha}$  is the energy for repatom  $\alpha$ . Weight functions can be physically interpreted as the number of atoms represented by repatom  $\alpha$ . Therefore, the weight function is large in the region where the repatom density is low and vice versa.

Therefore, the weight function has to be such that;

$$\sum_{\alpha=1}^{N_{rep}} n_{\alpha} = N \quad (2.7)$$

Therefore, if  $n_{\alpha} = 1$ , then all the atoms in the region considered to be repatom.

Note that in Eq. (2.5) the sum over the displacement of atom  $\alpha$  is simpler due to the support of finite element interpolation function. However, the displacement of any atom located inside an element is determined by the sum over the three rep atoms overlap finite element nodes of that element. Therefore, the energy minimization can be calculated from neighbour environment from the interpolated displacement. As a result, the energy of each repatom,  $E_{\alpha}$ , can be determined from its deformed environment and the next step will be the same minimization procedure.

In force-base QC formulation, forces are derivatives of the total energy on each rep atom. Therefore, in equilibrium when energy is minimized, the force will be zero. In other words, force base QC adopts a different approach that energy minimization physically corresponds to solving the configuration in which the force on each degree of freedom in zero. The formulation can be started from the derivatives of energy with respect to each repatom displacement as follows:

$$f_{\alpha} \equiv \frac{\partial E^{tot,h}}{\partial u_{\alpha}} = \sum_{i=1}^N \frac{\partial E_i(u^h)}{\partial u^h} \frac{\partial u^h}{\partial u_{\alpha}} \quad (2.8)$$

Let us recall that  $u^h$  is the interpolated displacement field and  $u^{\alpha}$  is the displacement of a specific repatom. Since we have the following equation from before

$$N_{\alpha} = \frac{\partial u^h}{\partial u^{\alpha}} \quad (2.9)$$

the force expression becomes:

$$f_\alpha = \sum_{i=1}^N \frac{\partial E_i(u^h)}{\partial u^h(X_i)} N_\alpha(X_i) \quad (2.10)$$

When there is a high repatom density, the clusters can be decreased in such a way that there is no overlap between clusters. In this case, the force can be approximated as follows:

$$f_\alpha \approx \sum_{\alpha}^{N_{rep}} n_\alpha \left[ \sum_{c \in C_\alpha} g_c N_\alpha(X_c) \right] \quad (2.11)$$

where  $C_\alpha$  is a set of atoms in the cluster around repatom  $\alpha$  and  $g_c = \frac{\partial E_i(u^h)}{\partial u^h(X_i)}$ .

The full non-local formulation as discussed in this section is more accurate than local formulation. In both energy-based and force-based non-local formulation when the region is refined down to the atomic scale, it reduces to lattice static, correctly capturing details of dislocation cores, stacking faults and grain boundaries[94]. However, the non-local approach has disadvantages. The main limitation is the increase of the computational costs comparing to the local formulation. Another issue arises from the fact that for each repatom, in order to evaluate energy or force it is required to map a cluster of atoms and their neighbors to a deformed shape followed by the determination of interatomic potentials for that cluster. The latter needs more calculation than the local approach.

To sum up the last two sections of this chapter, the local QC is a formulation for crystalline solids with simple lattice structure where the deformation gradient is uniform within each element and the Cauchy-Born approximation is valid. However, non-local QC is a formulation dealing with non-uniform such as free surfaces and interfaces where full atomistic details are required.



### 2.7.3 Coupled Local/Non-Local Quasi-Continuum Method

Recalling the advantages and disadvantages of local and non-local QC formulation from previous sections, sometimes it is desirable to have advantages of both approaches in one simulation by coupling local/non-local formulation. Therefore, in the same configuration the non-local QC can be used where the atomic scale accuracy is required and the local QC can be used where the deformation happens slowly to take advantage of the computational efficiency. Note that for combining the local and non-local QC, the energy-based formulation should be used for non-local approach. In this approach, the energy of repatoms is approximated firstly. Then, the total number of repatoms  $N_{rep}$  are divided into  $N_{loc}$  for local repatoms and  $N_{nl}$  for non-local repatoms, such that;

$$N_{loc} + N_{nl} = N_{rep} \quad (2.12)$$

Then, the energy is approximated as:

$$E^{tot,h} \approx \sum_{\alpha=1}^{N_{loc}} n_{\alpha} E_{\alpha}(u^h) + \sum_{\alpha=1}^{N_{nl}} n_{\alpha} E_{\alpha}(u^h) \quad (2.13)$$

The important decision is how to determine which atom is local, and which one is non-local. Since the Cauchy-Born rule of local formulation can describe any uniform deformation, it can be still considered to be local if the deformation is uniform regardless how large it is. However, if there is a variation in the deformation gradient at the atomic scale, the repatom should be treated as non-local.

The followings are some applications of QC method from literature. The density functional theory (DFT) of local quasi-continuum was introduced by Fago et al. in 2004 to predict dislocation of nucleation [95]. In the same year, Diestler et al. extended the QC treatment

of multiscale to solids with non-zero temperature [96]. In 2005, a nanoscale meshfree particle method with the implementation of the QC was proposed by Xiao and Yang [97]. Dupuy et al in the same year developed finite temperature QC, which was the MD without considering all atoms. In this work, they suggested a new approach as an alternative to MD which was more efficient, and validated the method by recovering equilibrium properties of single crystal Ni as a function of temperature [98]. In 2006, Iglesias and Leiva applied the 3D QC method to an indentation process taking into account the atomic structure of the indenter and the substrate subject to indentation [99]. In the same year, Hayes et al used local QC to predict dislocation nucleation during nanoindentation of Al<sub>3</sub>Mg [100] while the finite-temperature QC method was used for multiscale analysis of silicon nanostructure by Tang et al. [101] and carbon nanotube by Park et al. [102-103]. In 2007, Sansoz and Molinari used this method for microstructure effects on the mechanical behaviour of FCC bicrystals [104]. In 2008, Park et al adapted the non-local QC for deformations of curved crystalline structures [105]. From 2009 to 2011 QC was applied for simulations of many materials such as; Nano metric cutting of single crystal copper [106], strengthening and weakening effect of Cu/Ag interface of nanoindentation [107], crack propagation of nanocrystalline Ni [108], and crack propagation of BCC-Fe [109]. Moreover, many modifications and improvements have been done on this method so far to make it even more practical and appealing for simulating different materials. For instance, a local QC method for 3D multilattice crystalline materials was proposed by Sorkin et al in 2014 with application to shape-memory alloys [110]. Beex et al. in 2014 and 2015 did some QC based research and published several papers on the multiscale quasi-continuum method for lattice models with bond failure and fibre sliding [111,112] and for dissipative lattice models and

discrete networks [113,114]. QC-based multiscale approaches for plate-like beam lattices experiencing in-plane and out-of-plane deformation [115]. Finally, the most recent application is the investigation of mechanical reliability of an electronic textile by the virtual-power-based QC method [116].

## 2.8 Bridging Scale Method

The bridging scale method was developed by Wagner and Liu in 2003 [117] in order to couple atomistic and continuum concurrently in two- and three- dimension. The fundamental idea behind this formulation is combining both MD and FE in a unified system. It means that both simulations run and exchange relevant information at the same time. The fundamental principle of this method is the decomposing of the total displacement  $U(x)$  into fine and coarse scales, such that,

$$U(x) = u(x) + u'(x) \quad (2.14)$$

where  $u(x)$  is the coarse scale part of the displacement and  $u'(x)$  is the fine scale part of the displacement. When both systems, continuum and atomic, overlap we come across some redundancy in the region. In order to remove the unwanted redundancy of atomic region from the system, an external force should be added to the system to compensate the removed MD degrees of freedom effects. This force is called impedance force in bridging scale method.

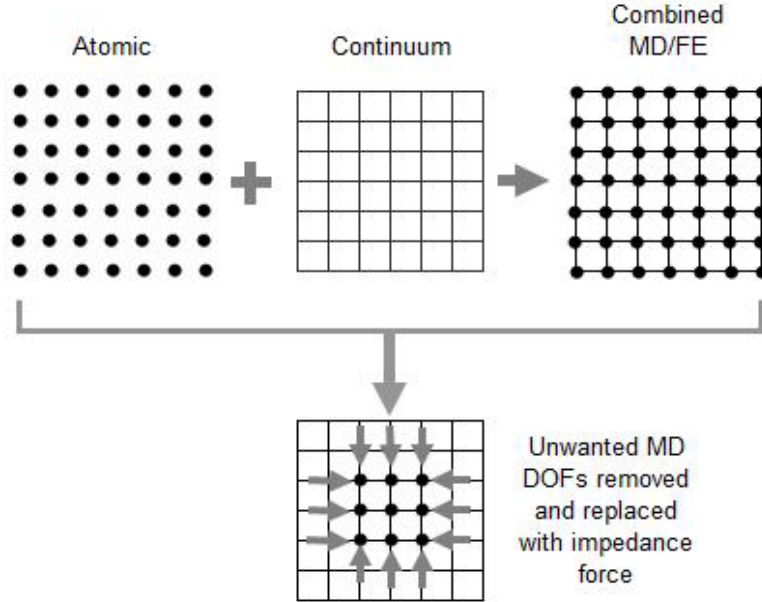


Figure 2.5 Bridging scale model

Figure 2.5 illustrates the bridging scale scheme. On the top, atomic region shown in 2D on the left hand side, continuum region in the middle and on the right hand side both atomic and continuum overlapped. At the bottom of the figure, the combined system of two regions has shown as a unified system with illustration impedance force. In this method, FEM can be found everywhere in the body. However, MD only appears in the regions where higher accuracy is required.

In this method the equation of motion in the continuum can be written as:

$$M\ddot{d} = N^T F$$

where  $M$  is finite element mass matrix,  $N$  is finite element shape function and  $d$  is nodal displacement.

Atomic region equation of motion is as follows:

$$M_A \ddot{u} = F$$

$M_A$  is atomic mass matrix,  $u$  is the MD displacement and  $F$  is the total force for MD.

Note that the MD equation of motion is only solved in the MD region. However, the FE equation of motion is solved across the entire system.

In the coupling MD and FEM region, where both scales exist and the impedance force has been applied, the equations of motions are as follows:

$$M_A \ddot{u} = f(t) + f^{imp}(t)$$

$$M \ddot{d} = N^T F$$

The first term is the interatomic force and the second term is the impedance force. As we already introduced the impedance force in chapter 1, this force contains time history kernel and acts to dissipate fine scale energy from MD simulation into the surrounding continuum. Note that the time history kernel functions are the time-delayed response to a delta function input, reflecting the underlying lattice structure. Accurate and efficient calculations of the kernel functions are crucial for the overall accuracy of the multi-scale algorithm. The existence of impedance force is one of the distinguished features of bridging scale method. Another important feature is the fact that the total energy is the linear combination of the molecular and continuum energies. A scaling parameter  $\alpha$  is introduced in the handshaking area. In developing our method in this dissertation we used this definition of bridging scale. Details for this method can be found in the works of Liu et al. 2006 [1]. Park and Liu 2004 [118] wrote an introductory paper and tutorial about multi-scale analysis in solids with a focus on bridging scale method, Qian et al. 2008 [119] published a paper about concurrent coupling of analysis of nanostructure using the similar approach, Wagner and Liu 2001 [120] used meshfree FEM instead of conventional FEM in bridging scale approach, Park et al. 2005 [121] published another paper about coupling atomistic/continuum in 2D using bridging scale method and Karpov et al. [122] present a coupling approach for material

with dynamic internal structure in 2010.

Study of different concurrent method which introduced in this chapter helped us to understand different formulations and the strength and limitations of each method. In this research two definitions have been adapted from previous methods. First, is the representative atoms adapted from quasi continuum method. Second is the definition of the total energy in the handshaking area adapted from bridging scale method which implies the total energy is the linear combination of the molecular and continuum energies.

# Chapter 3 THEORETICAL DEVELOPMENT AND FORMULATION

## 3.1 Introduction

The current work is motivated by the need for a multiscale modeling method that couples continuum mechanics and atomic or molecules dynamics. The essential part of the work concerns the transformation of information from continuum domain to atomistic domain smoothly and seamlessly. In other words, the multi-scale modeling leads to a coupled system of equations of FEM in continuum domain and MD in atomistic domain. This approach is aimed to increase substantially the efficiency of the simulations without compromising accuracy. Among all the coupling approaches in the literature, the approach based on the energy conservation is most appealing, in which the Hamiltonians of the continuum and atomics meet and overlap in the handshaking zone. However, the description of the Hamiltonian of traditional FEM is based on the nodal displacement field, while the MD describes the position of atoms/molecules using their position vectors. Extra procedures are required to couple them together. To overcome this inconsistency and unify the description, a new 2D Nodal Position Finite Element Method (NPFEM) is proposed here [21]. The new formulation, by using nodal positions as state variables instead of nodal displacements, enables the direct coupling of the Hamiltonians of FEM and MD for multi-scale modeling. Furthermore, it addresses the limitations of existing FEM in dealing with large rigid-body motion coupled with the small elastic deformation. As a result, it

eliminates the need to decouple the elastic deformation from the rigid-body motion and consequently the errors caused by approximation in kinematic relationship and the accumulated numerical errors arising from the incremental solution procedure of existing nonlinear FEM.

## 3.2 Nodal Position Finite Element Method

### 3.2.1 Potential Energy and Stiffness Matrix

Consider a quadrilateral plane element in the global coordinate system  $OXY$  as shown in Figure 3.1. The nodal coordinates are denoted as  $(X_i, Y_i, i = 1, 2, 3, 4)$ . Assume the element moves to a new position under external loads with new nodal coordinates, such as  $(\tilde{X}_i, \tilde{Y}_i)$ . To calculate the strain energy due to the elastic deformation within element, let us define a local coordinate system  $(x, y)$  with  $x$ -axis along one side of the element and  $y$ -axis perpendicular to the  $x$ -axis. In addition, let us place the undeformed element (dashed line in Figure 3.1) in the local coordinate system as a reference state for calculating the strain energy. Thus, one can calculate the strain energy of the element without the need to decouple the elastic motion from the rigid-body motion. Denote the nodal coordinate vectors of the deformed and undeformed element in the local coordinates as

$$\tilde{\mathbf{x}}_e = \{\tilde{x}_1, \tilde{y}_1, \tilde{x}_2, \tilde{y}_2, \tilde{x}_3, \tilde{y}_3, \tilde{x}_4, \tilde{y}_4\}^T \quad (3.1)$$

$$\mathbf{x}_e = \{\tilde{x}_1, \tilde{y}_1, \tilde{x}_1 + a, \tilde{y}_1, \tilde{x}_1 + a, \tilde{y}_1 + b, \tilde{x}_1, \tilde{y}_1 + b\}^T \quad (3.2)$$

Further, assume the position vectors of an arbitrary point  $P$  inside the element after and before deformation can be interpolated using by-linear shape functions and nodal



coordinates, such that:

$$\tilde{\mathbf{r}} = \mathbf{N}\tilde{\mathbf{x}}_e, \quad \mathbf{r} = \mathbf{N}\mathbf{x}_e \quad (3.3)$$

where  $\tilde{\mathbf{r}} = \{\tilde{x}, \tilde{y}\}^T$ ,  $\mathbf{r} = \{x, y\}^T$ , and  $\mathbf{N}$  is the matrix of shape functions:

$$\mathbf{N} = \begin{Bmatrix} N_1(\xi, \eta) & 0 & N_2(\xi, \eta) & 0 & N_3(\xi, \eta) & 0 & N_4(\xi, \eta) & 0 \\ 0 & N_1(\xi, \eta) & 0 & N_2(\xi, \eta) & 0 & N_3(\xi, \eta) & 0 & N_4(\xi, \eta) \end{Bmatrix}$$

$$(3.4)$$

The shape functions are defined as functions of  $\xi$  and  $\eta$ , such that,

$$N_1(\xi, \eta) = (1 - \xi)(1 - \eta), \quad N_2(\xi, \eta) = \xi(1 - \eta), \quad N_3(\xi, \eta) = \xi\eta, \quad N_4(\xi, \eta) = (1 - \xi)\eta \quad (3.5)$$

where  $\xi = \frac{x}{a}$ ,  $\eta = \frac{y}{b}$ , and  $(a, b)$  are the length and width of the undeformed element.

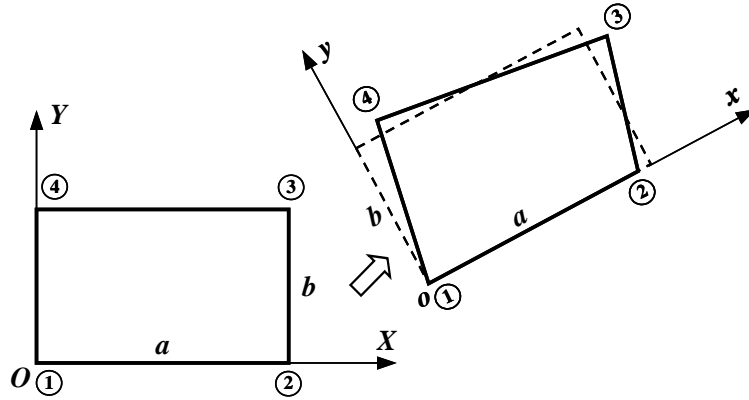


Figure 3.1 Element before and after displacement

The dashed line in after displacement element shows undeformed (original)

element and the solid line shows deformed element

Accordingly, the displacement in the element can be obtained as follows:

$$\mathbf{u} = \tilde{\mathbf{r}} - \mathbf{r} = \mathbf{N} \{ \tilde{\mathbf{x}}_e - \mathbf{x}_e \} \quad (3.6)$$

where  $\mathbf{u} = \{u, v\}^T$ .

Substituting Eqs.(3.1), (3.2), (3.4) into (3.6) yields the displacement vector:

$$\begin{Bmatrix} u \\ v \end{Bmatrix} = \begin{bmatrix} N_1 & 0 & N_2 & 0 & N_3 & 0 & N_4 & 0 \\ 0 & N_1 & 0 & N_2 & 0 & N_3 & 0 & N_4 \end{bmatrix} \begin{Bmatrix} \tilde{x}_1 - x_1 \\ \tilde{y}_1 - y_1 \\ \vdots \\ \tilde{x}_4 - x_4 \\ \tilde{y}_4 - y_4 \end{Bmatrix} \quad (3.7)$$

One of the most fundamental definitions in continuum mechanic, when problems deal with deformation, is strain. Strain describes deformation in terms of displacement or in other words, strain is displacement gradient and usually shown as  $\epsilon$  in formulations. Therefore,

strain in x direction is  $\epsilon_X = \frac{\partial u}{\partial x}$  and in y direction is  $\epsilon_Y = \frac{\partial v}{\partial y}$ . These partial derivatives are

valid for normal strain, where the deformation is only extension or compression in length.

However, when deformation also dealing with rotation, another component should be

added:  $\tau_{XY} = \frac{1}{2} \left( \frac{\partial u}{\partial y} + \frac{\partial v}{\partial x} \right)$ .

The Green-Lagrangian formulation of strain is well known for large deformation considering both linear and nonlinear terms in orthogonal Cartesian coordinates.

The Green-Lagrangian strain of the element is defined as:

$$\epsilon_{ij} = \frac{1}{2} \left( \frac{\partial u_i}{\partial x_j} + \frac{\partial u_j}{\partial x_i} + \frac{\partial u_k}{\partial x_i} \frac{\partial u_k}{\partial x_j} \right), \quad (i, j = 1, 2) \quad (3.8)$$

Or in the expanded form,

$$\begin{aligned}\varepsilon_X &= \varepsilon_{XL} + \varepsilon_{XN} = \frac{\partial u}{\partial x} + \frac{1}{2} \left[ \left( \frac{\partial u}{\partial x} \right)^2 + \left( \frac{\partial v}{\partial x} \right)^2 \right] \\ \varepsilon_Y &= \varepsilon_{YL} + \varepsilon_{YN} = \frac{\partial v}{\partial y} + \frac{1}{2} \left[ \left( \frac{\partial u}{\partial y} \right)^2 + \left( \frac{\partial v}{\partial y} \right)^2 \right]\end{aligned}\quad (3.9)$$

$$\tau_{XY} = \tau_{XYL} + \tau_{XYN} = \frac{\partial u}{\partial y} + \frac{\partial v}{\partial x} + \frac{1}{2} \left[ \frac{\partial u}{\partial x} \frac{\partial u}{\partial y} + \frac{\partial v}{\partial x} \frac{\partial v}{\partial y} \right]$$

Denote linear strain vector as:

$$\{\varepsilon_L\} = \begin{Bmatrix} \varepsilon_{XL} \\ \varepsilon_{YL} \\ \tau_{XYL} \end{Bmatrix} = \begin{bmatrix} \frac{\partial}{\partial x} & 0 \\ 0 & \frac{\partial}{\partial y} \\ \frac{\partial}{\partial y} & \frac{\partial}{\partial x} \end{bmatrix} \begin{Bmatrix} u \\ v \end{Bmatrix}\quad (3.10)$$

Substituting Eq.(3.7) yields the linear strain in the element as,

$$\{\varepsilon_L\} = \begin{bmatrix} \frac{\partial}{\partial x} & 0 \\ 0 & \frac{\partial}{\partial y} \\ \frac{\partial}{\partial y} & \frac{\partial}{\partial x} \end{bmatrix} \mathbf{N} \{\tilde{\mathbf{x}}_e - \mathbf{x}_e\} = \mathbf{B}_L \{\tilde{\mathbf{x}}_e - \mathbf{x}_e\}\quad (3.11)$$

where  $\mathbf{B}_L$  is the strain matrix defined as

$$\mathbf{B}_L = \begin{bmatrix} \frac{\partial N_1}{\partial X} & 0 & \frac{\partial N_2}{\partial X} & 0 & \frac{\partial N_3}{\partial X} & 0 & \frac{\partial N_4}{\partial X} & 0 \\ 0 & \frac{\partial N_1}{\partial Y} & 0 & \frac{\partial N_2}{\partial Y} & 0 & \frac{\partial N_3}{\partial Y} & 0 & \frac{\partial N_4}{\partial Y} \\ \frac{\partial N_1}{\partial Y} & \frac{\partial N_1}{\partial X} & \frac{\partial N_2}{\partial Y} & \frac{\partial N_2}{\partial X} & \frac{\partial N_3}{\partial Y} & \frac{\partial N_3}{\partial X} & \frac{\partial N_4}{\partial Y} & \frac{\partial N_4}{\partial X} \end{bmatrix}\quad (3.12)$$

Similarly, the non-linear strain can be written in a matrix form,

In the expanded Green-Lagrange strain discussed in (3.9) there are two components, linear and nonlinear, the nonlinear part of the equation is valid for nonlinear strain when problem deals with large and irreversible deformation.

$$\{\varepsilon_N\} = \frac{1}{2} \begin{bmatrix} \frac{\partial u}{\partial x} & \frac{\partial v}{\partial x} & 0 & 0 \\ 0 & 0 & \frac{\partial u}{\partial y} & \frac{\partial v}{\partial y} \\ \frac{1}{2} \frac{\partial u}{\partial y} & \frac{1}{2} \frac{\partial v}{\partial y} & \frac{1}{2} \frac{\partial u}{\partial x} & \frac{1}{2} \frac{\partial v}{\partial x} \end{bmatrix} \begin{Bmatrix} \frac{\partial u}{\partial x} \\ \frac{\partial v}{\partial x} \\ \frac{\partial u}{\partial y} \\ \frac{\partial v}{\partial y} \end{Bmatrix} = \frac{1}{2} \mathbf{A} \begin{Bmatrix} \frac{\partial u}{\partial x} \\ \frac{\partial v}{\partial x} \\ \frac{\partial u}{\partial y} \\ \frac{\partial v}{\partial y} \end{Bmatrix} \quad (3.13)$$

where

$$\mathbf{A} = \begin{bmatrix} \frac{\partial u}{\partial x} & \frac{\partial v}{\partial x} & 0 & 0 \\ 0 & 0 & \frac{\partial u}{\partial y} & \frac{\partial v}{\partial y} \\ \frac{1}{2} \frac{\partial u}{\partial y} & \frac{1}{2} \frac{\partial v}{\partial y} & \frac{1}{2} \frac{\partial u}{\partial x} & \frac{1}{2} \frac{\partial v}{\partial x} \end{bmatrix} \quad (3.14)$$

Considering

$$\begin{Bmatrix} \frac{\partial u}{\partial x} \\ \frac{\partial v}{\partial x} \\ \frac{\partial u}{\partial y} \\ \frac{\partial v}{\partial y} \end{Bmatrix} = \begin{bmatrix} \frac{\partial}{\partial x} & 0 \\ 0 & \frac{\partial}{\partial x} \\ \frac{\partial}{\partial y} & 0 \\ 0 & \frac{\partial}{\partial y} \end{bmatrix} \begin{Bmatrix} u \\ v \end{Bmatrix} = \begin{bmatrix} \frac{\partial}{\partial x} & 0 \\ 0 & \frac{\partial}{\partial x} \\ \frac{\partial}{\partial y} & 0 \\ 0 & \frac{\partial}{\partial y} \end{bmatrix} \mathbf{N} \{\tilde{\mathbf{x}}_e - \mathbf{x}_e\} = \boldsymbol{\theta} \{\tilde{\mathbf{x}}_e - \mathbf{x}_e\} \quad (3.15)$$

we have:

$$\boldsymbol{\theta} = \begin{bmatrix} \frac{\partial N_1}{\partial X} & 0 & \frac{\partial N_2}{\partial X} & 0 & \frac{\partial N_3}{\partial X} & 0 & \frac{\partial N_4}{\partial X} & 0 \\ 0 & \frac{\partial N_1}{\partial X} & 0 & \frac{\partial N_2}{\partial X} & 0 & \frac{\partial N_3}{\partial X} & 0 & \frac{\partial N_4}{\partial X} \\ \frac{\partial N_1}{\partial Y} & 0 & \frac{\partial N_2}{\partial Y} & 0 & \frac{\partial N_3}{\partial Y} & 0 & \frac{\partial N_4}{\partial Y} & 0 \\ 0 & \frac{\partial N_1}{\partial Y} & 0 & \frac{\partial N_2}{\partial Y} & 0 & \frac{\partial N_3}{\partial Y} & 0 & \frac{\partial N_4}{\partial Y} \end{bmatrix} \quad (3.16)$$

$\boldsymbol{\theta}$  is represent nonlinear strain matrix.

Then, the non-linear strain can be expressed as follows,

$$\{\boldsymbol{\varepsilon}_N\} = \frac{1}{2} \mathbf{A} \boldsymbol{\theta} \{\tilde{\mathbf{x}}_e - \mathbf{x}_e\} = \frac{1}{2} \mathbf{B}_N \{\tilde{\mathbf{x}}_e - \mathbf{x}_e\} \quad (3.17)$$

where  $\mathbf{B}_N$  is the non-linear B matrix given by:

$$\mathbf{B}_N = \mathbf{A} \boldsymbol{\theta} \quad (3.18)$$

Therefore, the total strain can be expressed in terms of nodal position:

$$\boldsymbol{\varepsilon} = \left( \mathbf{B}_L + \frac{1}{2} \mathbf{B}_N \right) \{\tilde{\mathbf{x}}_e - \mathbf{x}_e\} \quad (3.19)$$

Furthermore, assume the material obeys the Hooke's law, such that,

$$\boldsymbol{\sigma} = \mathbf{D} \boldsymbol{\varepsilon} \quad (3.20)$$

where  $\boldsymbol{\sigma} = \{\sigma_x, \sigma_y, \tau_{xy}\}^T$  is the stress vector and  $\mathbf{D}$  is the 2D elastic matrix.

$$\mathbf{D} = \frac{E}{1 - \nu^2} \begin{bmatrix} 1 & \nu & 0 \\ \nu & 1 & 0 \\ 0 & 0 & \frac{1 - \nu}{2} \end{bmatrix}$$

where E is the Young modulus and  $\nu$  is the Poisson's ratio.

In general, when a body goes under deformation energy will be stored in the system called

strain energy. The elastic strain energy can be released to the system when the load is removed. Therefore, internal strain energy is equal to the work done by external force.

Once the kinematic and constitutive relationships in the element are defined, the strain energy can be expressed as:

$$U = \int_A \frac{1}{2} \boldsymbol{\varepsilon}^T \boldsymbol{\sigma} t dA = \frac{1}{2} (\tilde{\mathbf{x}}_e - \mathbf{x}_e)^T \mathbf{K} (\tilde{\mathbf{x}}_e - \mathbf{x}_e) \quad (3.21)$$

where A is area and t is the thickness of the element.

If strain from Eq. (3.19) and stress from Eq. (3.20) are substituted in the above equation

The stiffness matrix can be determined as follows:

$$\mathbf{K} = t \int_A (\mathbf{B}_L^T + \frac{1}{2} \mathbf{B}_N^T) \mathbf{D} (\mathbf{B}_L + \frac{1}{2} \mathbf{B}_N) dA \quad (3.22)$$

Where  $\mathbf{K}$  is the stiffness matrix of element and  $t$  is the thickness of element.

The stiffness matrix in Eq. (3.16) can be further decomposed into linear and nonlinear stiffness matrices such that:

$$\mathbf{K} = \mathbf{K}_L + \mathbf{K}_{N1} + \mathbf{K}_{N2} \quad (3.23)$$

where

$$\mathbf{K}_L = t \int_A \mathbf{B}_L^T \mathbf{D} \mathbf{B}_L dA, \quad \mathbf{K}_{N1} = \frac{1}{2} t \int_A (\mathbf{B}_N^T \mathbf{D} \mathbf{B}_L + \mathbf{B}_L^T \mathbf{D} \mathbf{B}_N) dA, \quad \mathbf{K}_{N2} = \frac{1}{4} t \int_A \mathbf{B}_N^T \mathbf{D} \mathbf{B}_N dA$$

It is interesting to note that the element stiffness matrix in NPFEM is the same as in the existing finite element method. Since the element stiffness matrix is a function of element properties such as shape of the element which is determined by shape function, size of the element which is determined by length, width and thickness of the element as well as

mechanical properties of material such as Young's modulus and Poisson ratio. Therefore, it is independent of formulation of FE and NPFEM.

### 3.2.2 Kinetic Energy and Mass Matrix

Kinetic energy is that part of the energy which is related to the motion of a body. The popular equation expressing the amount of kinetic energy is directly proportional to the mass and velocity square of the body  $T = \frac{1}{2}mv^2$ . Since  $m = \rho V$  where  $\rho$  is density and  $V$  is the volume. If  $\Delta T$  is chosen for kinetic energy of a unit of  $\Delta m$ , then we can integrate it over the element to find the kinetic energy of the element.

The kinetic energy of the element is defined as,

$$T = \frac{1}{2} \int_A \rho t \dot{\mathbf{r}} \cdot \dot{\mathbf{r}} dA \quad (3.24)$$

where  $\rho$  and  $t$  are the material density and thickness of the element respectively.

Assume the velocity and acceleration of any point inside the element can be interpreted by its nodal values using the same shape function in Eq. (3.3) as follows:

$$\dot{\mathbf{r}} = \mathbf{N} \dot{\mathbf{x}}_e, \quad \ddot{\mathbf{r}} = \mathbf{N} \ddot{\mathbf{x}}_e \quad (3.25)$$

Accordingly, the kinetic energy of the element is written as,

$$T = \frac{1}{2} \int_A \rho t \dot{\mathbf{r}} \cdot \dot{\mathbf{r}} dA = \frac{1}{2} \dot{\mathbf{x}}_e^T \mathbf{M} \dot{\mathbf{x}}_e \quad (3.26)$$

where  $\mathbf{M}$  is the mass matrix defined as

$$\mathbf{M} = t \int_A \rho \mathbf{N}^T \mathbf{N} dA$$

Mass matrix of individual element represents distributed mass density throughout the

element.

Again, it is interesting to note that the element mass matrix in NPFEM is the same as in the existing finite element method. This is due to the fact that element mass matrix or mass distribution throughout the FE is a function of element properties and material such as element shape and size, thickness, material density. All of these properties are independent of FEM or NPFEM formulation.

### 3.2.3 Equation of Motion of NPFEM

Based on the potential and kinetic energy of the element, the discrete equation of motion of the NPFEM can be derived from the variational principle, such that,

$$\delta(U - T) - \delta\tilde{\mathbf{x}}_e^T \mathbf{F} = \delta\tilde{\mathbf{x}}_e^T [\mathbf{M}\ddot{\tilde{\mathbf{x}}}_e + \mathbf{K}\{\tilde{\mathbf{x}}_e - \mathbf{x}_e\} - \mathbf{F}] = 0 \quad (3.27)$$

where  $\mathbf{F}$  is the external force vector.

For an arbitrary  $\delta\tilde{\mathbf{x}}_e^T$ , there must exist

$$\mathbf{M}\ddot{\tilde{\mathbf{x}}}_e + \mathbf{K}\{\tilde{\mathbf{x}}_e - \mathbf{x}_e\} = \mathbf{F} \quad (3.28)$$

Considering the shape of the undeformed element  $\mathbf{x}_e$  is related to the deformed element  $\tilde{\mathbf{x}}_e$

by

$$\mathbf{x}_e = \mathbf{Q}\tilde{\mathbf{x}}_e + \mathbf{x}_0 \quad (3.29)$$

where



$$\mathbf{Q} = \begin{bmatrix} 1 & 0 & 0 & 0 & 0 & 0 & 0 & 0 \\ 0 & 1 & 0 & 0 & 0 & 0 & 0 & 0 \\ 1 & 0 & 0 & 0 & 0 & 0 & 0 & 0 \\ 0 & 0 & 0 & 1 & 0 & 0 & 0 & 0 \\ 1 & 0 & 0 & 0 & 0 & 0 & 0 & 0 \\ 0 & 1 & 0 & 0 & 0 & 0 & 0 & 0 \\ 1 & 0 & 0 & 0 & 0 & 0 & 0 & 0 \\ 0 & 1 & 0 & 0 & 0 & 0 & 0 & 0 \end{bmatrix} \text{ and } \mathbf{x}_0 = \begin{bmatrix} 0 \\ 0 \\ a \\ 0 \\ a \\ b \\ 0 \\ b \end{bmatrix} \quad (3.30)$$

Substituting Eq. (3.29) into Eq. (3.28) yields

$$\mathbf{M}\tilde{\mathbf{x}}_e + \mathbf{K}_e\tilde{\mathbf{x}}_e = \mathbf{F} + \mathbf{F}_{ke} \quad (3.31)$$

where

$$\mathbf{K}_e = (\mathbf{I} - \mathbf{Q})^T \mathbf{K} (\mathbf{I} - \mathbf{Q}) \text{ and } \mathbf{F}_{ke} = (\mathbf{I} - \mathbf{Q})^T \mathbf{K} \mathbf{x}_0$$

$\mathbf{K}_e$  represents global stiffness matrix,  $\mathbf{F}_{ke}$  is the equivalent nodal force vector due to the elasticity of the element in the global coordinates, and  $\mathbf{F}$  is the external force, respectively.

Eq. (3.31) is the discrete equation of motion. It should be noted that (i) the equivalent elastic nodal force vector  $\mathbf{F}_{ke}$  is new in the newly developed NPFEM and does not exist in the existing finite element methods; (ii) the NPFEM can be used with other existing elements except one needs to re-define the  $\mathbf{Q}$  matrix and  $\mathbf{x}_0$  vector shown in Eq. (3.30).

Mathematically Eq. (3.31) represents a system of differential equations of second order and the solution to the equations can be obtained by standard procedures for the solution of differential equations like direct integration such as; the central difference method, the Houbolt method, the Wilson  $\theta$  method, and Newmark method or mode superposition. Among all of existing methods Newmark method has been chosen to solve the above equations for displacement in this research.

### 3.3 Molecular Dynamics

The formulation of molecular dynamics starts with the variational principle in the atomic region. Consider the total energy in the atomic region as

$$\Pi^M = U^M - T^M - W^{ext} = U^M - \sum_{i=1}^n \frac{1}{2} m_i \dot{\mathbf{r}}_i \cdot \dot{\mathbf{r}}_i - W^{ext} \quad (3.32)$$

where  $U^M$  is the potential energy and  $W^{ext}$  is the work done by external forces.

The work done by external force can be written

$$W^{ext} = \sum_{i=1}^n \mathbf{f}_i^{ext} \cdot (\tilde{\mathbf{r}} - \mathbf{r}_0)_i \quad (3.33)$$

Now, let us focus on the dynamic relation between a pair of atoms. The potential between atoms is assumed as the Lennard-Jones potential:

$$U_{ij}^M = 4\varepsilon \left[ \left( \frac{\sigma}{r_{ij}} \right)^{12} - \left( \frac{\sigma}{r_{ij}} \right)^6 \right] \quad (3.34)$$

where  $\varepsilon$  is the depth of potential well,  $\sigma$  is the finite distance at which the inter particle potential is zero. This is similar to bond length in molecules which is a length between two atoms' nuclei in a bonded molecule.  $r_{ij}$  is the distance between two particles.

The equation of motion of MD can be derived from

$$\delta \Pi_{ij}^M = \delta U_{ij}^M - \delta T_{ij}^M - \delta W_{ij}^{ext} = \delta U_{ij}^M - \sum_{i=1}^2 m_i \dot{\mathbf{r}}_i \cdot \delta \dot{\mathbf{r}}_i - \delta W_{ij}^{ext} = 0 \quad (3.35)$$

where

$$\delta W_{ij}^{ext} = \sum_{i=1}^2 \delta \tilde{\mathbf{r}}_i \cdot \mathbf{f}_i^{ext} \quad (3.36)$$

$$\delta U_{ij}^M = \frac{24\varepsilon}{r_{ij}^2} \left( \frac{\sigma}{r_{ij}} \right)^6 \left[ 1 - 2 \left( \frac{\sigma}{r_{ij}} \right)^6 \right] r_{ij} \delta r_{ij} \quad (3.37)$$

Consider  $r_{ij} = \sqrt{\sum_{k=1}^2 (x_{ik} - x_{jk})^2}$ , then

$$\begin{aligned} \delta r_{ij} &= \frac{\partial r_{ij}}{\partial x_{ik}} \delta x_{ik} + \frac{\partial r_{ij}}{\partial x_{jk}} \delta x_{jk} \\ &= \frac{1}{r_{ij}} \sum_{k=1}^2 (x_{ik} - x_{jk}) \delta x_{ik} - \frac{1}{r_{ij}} \sum_{k=1}^2 (x_{ik} - x_{jk}) \delta x_{jk} \end{aligned} \quad (3.38)$$

Rearrange the above equations leads to the matrix form:

$$\begin{aligned} \delta r_{ij} &= \frac{1}{r_{ij}} \left[ (X_{i1} - X_{j1}) \delta X_{i1} + (X_{i2} - X_{j2}) \delta X_{i2} \right] - \\ &\quad \frac{1}{r_{ij}} \left[ (X_{i1} - X_{j1}) \delta X_{j1} + (X_{i2} - X_{j2}) \delta X_{j2} \right] \\ &= \frac{1}{r_{ij}} \left\{ \begin{matrix} \delta X_{i1} & \delta X_{i2} & \delta X_{j1} & \delta X_{j2} \end{matrix} \right\} \begin{Bmatrix} X_{i1} - X_{j1} \\ X_{i2} - X_{j2} \\ -X_{i1} + X_{j1} \\ -X_{i2} + X_{j2} \end{Bmatrix} \\ &= \frac{1}{r_{ij}} \left\{ \begin{matrix} \delta X_{i1} & \delta X_{i2} & \delta X_{j1} & \delta X_{j2} \end{matrix} \right\} \begin{Bmatrix} 1 & 0 & -1 & 0 \\ 0 & 1 & 0 & -1 \\ -1 & 0 & 1 & 0 \\ 0 & -1 & 0 & 1 \end{Bmatrix} \begin{Bmatrix} X_{i1} \\ X_{i2} \\ X_{j1} \\ X_{j2} \end{Bmatrix} \\ &= \delta \left\{ \begin{matrix} X_{i1} & X_{i2} & X_{j1} & X_{j2} \end{matrix} \right\} \frac{1}{r_{ij}} \begin{Bmatrix} 1 & 0 & -1 & 0 \\ 0 & 1 & 0 & -1 \\ -1 & 0 & 1 & 0 \\ 0 & -1 & 0 & 1 \end{Bmatrix} \begin{Bmatrix} X_{i1} \\ X_{i2} \\ X_{j1} \\ X_{j2} \end{Bmatrix} \quad (3.39) \end{aligned}$$

Substituting Eq. (3.39) into Eq. (3.37) yields:

$$\begin{aligned}
\delta U_{ij}^M &= \frac{24\varepsilon}{r_{ij}^2} \left( \frac{\sigma}{r_{ij}} \right)^6 \left[ 1 - 2 \left( \frac{\sigma}{r_{ij}} \right)^6 \right] \delta \{x_{i1} \quad x_{i2} \quad x_{j1} \quad x_{j2}\} \frac{1}{r_{ij}} \begin{Bmatrix} 1 & 0 & -1 & 0 \\ 0 & 1 & 0 & -1 \\ -1 & 0 & 1 & 0 \\ 0 & -1 & 0 & 1 \end{Bmatrix} \begin{Bmatrix} x_{i1} \\ x_{i2} \\ x_{j1} \\ x_{j2} \end{Bmatrix} \\
&= \delta \{x_{i1} \quad x_{i2} \quad x_{j1} \quad x_{j2}\} \mathbf{K}_{MD} \begin{Bmatrix} x_{i1} \\ x_{i2} \\ x_{j1} \\ x_{j2} \end{Bmatrix}
\end{aligned} \tag{3.40}$$

where  $\mathbf{K}_{MD}$  is the stiffness matrix analog to FEM

$$\mathbf{K}_{MD} = \frac{f(r_{ij})}{r_{ij}} \begin{bmatrix} 1 & 0 & -1 & 0 \\ 0 & 1 & 0 & -1 \\ -1 & 0 & 1 & 0 \\ 0 & -1 & 0 & 1 \end{bmatrix} \text{ and } f(r_{ij}) = \frac{24\varepsilon}{r_{ij}^2} \left( \frac{\sigma}{r_{ij}} \right)^6 \left[ 1 - 2 \left( \frac{\sigma}{r_{ij}} \right)^6 \right] \tag{3.41}$$

It should be noted that the stiffness matrix  $\mathbf{K}_{MD}$  in Eq. (3.41) is highly nonlinear because it is the function of distance between two particles. Furthermore, the variation of the kinetic energy can be simplified; such that,

$$-\sum_{i=1}^2 m_i \dot{\mathbf{r}}_i \cdot \delta \dot{\mathbf{r}} = \delta \{x_{i1} \quad x_{i2} \quad x_{j1} \quad x_{j2}\} \mathbf{M}_{MD} \begin{Bmatrix} \ddot{x}_{i1} \\ \ddot{x}_{i2} \\ \ddot{x}_{j1} \\ \ddot{x}_{j2} \end{Bmatrix} \tag{3.42}$$

where (if assume  $m_i = m_j = m$ )

$$\mathbf{M}_{MD} = \begin{bmatrix} m & 0 & 0 & 0 \\ 0 & m & 0 & 0 \\ 0 & 0 & m & 0 \\ 0 & 0 & 0 & m \end{bmatrix}$$

Thus, dynamic relationship between a pair of atoms is

$$\mathbf{M}_{MD} \begin{Bmatrix} \ddot{X}_{i1} \\ \ddot{X}_{i2} \\ \ddot{X}_{j1} \\ \ddot{X}_{j2} \end{Bmatrix} + \mathbf{K}_{MD} \begin{Bmatrix} X_{i1} \\ X_{i2} \\ X_{j1} \\ X_{j2} \end{Bmatrix} = \begin{Bmatrix} f_{i1} \\ f_{i2} \\ f_{j1} \\ f_{j2} \end{Bmatrix} \quad (3.43)$$

The equation of motion in the molecular dynamic domain can be obtained by adding all pairs together.

### 3.4 Coupling of FEM/MD

The coupling of MD and FEM in the transition or handshaking zone is achieved by ensuring the energy conservation. Consider the transition or handshaking zone shown in Figure 3.2 Transition region from molecules domain (M) to continuum domain (C) from the molecules domain (M) to continuum domain (C). This transition region is called CM.

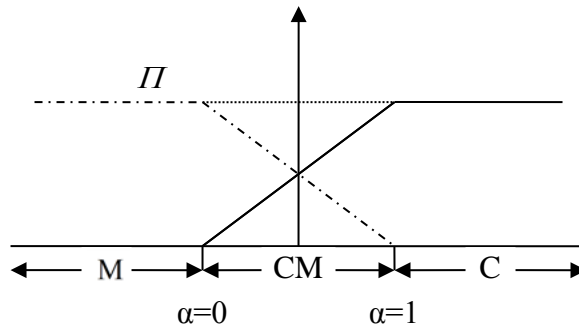


Figure 3.2 Transition region from molecules domain (M) to continuum domain (C)

It is assumed that the energy in the CM zone is continuously passing through the zone, such that,[22].

$$\Pi_{CM} = \alpha\Pi_C + (1-\alpha)\Pi_M \quad (3.44)$$

In Eq. (3.44),  $\Pi$  is the Hamiltonian function and the subscript “C”, “CM” and “M”

represent the corresponding zones, and  $\alpha$  is the weight linearly varying from 0 to 1. It enforces the total energy is conservative in the handshaking area.

Then, the total energy in the coupling region can be written as:

$$\Pi_{CM} = \alpha T_C - \alpha U_C - \alpha W_C^{ext} + (1 - \alpha) T_M - (1 - \alpha) U_M - (1 - \alpha) W_M^{ext} \quad (3.45)$$

Or it can be reorganized like:

$$\Pi_{CM} = \alpha T_C + (1 - \alpha) T_M - \alpha U_C - (1 - \alpha) U_M - \alpha W_C^{ext} - (1 - \alpha) W_M^{ext} \quad (3.46)$$

where  $\Pi_{CM}$  is total Hamiltonian of handshaking area,  $T_C$  is kinetic energy of continuum region,  $U_C$  is potential energy of the continuum region,  $W_C^{ext}$  work done by external force. Moreover,  $T_M$ ,  $U_M$ , and  $W_M^{ext}$  are kinetic, potential energy and work done by external force in molecular dynamic region. Eq. (3.46) shows that the energy within the handshaking region goes from entirely atomistic at MD boundary, to entirely continuum at FE boundary [123].

Thus, the equation of motion in the transition zone can be derived by the same steps,

$\delta \Pi_{CM} = 0$ , as in the previous sections.

### 3.5 Numerical Integration Scheme

Once the equations of motion of the system in different zones derived, the total equation of motion of the system can be assembled and written as follows,

$${}^{t+\Delta t} \mathbf{M} {}^{t+\Delta t} \ddot{\mathbf{X}} + {}^{t+\Delta t} \mathbf{K} {}^{t+\Delta t} \mathbf{X} = {}^{t+\Delta t} \mathbf{F} \quad (3.47)$$

where  $\mathbf{M}$  is mass matrix,  $\ddot{\mathbf{X}}$  is acceleration vector,  $\mathbf{K}$  is stiffness matrix,  $\mathbf{X}$  is position vector,  $t$  is current position and  $\Delta t$  is time step.

There are many numerical integration schemes available in the literature [124]. Among

them, two numerical integration methods were chosen namely, the Newmark time integration scheme [20], and Stormer-Verlet leapfrog [17]. Both numerical integrations were used to model continuum (NPFEM) and atomic (MD) domain for comparison. However, at the end, the Newmark Method was chosen as the best match for this research for the sake of simplicity.

The Newmark time integration scheme adopts the following time stepping scheme,

$$\{ {}^{t+\Delta t} \dot{\mathbf{X}} \} = \{ {}^t \dot{\mathbf{X}} \} + [(1-\alpha)\{ {}^t \ddot{\mathbf{X}} \} + \alpha\{ {}^{t+\Delta t} \ddot{\mathbf{X}} \}] \Delta t \quad (3.48)$$

$$\{ {}^{t+\Delta t} \mathbf{X} \} = \{ {}^t \mathbf{X} \} + \{ {}^t \dot{\mathbf{X}} \} \Delta t + \left[ \left( \frac{1}{2} - \beta \right) \{ {}^t \ddot{\mathbf{X}} \} + \beta \{ {}^{t+\Delta t} \ddot{\mathbf{X}} \} \right] \Delta t^2 \quad (3.49)$$

where  $\Delta t$  is the time integration step,  $\alpha$  and  $\beta$  are the integration parameters, respectively.  $\alpha$  and  $\beta$  are two variables that control two factors in this method; the stability of the method and the damping of the system in this method. For example for  $\alpha = 0.5$ , there is no numerical damping. Therefore, depending on the chosen value for  $\alpha$  and  $\beta$  different set of data will be generated. Two popular set of parameters are as follows:

1. Average acceleration method  $\alpha = \frac{1}{2}, \beta = \frac{1}{4}$
2. Constant acceleration method  $\alpha = \frac{1}{2}, \beta = \frac{1}{6}$

The integration parameters are chosen to be  $\alpha = 0.5$  and  $\beta = 0.25$  in order to ensure the energy conservation of the algorithm. In the current research, the Newmark integration scheme includes two parts: the initial preparation and the time integration loop. Since the global mass matrix is constant, it is calculated in the initial preparation phase and set outside of the time integration loop. However, the stiffness matrix and load vectors have

to be calculated at each time step because they are functions of time and positions.

The initial steps are shown as:

1. Initialize  ${}^0\mathbf{X}$ ,  ${}^0\dot{\mathbf{X}}$ ,  ${}^0\ddot{\mathbf{X}}$  ;
2. Calculate integration constants  $a_0 - a_7$  as:

$$a_0 = \frac{1}{\beta\Delta t^2}; \quad a_1 = \frac{\alpha}{\beta\Delta t}; \quad a_2 = \frac{1}{\beta\Delta t}; \quad a_3 = \frac{1}{2\beta} - 1;$$

$$a_4 = \frac{\alpha}{\beta} - 1; \quad a_6 = \Delta t(1 - \alpha); \quad a_7 = \alpha\Delta t;$$

3. Form mass matrix  $\mathbf{M}$ .

Each time step includes the following calculations:

1. Form stiffness matrix  ${}^{t+\Delta t}\mathbf{K}$  at time  $t + \Delta t$  ;
2. Form effective stiffness matrix  ${}^{t+\Delta t}\hat{\mathbf{K}}$  :

$${}^{t+\Delta t}\hat{\mathbf{K}} = {}^{t+\Delta t}\mathbf{K} + a_0\mathbf{M} \quad (3.50)$$

3. Calculate effective loads:

$${}^{t+\Delta t}\hat{\mathbf{F}} = {}^{t+\Delta t}\mathbf{F} + \mathbf{M} \left( a_0 {}^t\mathbf{X} + a_2 {}^t\dot{\mathbf{X}} + a_3 {}^t\ddot{\mathbf{X}} \right); \quad (3.51)$$

4. Solve for positions  ${}^{t+\Delta t}\mathbf{X}$  at time  $t + \Delta t$  :

$${}^{t+\Delta t}\mathbf{X} = \left( {}^{t+\Delta t}\hat{\mathbf{K}} \right)^{-1} {}^{t+\Delta t}\hat{\mathbf{F}} \quad (3.52)$$

5. Update accelerations and velocities at time  $t + \Delta t$  :

$${}^{t+\Delta t}\ddot{\mathbf{X}} = a_0 \left( {}^{t+\Delta t}\mathbf{X} - {}^t\mathbf{X} \right) - a_2 {}^t\dot{\mathbf{X}} - a_3 {}^t\ddot{\mathbf{X}} \quad (3.53)$$

$${}^{t+\Delta t}\dot{\mathbf{X}} = {}^t\dot{\mathbf{X}} + a_6 {}^t\ddot{\mathbf{X}} + a_7 {}^{t+\Delta t}\ddot{\mathbf{X}} \quad (3.54)$$



To summarize the procedure developed in this chapter, formulation started by deriving the stiffness and mass matrix for quadrilateral element in continuum region. The equation of motion has been written and forces determined. In atomic domain mass matrix and the equivalent stiffness matrix of pair particles have been formulated and the equation of motion has been written in this region. Newmark numerical integration has been deployed to solve the equation of motion for positions, velocities and accelerations of all atoms and nodes. Therefore, the behaviour of the system can be predicted. Finally, knowing velocities and displacements, kinetic energy, potential energy as well as the total Hamiltonian of the system can be determined and if the Hamiltonian is constant or in other words, the total energy of the system is conserved then the method is working properly and valid.

# **Chapter 4 IMPLEMENTATION OF NPFEM, MD AND MULTISCALE METHOD**

## **4.1 Program Layout**

The new nodal position finite element method was used to simulate the behaviour of one quadrilateral element, 3-element and 25-element with initial velocities. The same schemes were also modeled by molecular dynamic method. At the end, all models were modeled by combination of NPFEM, MD and handshaking are NPFEM/MD in the middle where the two domains interact and transfer information. All were implemented using the FORTRAN 95 programming language. The FORTRAN compiler is the Compaq Visual FORTRAN Professional Edition 6.1.0.

The program consists of one Master routine and numerous supporting subroutines. The Master routine starts the program, defines the dimensions of dynamic arrays. Then it calls the input subroutine to input all data, executes all calculations by calling various subroutines like forming mass matrix, stiffness matrix, deploy time integration and solving to determine the position, displacement, velocity, acceleration, kinetic energy, potential energy, Hamiltonian and at the end call another subroutine to output all the results. The description of functionality and main routine are outlined in a flow chart shown in Table 4.1 and Figure 4.1 - Figure 4.3.

Table 4.1 Description of master routine.

Main Routine
Call routine to read control parameters and define dynamic dimensions
Call routine to input data from input file
Call routine to initialise arrays and apply initial conditions
Call routine to calculate initial status of system
Calculate Newmark time integration parameters
Call routine to form global mass matrix
Loop over each time increment, $t = t + \Delta t$
Call routine to compute stiffness matrix
Form effective stiffness matrix
Compute effective loadings
Call routine to apply boundary condition
Call routine to solve system equation for nodal positions
Compute values for nodal accelerations and velocities
Compute kinetic energy, potential energy and Hamiltonian
Output solutions

This table shows how the main routine involves with the subroutines and call them one by one to calculate global mass matrix. It also shows where the time integration starts and calculate global stiffness matrix to solve the equation of motion for positions, velocities and accelerations of all the nodes/particles and finally determination of the kinetic energy, potential energy and finally total Hamiltonian of the system. If the model is working properly a constant Hamiltonian is expected to show the energy conservation.

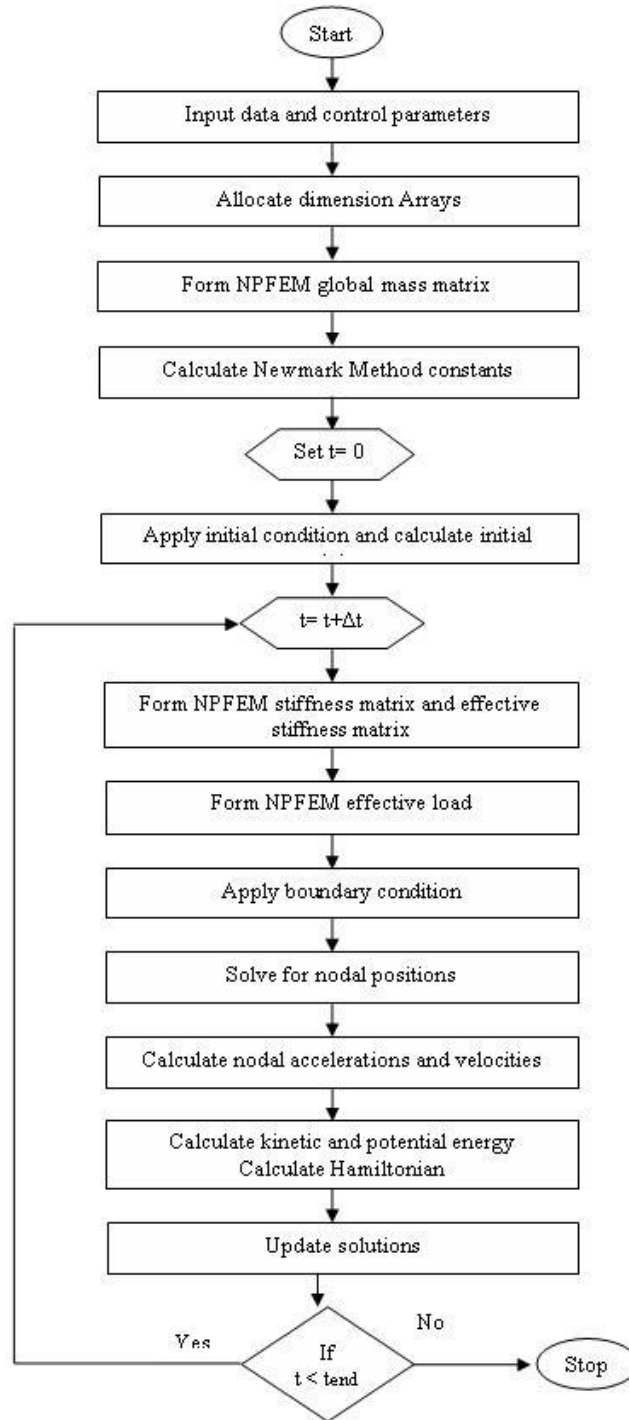


Figure 4.1 Flow chart of master routine for NPFEM.

For all three structures including one-element, 3-element and 25-element, all three models including NPFEM, MD and coupled MD/NPFEM have been used and the results compared in chapter 5. Figure 4.1 demonstrates the flow chart of master routine when the whole system is modeled by the newly proposed NPFEM. This shows clearly where the global NPFEM mass matrix forms. Moreover, Figure 4.6 shows the flow chart of NPFEM mass matrix subroutine in details. In the beginning of the master routine program inputs data and control parameters, form corresponding mass matrix, apply initial conditions, initializing for the time integration. The next step is the time integration where the NPFEM stiffness matrix, NPFEM effective stiffness matrix as well as effective loads are calculated and after applying the boundary conditions the equation will be solved for nodal positions. Based on calculated nodal positions, nodal velocities and accelerations will be determined in each time step. Kinetic energy can be determined using mass matrix and nodal velocities. Nodal displacements are always the difference of current positions and original positions and it is applicable in determination of the potential energy. Finally, the total Hamiltonian of the system is the summation of the kinetic and the potential energy in each time step. At this time all the nodal positions, velocities and accelerations should be updated before going to the new time step. In the new time step, stiffness matrix, effective stiffness matrix, effective loads, positions, velocities, accelerations, kinetic and potential energy and total Hamiltonian will be updated. If the NPFEM model works properly and accurately, a constant Hamiltonian is expected at the end.

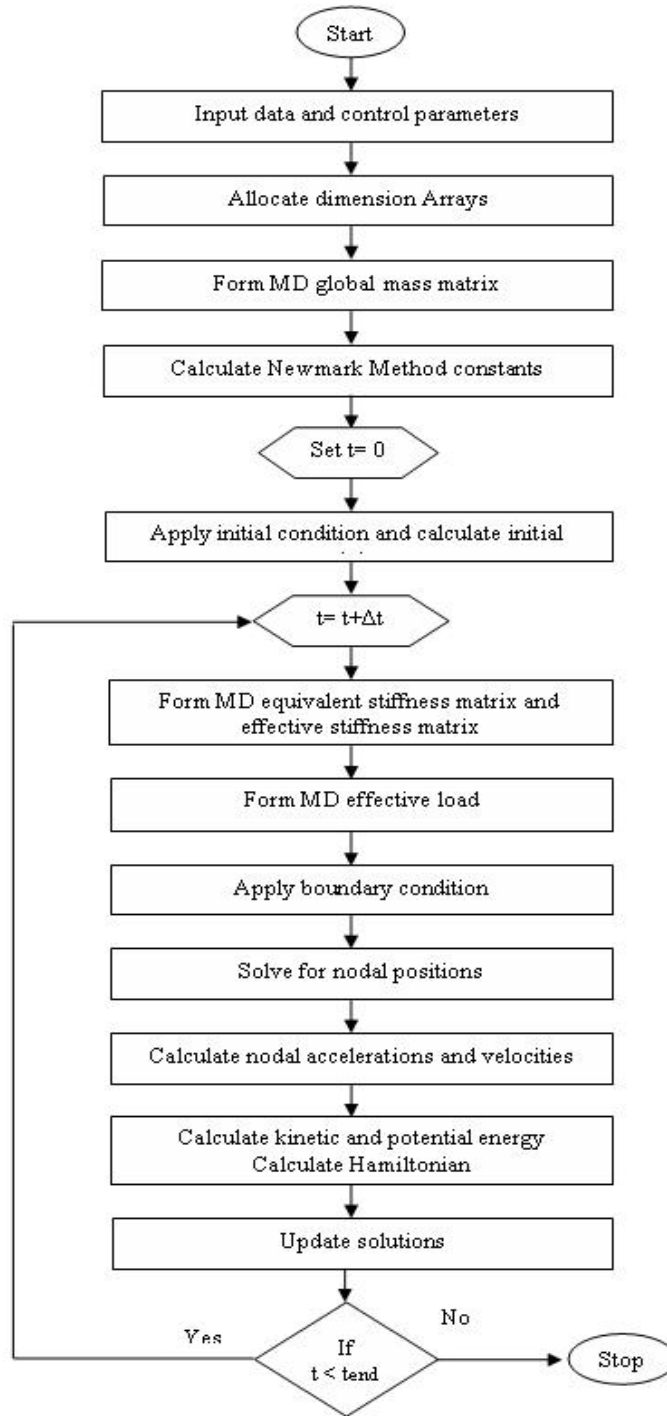


Figure 4.2 Flow chart of master routine for MD.

The second model which is used in this research is MD. Figure 4.2 demonstrates the flow chart of MD model. In figure 4.1 we already showed the flow chart of NPFEM and discussed the details of the model's algorithm and the outputs. In MD model, first the data and the control parameters are input and the array's dimensions are allocated. The global MD mass matrix is formed. The details of MD mass matrix calculation are discussed in details in chapter 3 and the flow chart is shown in figure 4.7. Before starting the time integration, it is necessary to calculate Newmark constants and apply the initial condition. The time integration starts and the first steps are calculating the equivalent stiffness matrix in MD and corresponded effective stiffness matrix. From this point the procedure is very similar to what has already done in NPFEM model since the same time integrator, the Newmark method, has been used for both model and this is required because in the third model both method would be combined in the same main routine. Therefore, the equation will be solved for the nodal positions in each time step and velocities, accelerations are calculated based on that. This information should be updated before starting the new time step. In the new time step, equivalent MD stiffness matrix, effective stiffness matrix, effective loads, positions, velocities, accelerations, kinetic and potential energy and total Hamiltonian will be recalculated. If the MD model works properly and accurately, the same scenario as NPFEM model, a constant Hamiltonian is expected at the end.

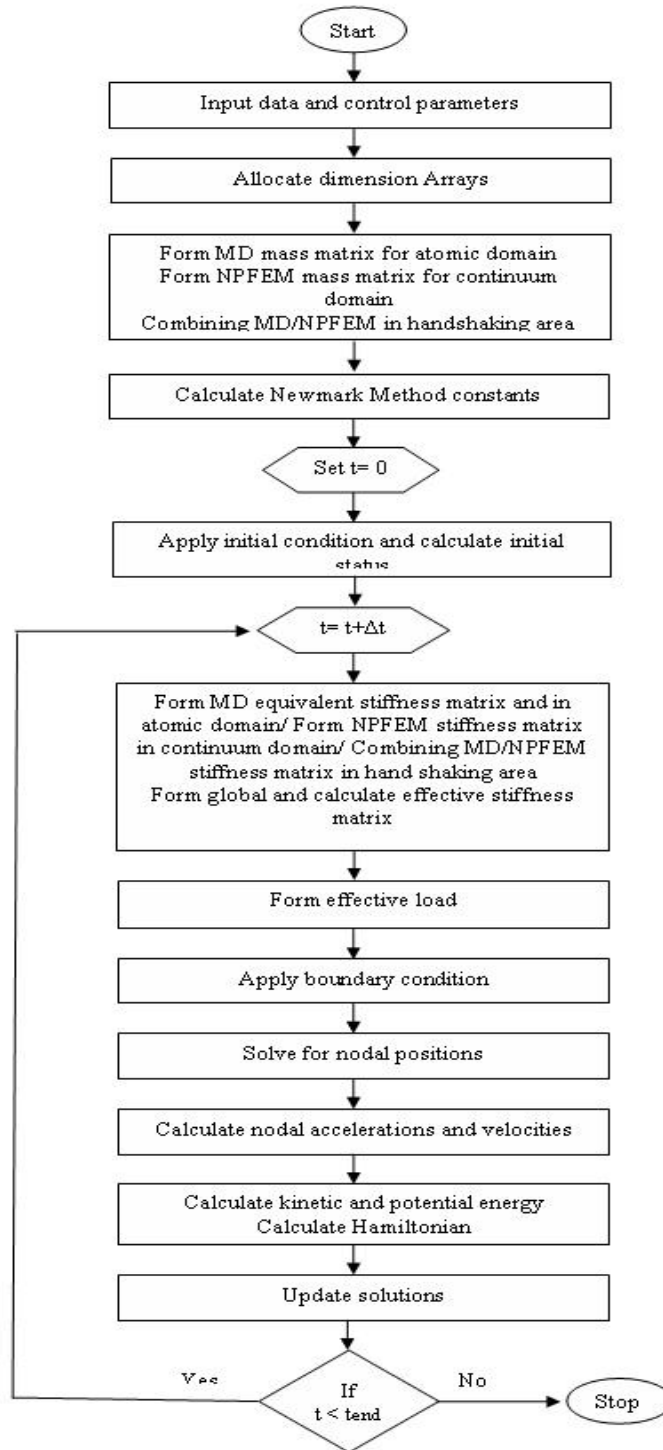


Figure 4.3 Flow chart of master routine for multiscale method.



The third model is coupling previous models, NPFEM and MD in the same main routine and combines these two models in the handshaking area. Figure 4.3 shows the main routine for coupling NPFEM/MD. The last algorithm is similar to those of NPFEM and MD except the mass and stiffness matrices. In coupling NPFEM/MD the main routine, instead of calling one subroutine as mass matrix calls three subroutines. One subroutine is formed for the continuum part of the lattice and uses NPFEM formulation to calculate mass matrix. The second subroutine is formed for the atomic part of the lattice and is based on the MD simulation principals. The third subroutine is based on the newly proposed multiscale bridging model to address the handshaking area where the continuum and the atomic domain overlap and share information. This subroutine carefully calculates the portion of the MD mass and NPFEM mass contribute in the handshaking area using the formulation derived and discussed in chapter 3. The same scenario is valid for the stiffness matrices. There are three subroutines; one address the continuum part of the lattice, the other subroutine addresses the atomic part of the lattice and the last one is uses for the handshaking area and follows the bridging scale method formulation already derived and presented in details in chapter 3. This main routine inputs data and control parameters, allocates arrays' dimension and calculates mass matrices in all domains. The routine continues with initializing for time integration and Newmark constants. The time integration starts with determination of stiffness matrices in all domains, calculating effective loads, applying boundary conditions and solving the equation of motion for the nodal positions. Calculating nodal velocities, accelerations followed by kinetic and potential energy as well as the total Hamiltonian at each time step is similar to the NPFEM and MD routines. If the coupling NPFEM/MD model works properly and accurately, a

constant Hamiltonian is expected for this simulation.

## **4.2 Evaluation Modules for Stiffness Matrices**

### **4.2.1 NPFEM for Continuum Domain**

The evaluation of NPFEM stiffness matrix is performed by the subroutine FORMFEGK in continuum domain. The global force also is evaluated in the same matrix for the same domain. This subroutine loops over the number of NPFEM quadrilateral elements and then calls another subroutine to assemble global stiffness matrix and the global force. This subroutine is called by the main routine in each time step and the stiffness matrix and the force is being updated each time based on updated nodal positions. Figure 4.4 illustrates the flow chart of the subroutine.

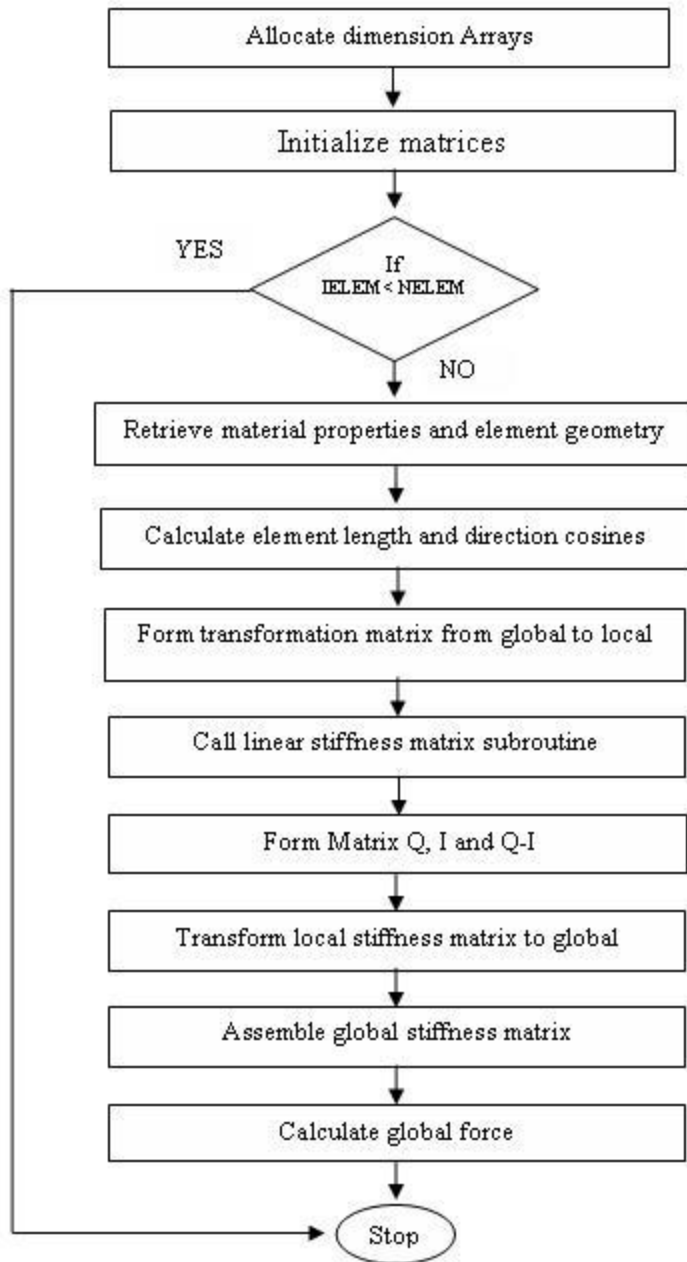


Figure 4.4 Evaluation modules for NPFEM global stiffness matrix.

### **4.2.2 MD for Atomic Domain**

The evaluation of MD stiffness matrix is performed by another subroutine FORMMDGK in atomic domain. In this subroutine, like the continuum domain, the global force is evaluated in the same matrix for the same domain. This subroutine loops over the number of MD pair atoms and then calls another subroutine to assemble the equivalent global stiffness matrix and the global force. This subroutine is called by the main routine in each time step and the stiffness matrix and the force is being updated each time based on updated atom positions. Figure 4.5 shows the flow chart of the subroutine.

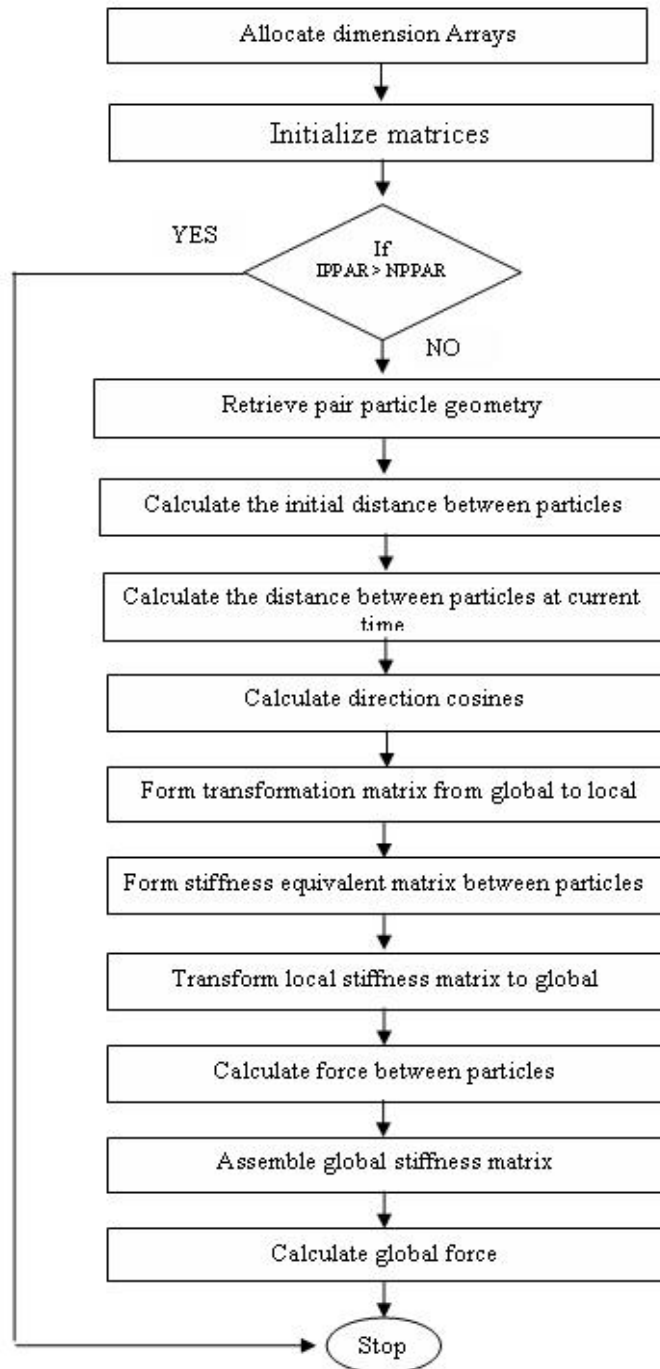


Figure 4.5 Evaluation modules for MD equivalent global stiffness matrix.

## **4.3 Evaluation Module for Mass Matrices**

### **4.3.1 NPFEM for Continuum Domain**

As we discussed in section 4.2 one of the most critical part of this implementation is the determination of stiffness matrices in both continuum and atomic region. Other matrices, which play an important role in this research, are mass matrices in each region. First, the integration in Eq. (3.26) has performed in Maple and then the result has converted to FORTRAN code. A subroutine called FORMFEMTX is used for calculation mass matrix in continuum region based on the derived equations and formulas from Nodal Position Finite Element Method. The mass matrix depends on material density, element size and element thickness. Therefore in this subroutine there is a loop over the number of elements and at the end use the same assembler as applied for stiffness matrix. Since the mass matrix does not update during the time integration, it is calculated before starting the time integration and remains constant during time integration process. Figure 4.6 illustrates the flowchart of the formation of NPFEM mass matrix.

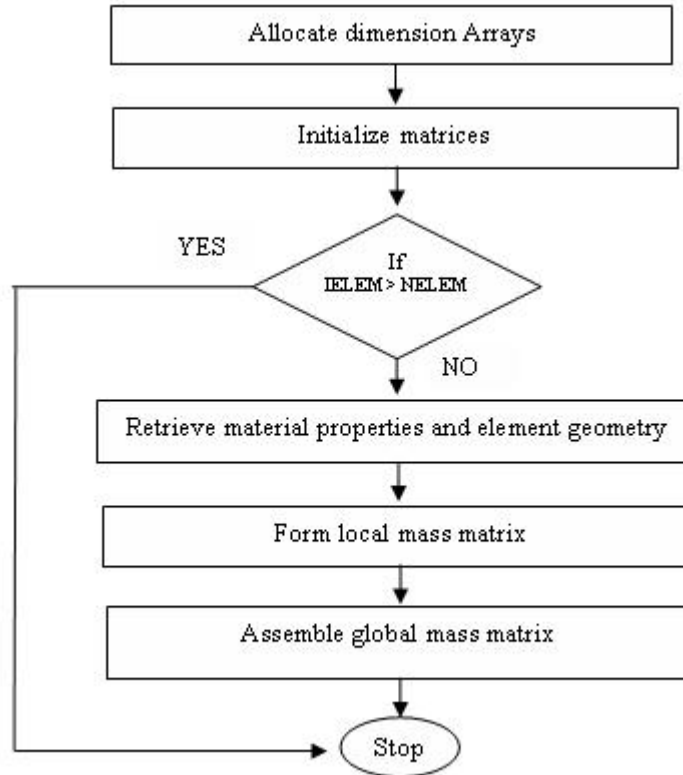


Figure 4.6 Evaluation module for NPFEM global mass matrix.

### 4.3.2 MD for Atomic Domain

Mass matrix in Atomic domain using Molecular Dynamic method is not as complicated as NPFEM. Here mass matrix is a diagonal matrix with diagonal entries equal to mass of each particle. Therefore, this matrix highly depends on particle mass which has been input in the beginning of the main routine. In this program, a subroutine called FORMMDMTX calculates the MD mass matrix. Figure 4.7 shows the flowchart of the routine calculate the mass matrix.

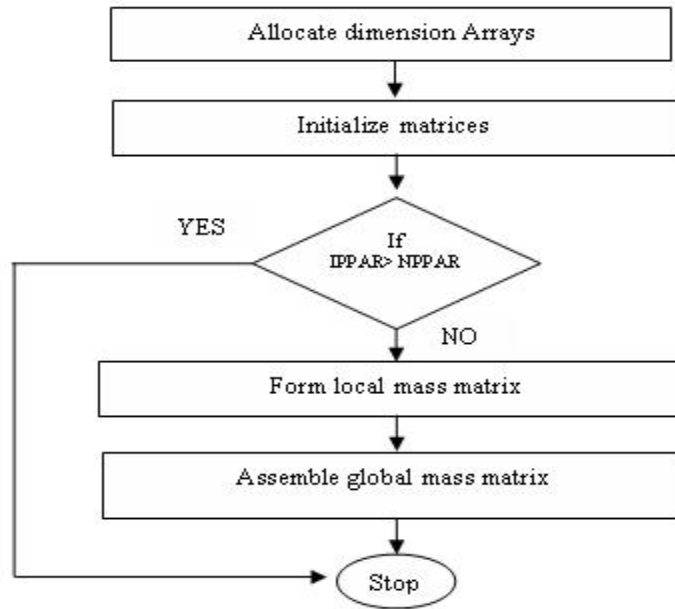


Figure 4.7 Evaluation module for MD global mass matrix.

In order to validate the formulation and implemented code, three different models have been chosen; one-element, 3-element and 25-element. Each model has been solved by three approaches discussed in this research; NPFEM, MD and multiscale MD/NPFEM. The results will be discussed in details in the next chapter. In all three models, the most important achievement is the fact that the energy is conserved and the Hamiltonian found to be constant in time. For the most complicated lattice with 25-element, one extra simulation has done. A sinusoidal wave has been applied to the top nodes of the lattice by changing the position of the top nodes and the behaviour of all the nodes have been studied under this condition. The results shows that the wave can successfully pass through the three different domains; continuum, handshaking and atomic, and finally reaches to the bottom layers.



## Chapter 5 RESULTS AND DISCUSSION

### 5.1 Modeling with One Element

In previous chapters a new multiscale modeling of molecules and continuum is proposed. This new model used bridging scale method for coupling MD and NPFEM methods to transfer information smoothly and seamlessly from one domain to the other through handshaking area. In this chapter, three examples including one-element, 3-element, and 25-element are studies and the results are compared with three different models; NPFEM, MD and NPFEM/MD. The first example is the study of a body illustrates in Figure 5.1 consists of one four-node element subject to an initial velocity on top nodes like a pulse and the system's reaction to this pulse. The system responses like velocity, displacement and the total energy of the system have been studied carefully in two dimensions in time. However, in this case we are mostly interested in the reaction of the body in y-direction where the initial velocity has been applied. The element was first modeled in continuum mechanics scale by Nodal Position Finite Element Method (NPFEM) Figure 5.1 (a) and then in atomic scale by Molecular Dynamics method (MD) Figure 5.2 (b) and finally the same element modeled with the proposed multiscale model by combining the two above-mentioned methods. The following figure is the illustration of the four-node element goes under the downward initial velocity.

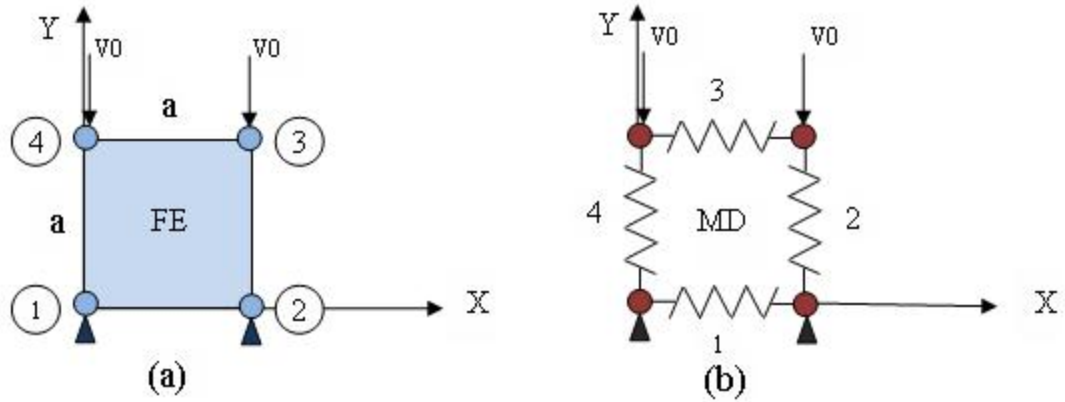


Figure 5.1 (a) four-node element in two dimensional plane scheme (b) four pair molecule interacting two by two

In this example, Figure 5.1 (a) illustrates four-nodded element modeled by NPFEM and Figure 5.1 (b) illustrates four pair molecules modeled by MD. Since this study is focused on methodology and developing new multiscale model and it is valid in any system of units, the dimensionless properties are used in these simulations. In Figure 5.1(a), the dimensionless properties of the element in continuum scale are: Young's modulus,  $E = 258.5$ ; element side length,  $a = 7.745$ ; thickness,  $t = 0.07745$ ; density,  $\rho = 51.5$  and the Poisson ratio,  $\nu = 0$ . An initial velocity  $V_0 = -0.01$  downwards is applied at top nodes and the following results have been obtained by running the NPFEM formulation by the Newmark numerical integration. The results are shown in Figure 5.2 - Figure 5.4. As expected, the displacement and velocity oscillates in a harmonic motion after the initial velocity pulse, because no internal material damping effect is considered. Figure 5.4 shows the time history of the Hamiltonian function of the element. For generating the results presented in Figure 5.2- Figure 5.4, the flowcharts shown in Figure 4.1, Figure 4.4 and Figure 4.6 are applied. The total energy of the element is conserved, which indicates the

NPFEM and the Newmark integration scheme are energy conserving as expected. It demonstrates that our codes are correct.

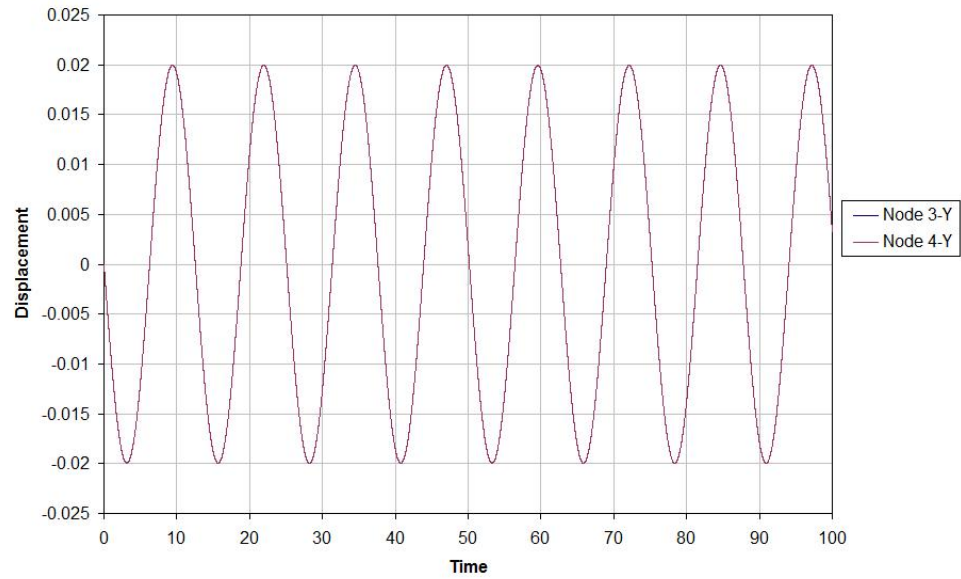


Figure 5.2 Time history of displacement in y direction of one element using NPFEM.

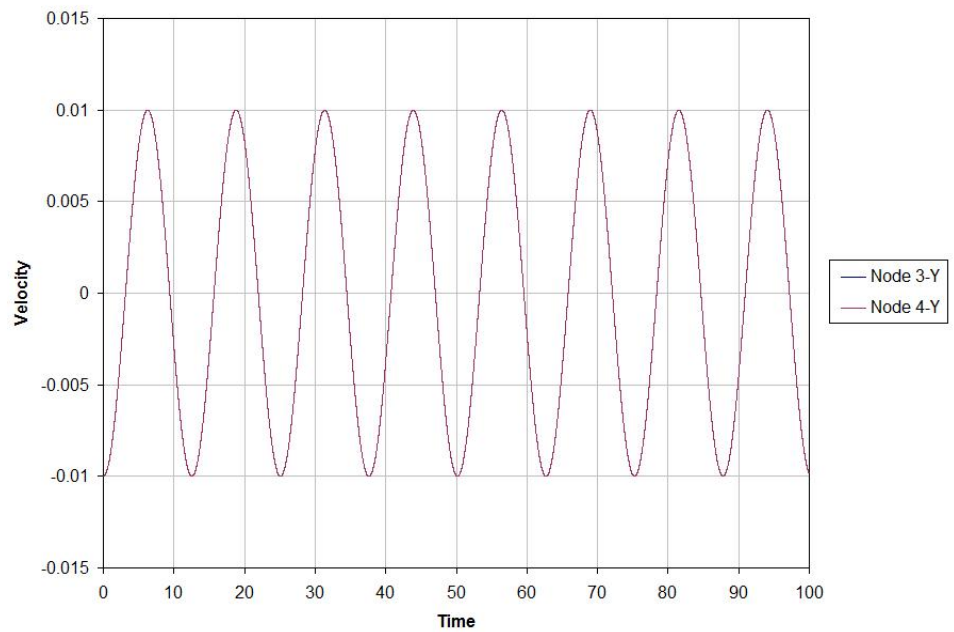


Figure 5.3 Time history of velocity in y direction of one element using NPFEM.

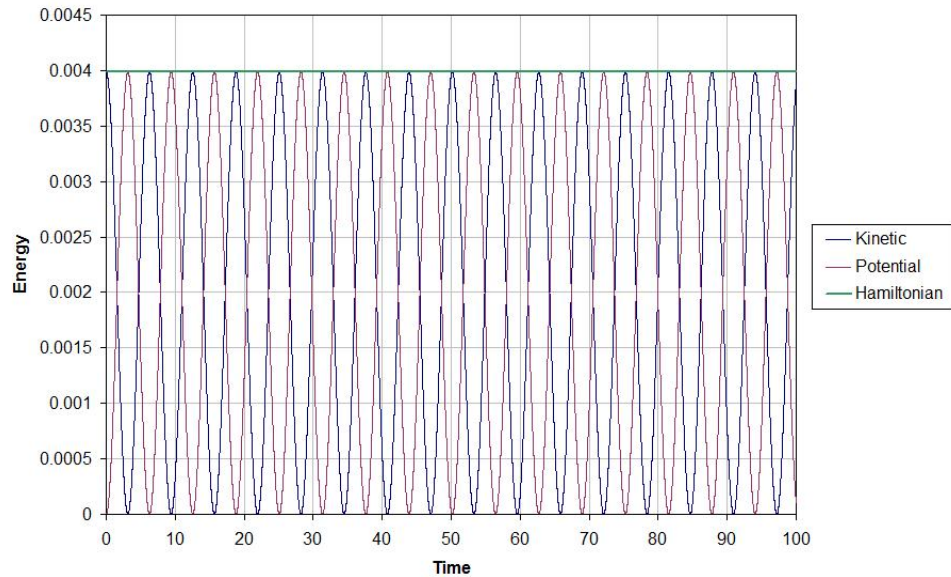


Figure 5.4 Time history of Hamiltonian of one element using NPFEM.

Figure 5.2 (b) shows the same body modeled with MD with four particles “equivalent atoms”. The dimensionless properties of equivalent atoms are: depth of potential well,  $\varepsilon = 8.33$ , the finite distance corresponding to zero the inter particle forces,  $\sigma = 6.9$  and the mass of each particle,  $m = 40.0$ . The results are shown in Figure 5.5 - Figure 5.7. As expected, the results of displacement and velocity are the same as that of NPFEM. The result of system energy, the Hamiltonian function, is almost the same as that of NPFEM, except for the small (2.5% of the correct value of Hamiltonian) oscillation around the correct value. This is due to nonlinearity of the stiffness matrix of MD. As shown in Eq. (3.41), the  $\mathbf{K}_{MD}$  is highly nonlinear. For generating the results presented in Figure 5.5- Figure 5.7, the flowcharts shown in Figure 4.2, Figure 4.5 and Figure 4.7 are applied. The energy conservation of the Newmark integration scheme adopted in the current study is valid only for linear systems. However, the fluctuation caused by the nonlinearity is small and

acceptable.

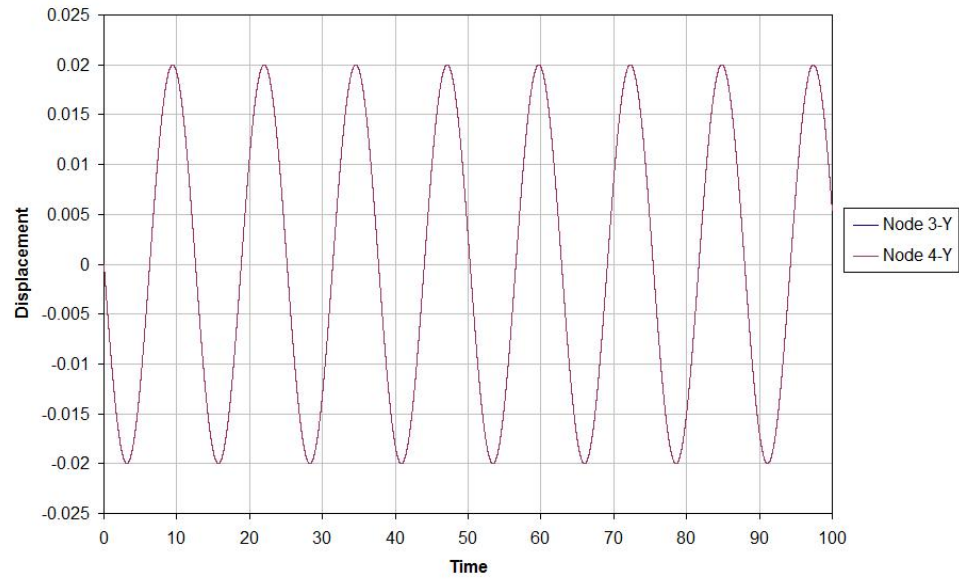


Figure 5.5 Time history of displacement in y direction of four particles using MD.

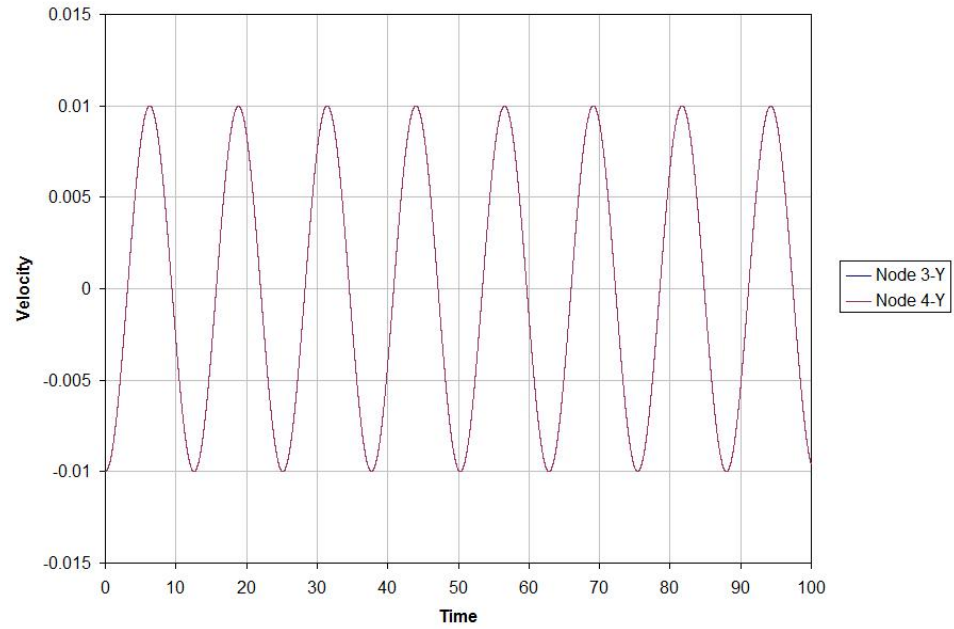


Figure 5.6 Time history of velocity in y direction of four particles using MD.

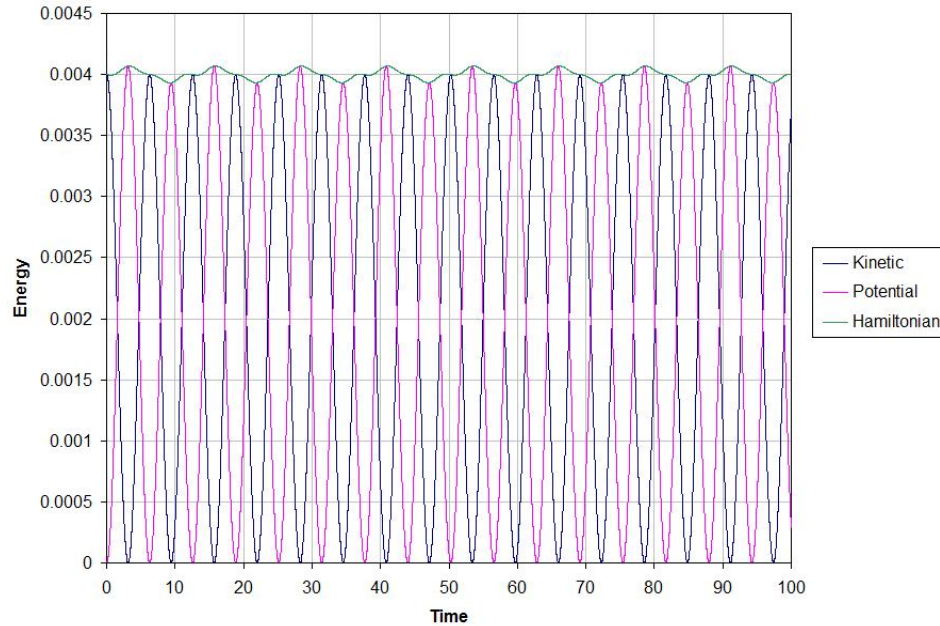


Figure 5.7 Time history of Hamiltonian of four particles using MD.

Finally, the same body has been modeled with coupled NPFEM/MD, where the 4-noded quadrilateral element is overlapped with four particles - “equivalent atoms” at four nodes. They are coupled as per Eq. (3.46). The results are shown in Figure 5.8 - Figure 5.10. The results of displacement and velocity are the same as that of NPFEM, which indicates that the NPFEM/MD coupling is effective to maintain the energy conservation in the transition zone. For generating the results presented in Figure 5.8- Figure 5.10, the flowcharts shown in Figure 4.3 is applied. The result of system energy, the Hamiltonian function, is almost the same as that of NPFEM. The oscillation due to nonlinearity of the stiffness mass of MD has been reduced to the level not noticeable. The results show that our codes are correct.

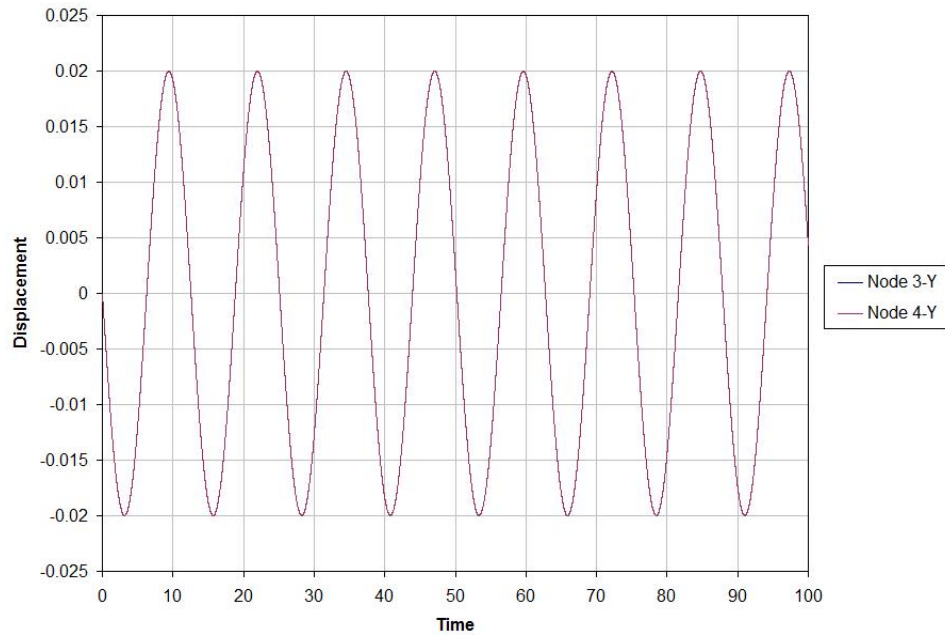


Figure 5.8 Time history of displacement in y direction using coupled NPFEM/MD.

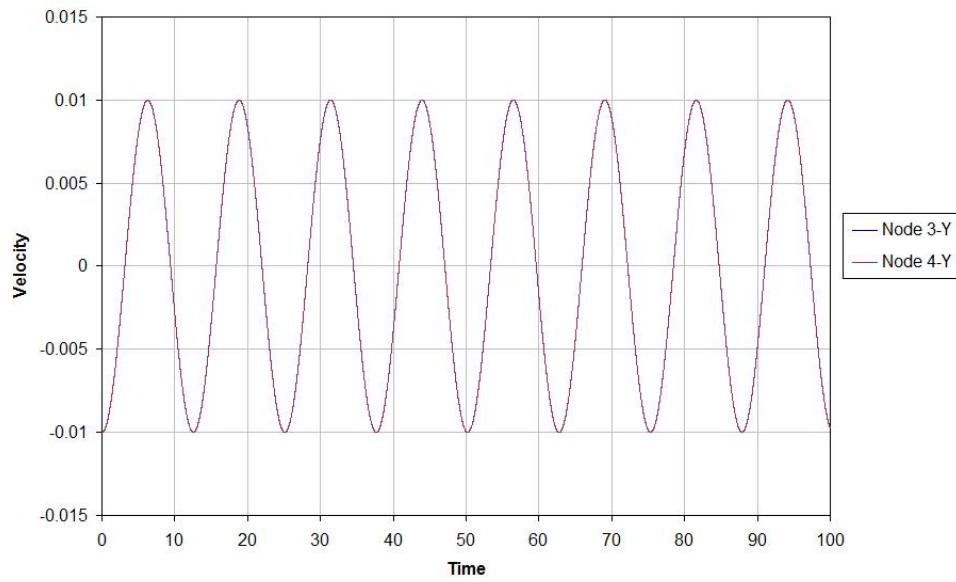


Figure 5.9 Time history of velocity in y direction using coupled NPFEM/MD.

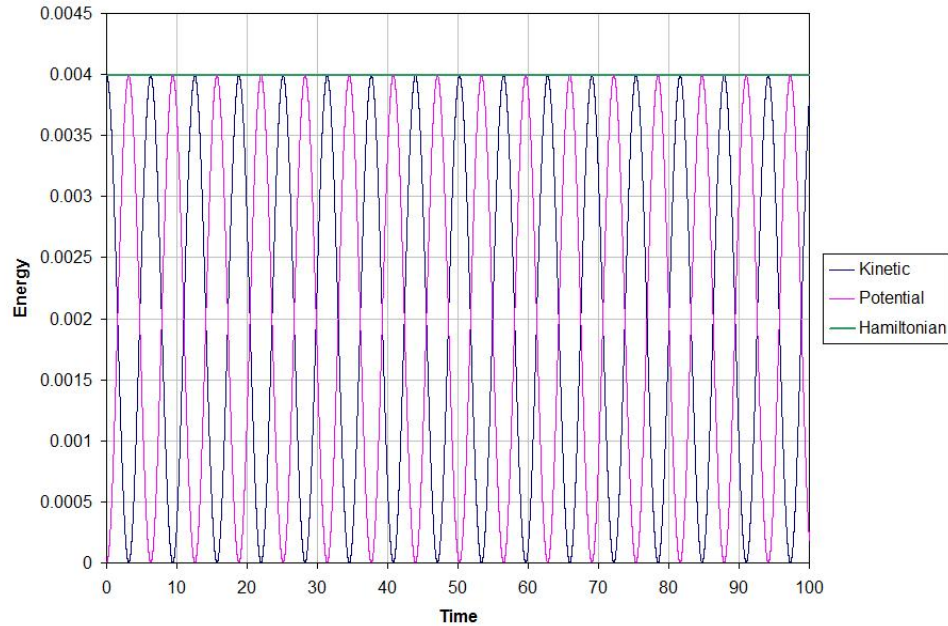


Figure 5.10 Time history of Hamiltonian using coupled NPFEM/MD.

## 5.2 Modeling with Three Elements

After the codes have been validated in the first sample with three different models, NPFEM, MD and coupled NPFEM/MD, the second example that has been studied involves three different zones, the FE, MD and FE/MD, as shown in Figure 5.11. Figure 5.11 (a) illustrates 3-element body with 8 nodes fixed at the bottom of the body only in y direction which is modeled by NPFEM. Figure 5.11 (b) illustrates the same body with 8 particles which two adjacent particles interact. Therefore, there are 10 pair particle and modeled by MD. Figure 5.11(c), illustrates the same body which is divided into three domains. The first domain is the MD domain. It is located at the bottom of the body. The domain on the top of the body is the FE domain. The domain in the middle is the handshaking/transition area which two domains interact and transfer information. Therefore, the middle element



is the combination of both models.

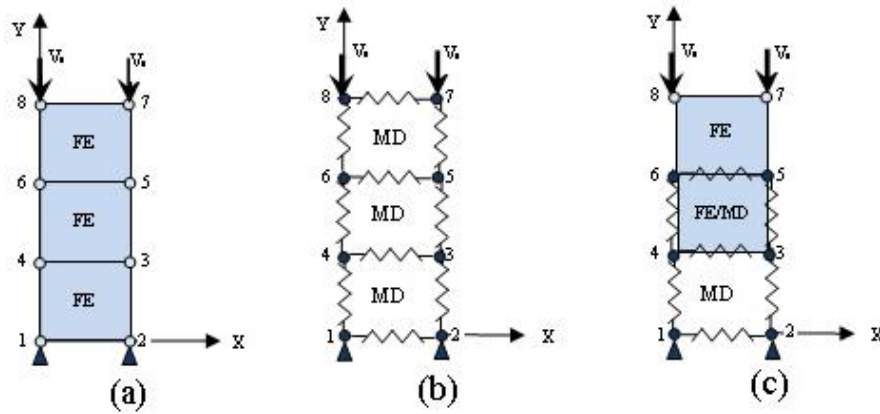


Figure 5.11 Three-element model.

The material properties in the FE and MD scales used in this sample are the same as those in the previous section. The initial conditions are the same as before: a velocity pulse  $V_0 = -0.01$  is applied at top nodes simultaneously downwards. Before conducting the multiple-scale modeling, the problem is analyzed by using only NPFEM, Figure 5.11 (a), and MD, Figure 5.11(b), separately for comparison and validation.

The results by NPFEM and MD are shown in Figure 5.12 - Figure 5.17. The results show that the dynamic characteristics obtained by continuum mechanics and molecular dynamics are different for the same body although the total system energy is kept the same. In the continuum mechanics based, NPFEM, the degrees of freedom of each node within one element are coupled both in the stiffness and mass matrices. In contrast, the element is replaced by four representative atoms at four nodes and the nodes are linked to their adjacent nodes by the LJ potentials. No diagonal LJ potentials are in the model. Furthermore, the mass matrix in MD is diagonal, which implies that there is no inertial

coupling between nodes. Thus, there exist higher order modes in NPFEM as shown in Figure 5.12 and Figure 5.13 than MD as shown in Figure 5.15 and Figure 5.16.

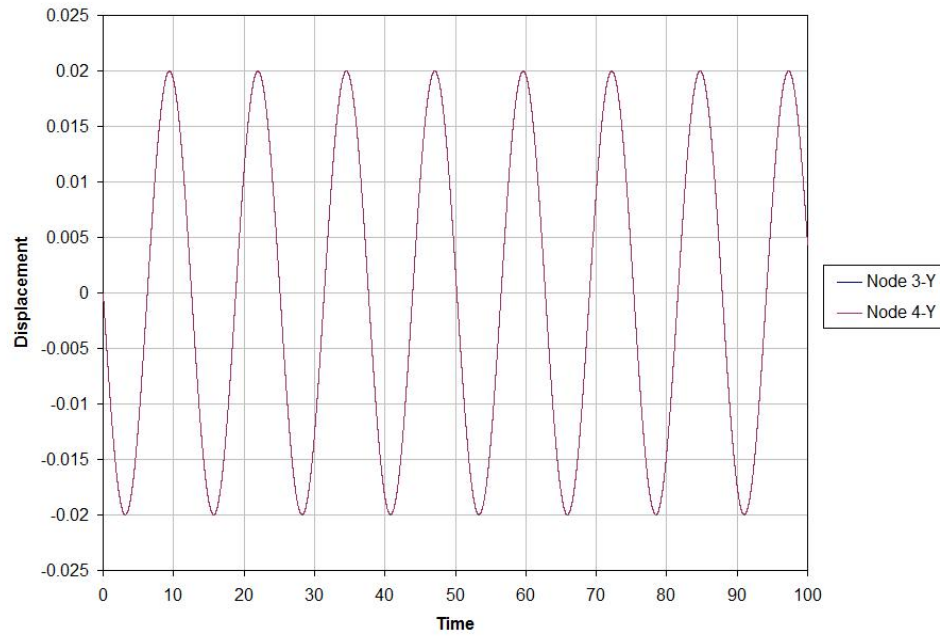


Figure 5.12 Time history of displacement of top nodes in Y direction by NPFEM – 3 element model.

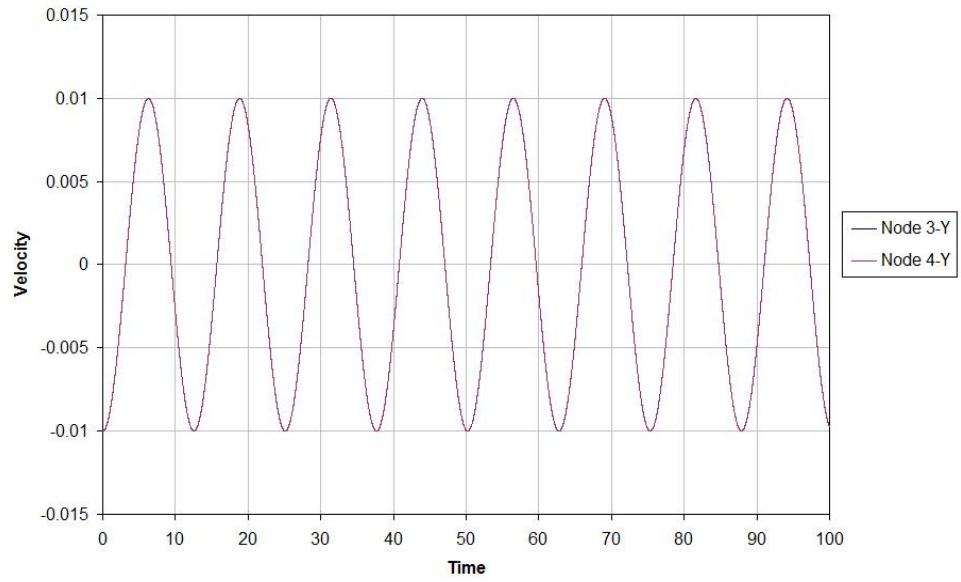


Figure 5.13 Time history of velocity of top nodes in Y direction by NPFEM – 3 elements model

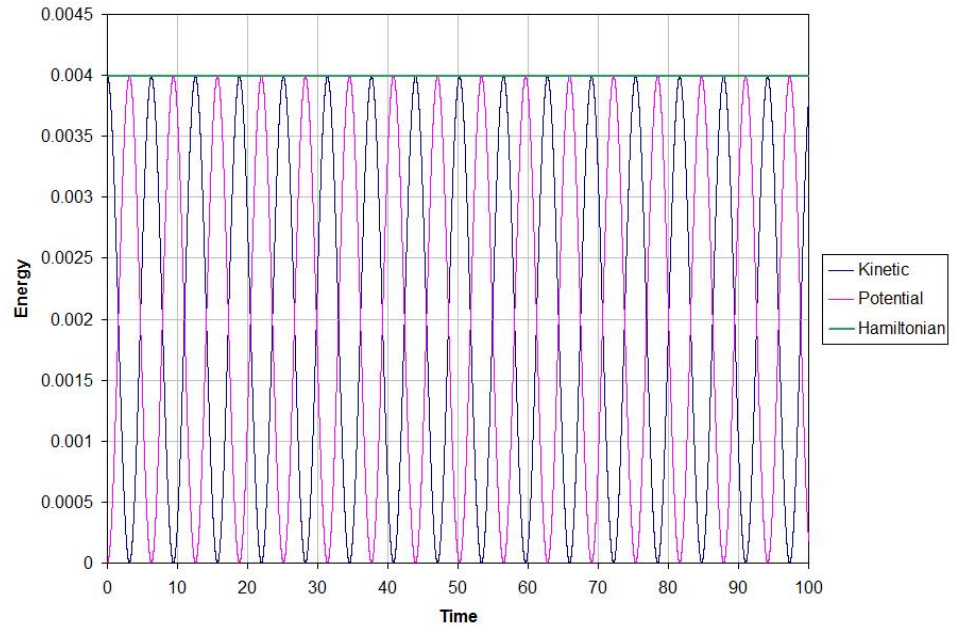


Figure 5.14 Time history of system Hamiltonian by NPFEM – 3 element model.

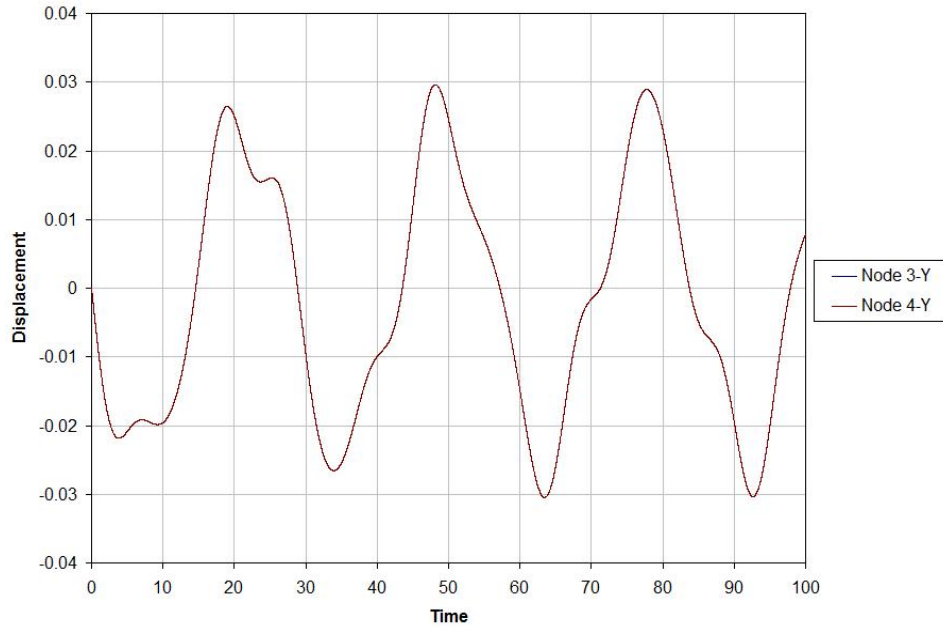


Figure 5.15 Time history of displacement of top nodes in Y direction by MD – 3 element model

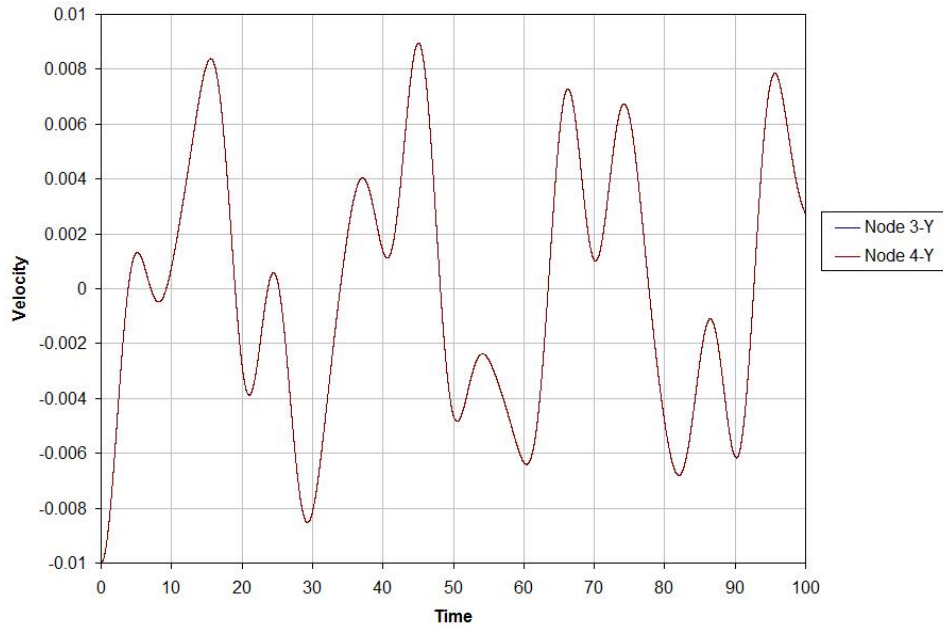


Figure 5.16 Time history of velocity of top nodes in Y direction by MD – 3 element model

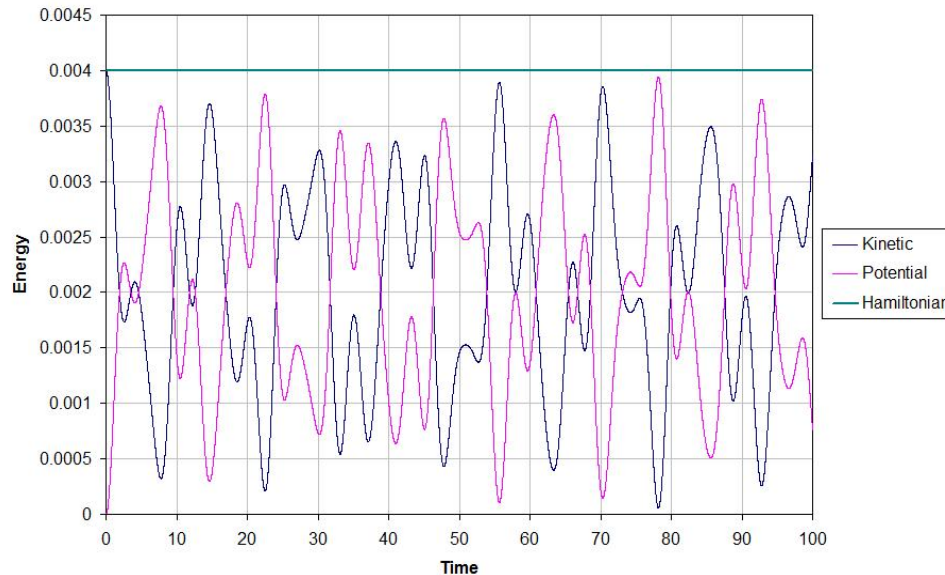


Figure 5.17 Time history of system Hamiltonian by MD – 3 element model.

The results with NPFEM and MD coupling are shown in Figure 5.18 - Figure 5.20. The body divided by three domains as shown in Figure 5.11 (c) the first domain at the bottom of the body consists of one element and is molecular domain the second domain is also consists of one element and located on the top of the element and is continuum domain. The last domain is in the middle of the body and consists of one element and considered and hand shaking area where both domains overlap and transfer information. As Figure 5.18 - Figure 5.20 clearly shown the dynamic characteristics, reflected by the displacement and velocity of top nodes, are different from the ones by either NPFEM or MD as expected. However, the total energy of the system remains the same. Thus, we can conclude that the coupling method used in the NPFEM/MD zone ensure energy conservation in the multiscale modeling.

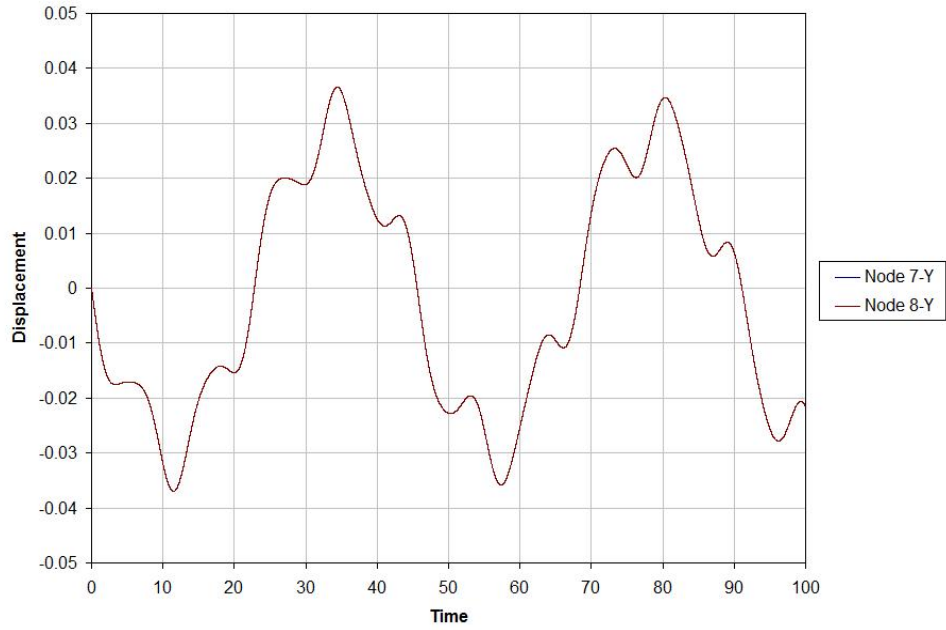


Figure 5.18 Time history of displacement of top nodes in Y direction by NPFEM/MD – 3 element model.

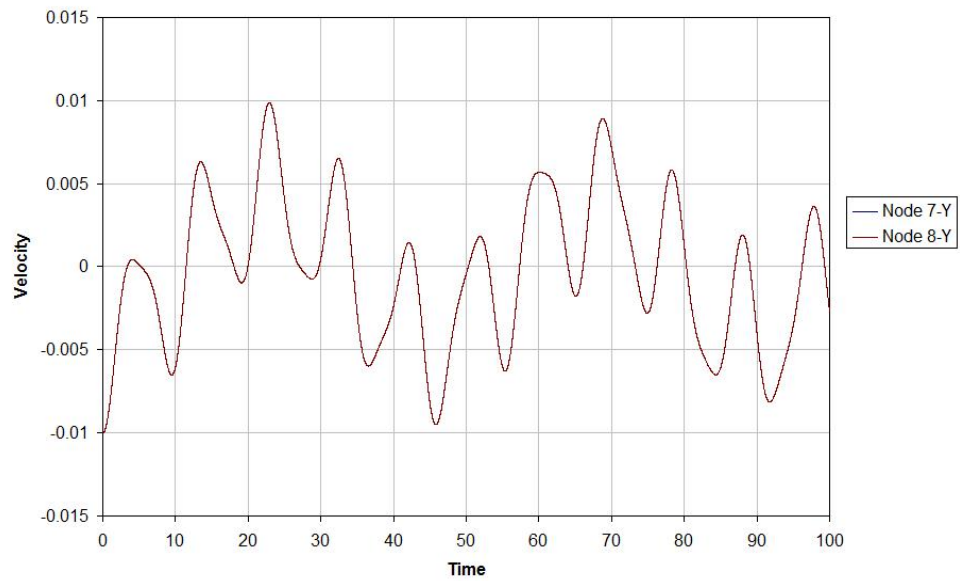


Figure 5.19 Time history of velocity of top nodes in Y direction by NPFEM/MD – 3 element model.

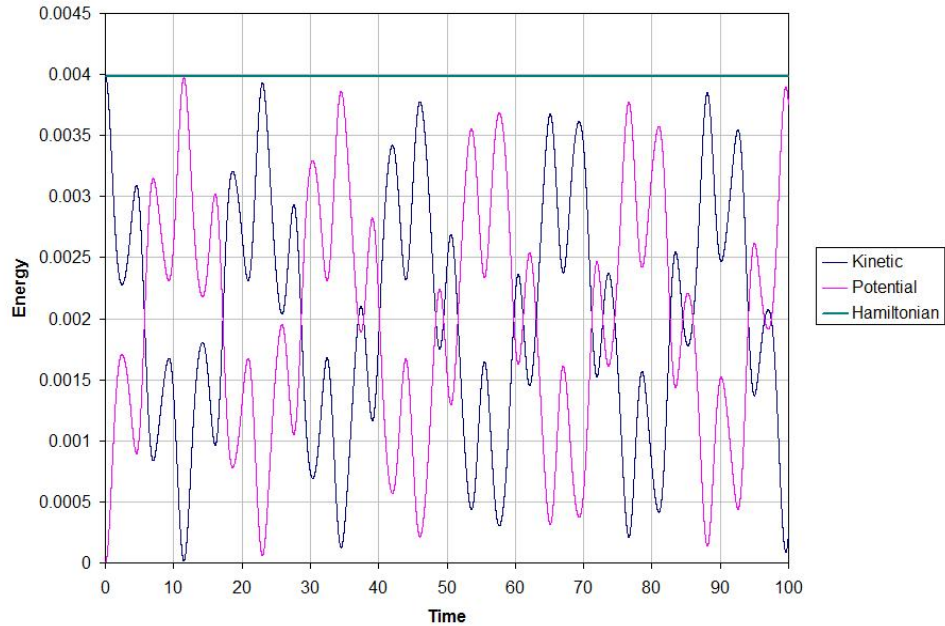


Figure 5.20 Time history of system Hamiltonian by NPFEM/MD – 3 element model.

### 5.3 Modeling with Five by Five Mesh/Lattice

The code has already been validated with two samples, one and three elements, each with three different models; NPFEM shown in Figures 5.2 - 5.4 and Figures 5.12 - 5.14, MD shown in Figures 5.5 - 5.7 and Figures 5.15 - 5.17 as well as coupled NPFEM/MD demonstrated in Figures 5.8 - 5.10 and Figures 5.18 - 5.20. The final and the most complicated case study has been performed is a lattice of 5 by 5 elements with 36 nodes/particles shown in Figure 5.21. For this model, 25 quadrilateral elements exist and for the body 72 by 72 mass and stiffness matrices have been determined manually for solving the total Hamiltonian of the system. One approach to ensure the method is valid is making the samples more complicated. In this study the number of nodes and as a result the number of elements has been increased in both directions. Therefore, in the handshaking region we have 5 elements instead of one and the stiffness and mass matrices

are much more complicated. Has the method worked accurately and the results shown energy conserved and information transferred from one region to the other smoothly, any other lattice should work as well. In this model, like the last two samples the body is divided into three domains. The first domain at the bottom of the body consists of 10 elements is MD. The second domain at the top of the body consists of 10 elements as well is NPFEM and the third domain in the middle of the body consists of 5 elements is the handshaking/transition area where two domains interact and transfer information. Therefore, in the handshaking area the two models, MD and NPFEM, are coupled and we have the combination of both models.

The material properties in NPFEM and MD domains in this sample are the same as those in previous sections for one and three elements samples. The initial condition is also the same as before: an initial velocity as a pulse of  $V_0 = -0.01$  is applied at the top nodes downwards. For simulation of this model, coupling MD/NPFEM, the problem is solved by using MD and NPFEM separately for comparison and validation.

The results by MD and NPFEM are presented in Figures 5.22 – 5.27. The results are consistent with that of obtained from three-element sample Figure 5.11. By means of it, although the dynamic characteristics of this model obtained by MD and NPFEM are different, the total energy of the system remains the same. In NPFEM model which is based on continuum mechanics principals, the degrees of freedom of each node within one element are coupled in both stiffness and mass matrices. However, when the nodes of this four noded element is replaced by four atoms in MD model, the atoms interact only with adjacent atoms through L-J potentials. In this study no diagonal L-J potentials are considered in the model. Moreover, in MD simulation no inertial exists between atomic



masses and the mass matrix is diagonal. As a result, higher order modes exist in NPFEM as shown in Figures 5.22 and 5.23 than MD as shown in Figures 5.25 and 5.26.

The results for coupled MD/NPFEM are shown in Figure 5.28 – 5.30. As expected and confirmed by previous sections' results the dynamic characteristics of the coupled MD/NPFEM reflected by displacement and velocity of the top nodes, are different than those modeled by MD or NPFEM separately. However, the total energy of the system, given by the Hamiltonian, remains the same. Therefore, it can be concluded that the coupling methodology used in MD/NPFEM ensure the energy conservation in the multiscale modeling.

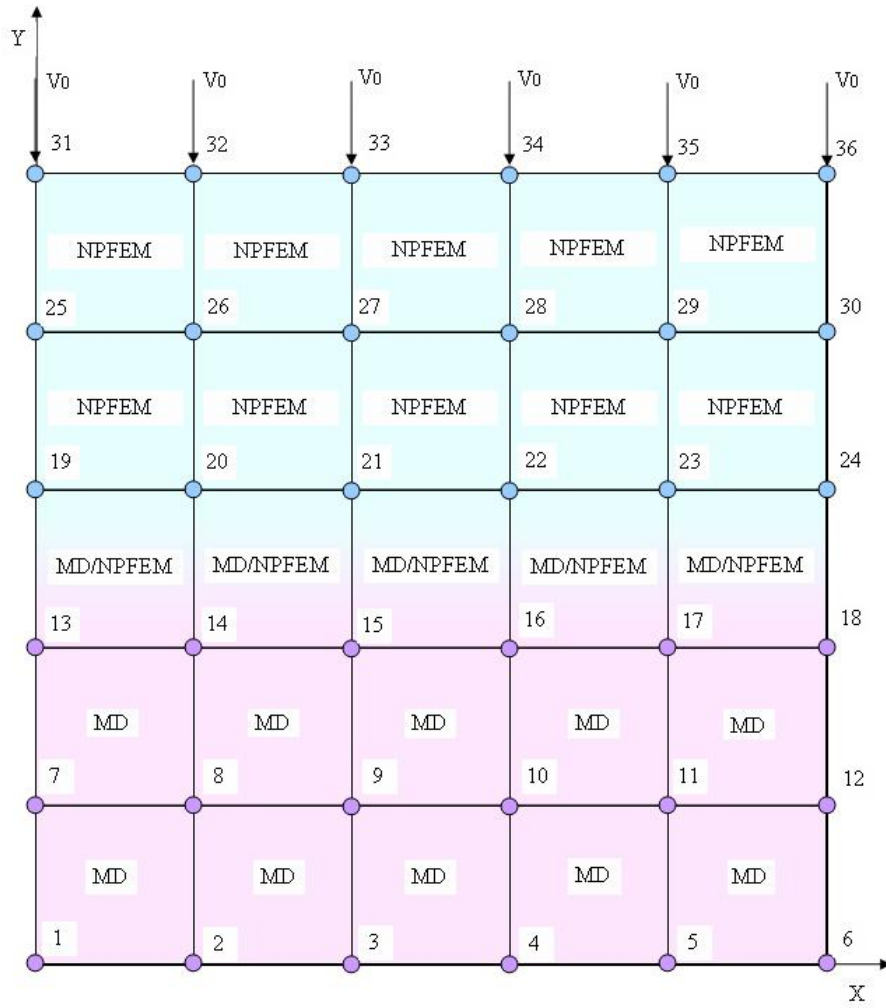


Figure 5.21 5 by 5 lattice.

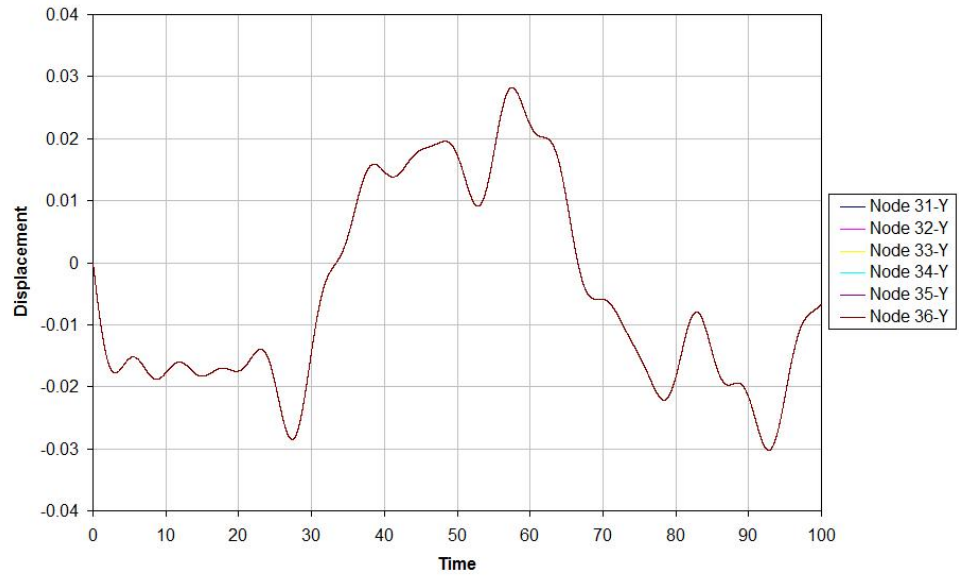


Figure 5.22 Time history of displacement of top nodes in Y direction by NPFEM 25-element model.

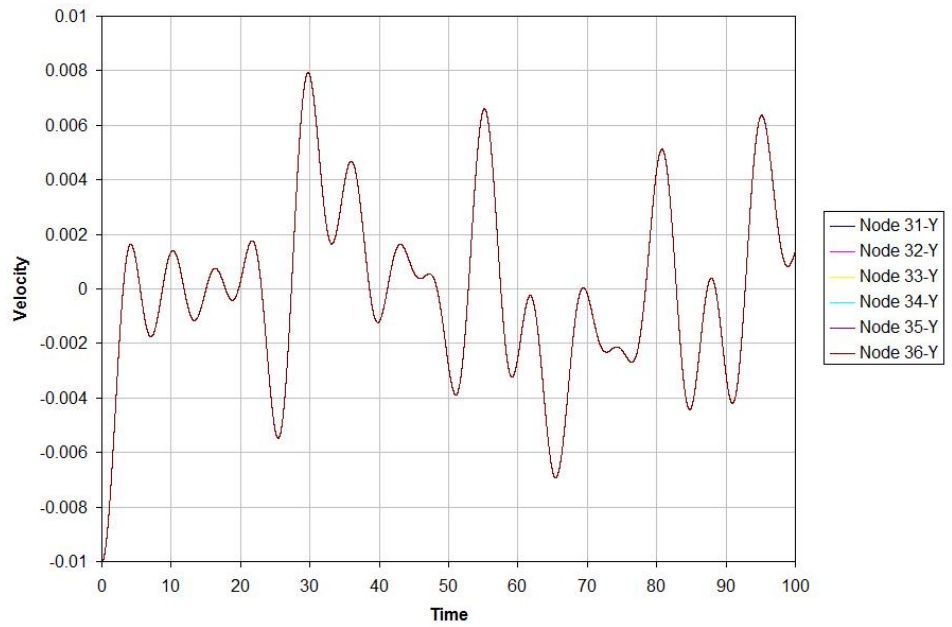


Figure 5.23 Time history of velocity of top nodes in Y direction by NPFEM 25-element model.

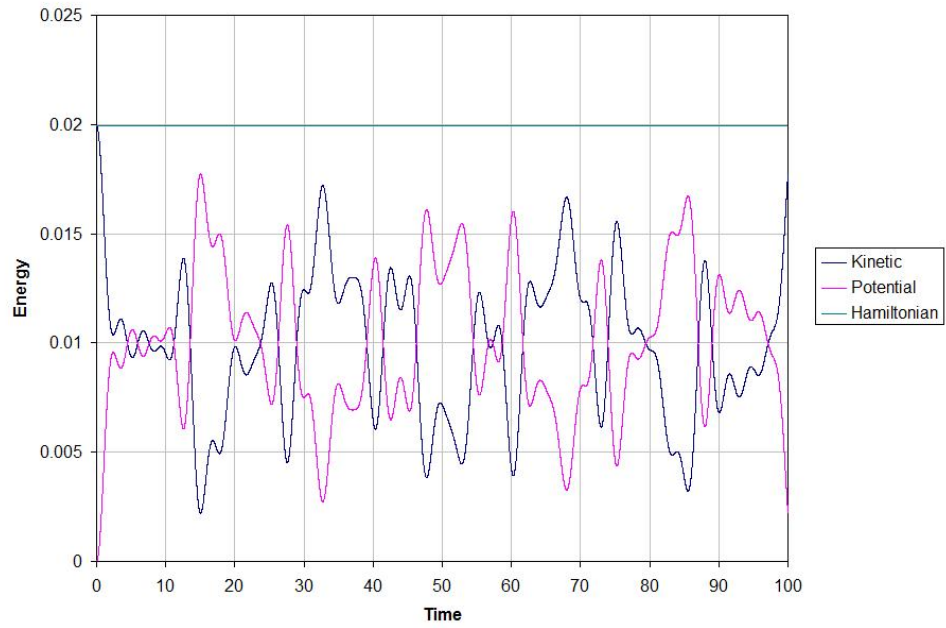


Figure 5.24 Time history of system Hamiltonian by NPFEM – 25 element model

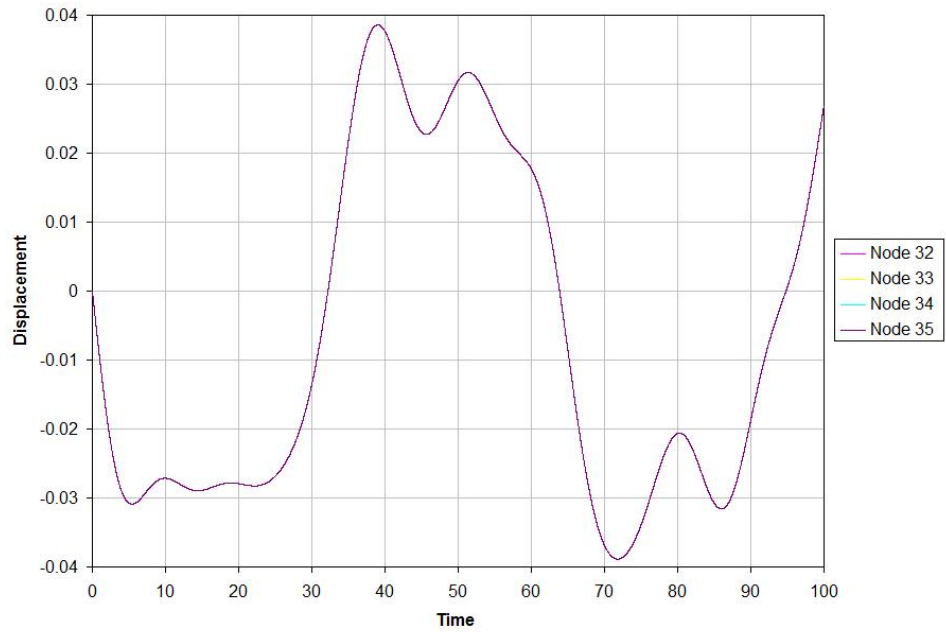


Figure 5.25 Time history of displacement of top nodes in Y direction by MD 25 element model.

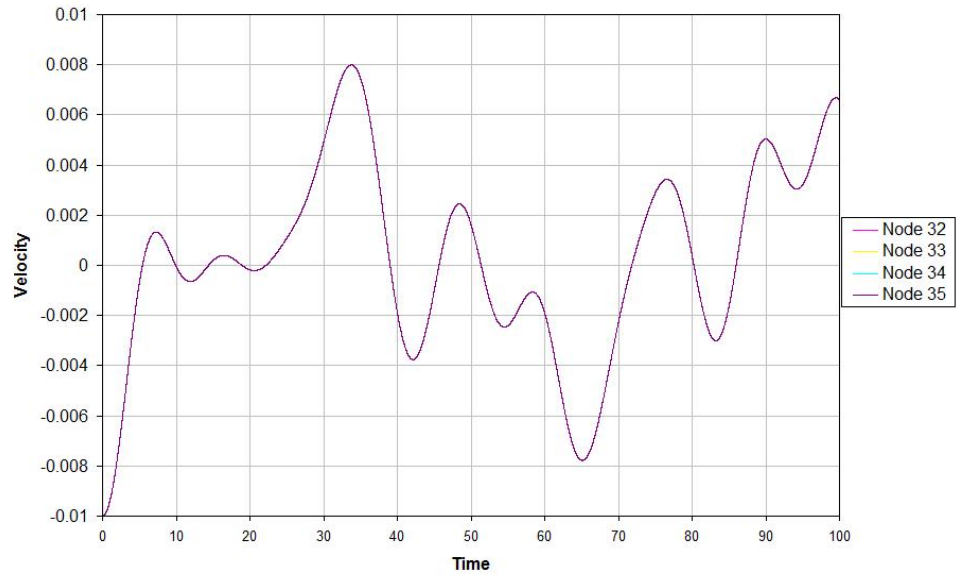


Figure 5.26 Time history of velocity of top nodes in Y direction by MD  
25-element model

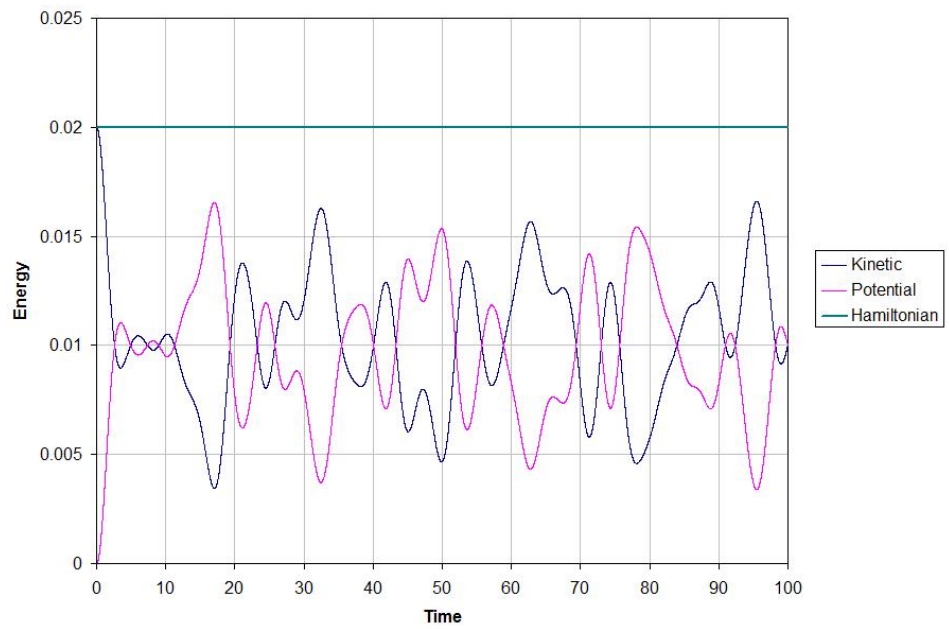


Figure 5.27 Time history of system Hamiltonian by MD – 25 element model

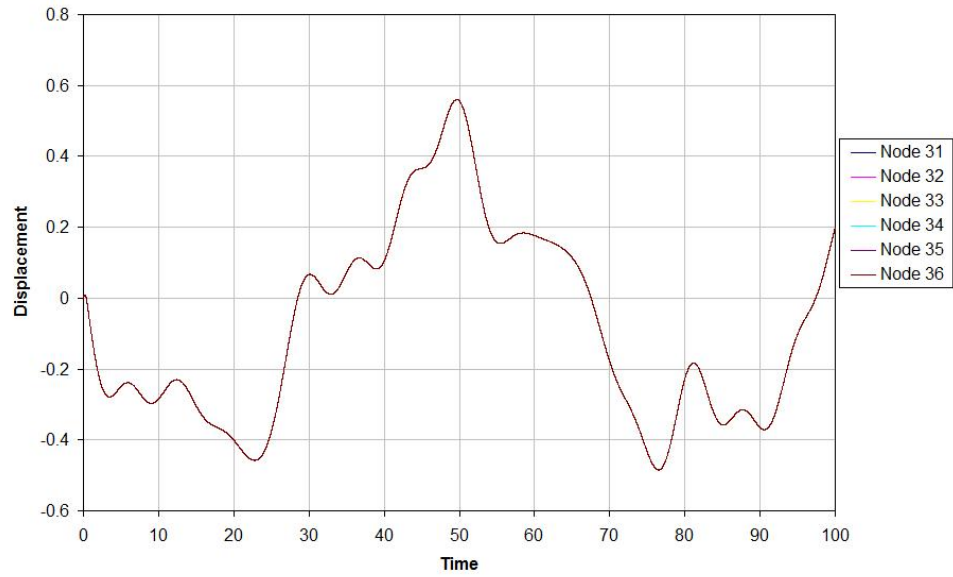


Figure 5.28 Time history of displacement of top nodes in Y direction by MD/NPFEM  
25 element model

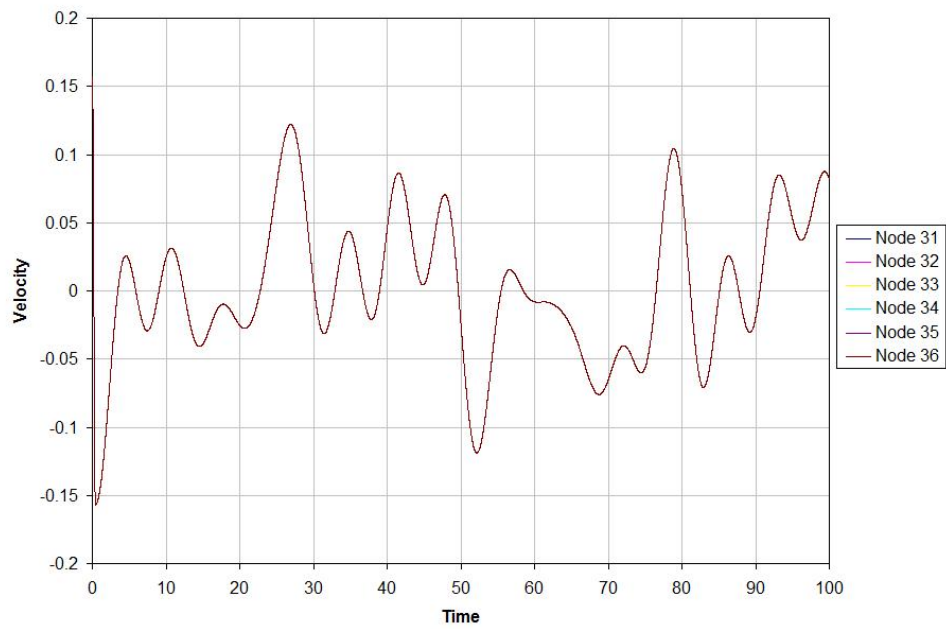


Figure 5.29 Time history of velocity of top nodes in Y direction by MD/NPFEM  
25 element model

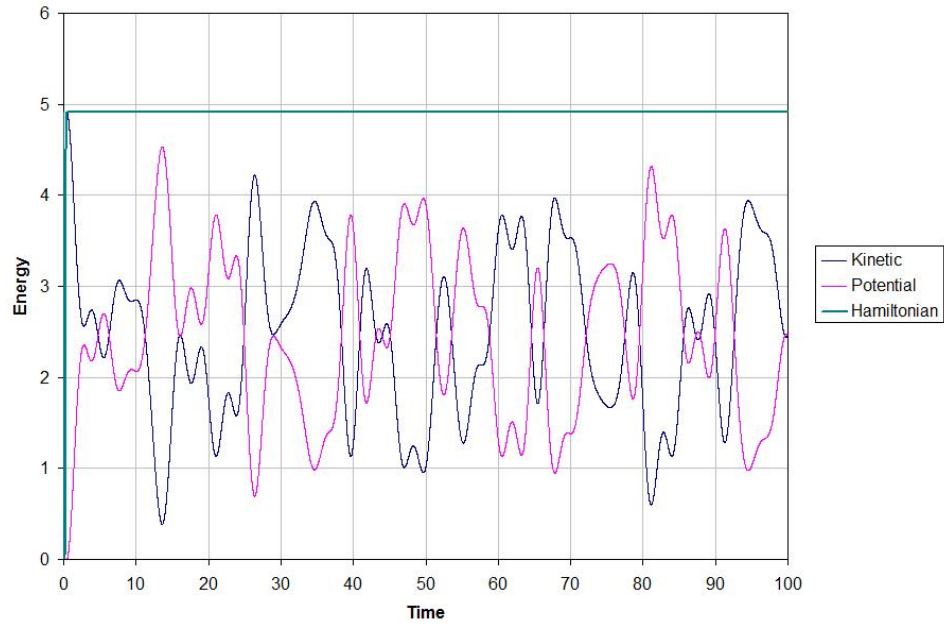


Figure 5.30 Time history of system Hamiltonian by MD/NPFEM – 25 element model

In this section, a body of 5 by 5 element model is studied when a velocity pulse is applied downward on all of the top nodes simultaneously. The results shown in Figure 5.22- 5.30 modeled with MD and NPFEM separately as well as MD/NPFEM coupled to observe dynamic characteristics such as displacement and velocity as well as total energy of the system. Figures 5.22 -5.24 illustrate the time history of displacement and velocity of the top nodes and the total Hamiltonian of the system respectively based on NPFEM formulation. Figures 5.25-5.27 illustrate the time history of displacement and velocity of the top nodes and the total Hamiltonian of the system respectively this time based on MD for the same 5 by 5 lattice. Moreover, Figures 5.28-5.30 illustrate the time history of displacement and velocity of the top nodes and the total Hamiltonian of the system using multiscale modeling of coupled NPFEM/MD using bridging scale method for comparison.

The results show that the total energy of the system is conserved. Following these results another simulation conducted for validation in such a way that a sinusoidal wave applied on the top nodes. Then the behaviour of all the nodes was observed from top to the bottom of the body in different layers. The purpose of this simulation is to ensure that the sinusoidal pulse can pass through all the layers especially the handshaking area. Therefore, the wave pass through two layers of continuum model, NPFEM, the handshaking/transition zone, MD/NPFEM and two layers of atomic model, MD, and reaches to the bottom of the lattice without losing energy. Figures 5.31 – 5.35 show the dynamic characteristics while the wave applies on top nodes and propagate in the body. A sinusoidal wave applied on the top nodes simultaneously and the reaction of the nodes in different layers was studied when the wave pass through all the layers and reach to the bottom of the lattice. Figure 5.31 shows the time history of displacement of the nodes/atoms on different layers in the middle of the body. In order to make the results more clearly, Figure 5.32 and 5.33 show the time history of displacement and velocity of the top nodes in the beginning of the motion. Figure 5.34 shows the total energy of the system is conserved. Finally, the last Figure, Figure 5.35, shows how the sinusoidal signal applied on the top nodes pass through the different layers and reaches to the bottom of the lattice. Therefore, two very important results are achieved; firstly, the information can pass through different domains smoothly specially through handshaking zone. Secondly, the total energy remains conserved.



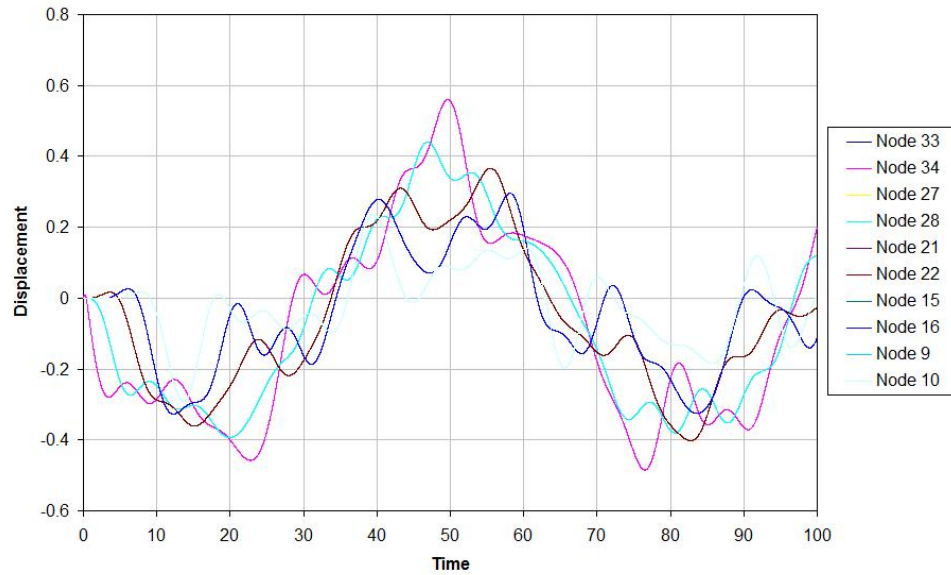


Figure 5.31 Time history of displacement indifferent layers in Y direction by MD/NPFEM 25 element model

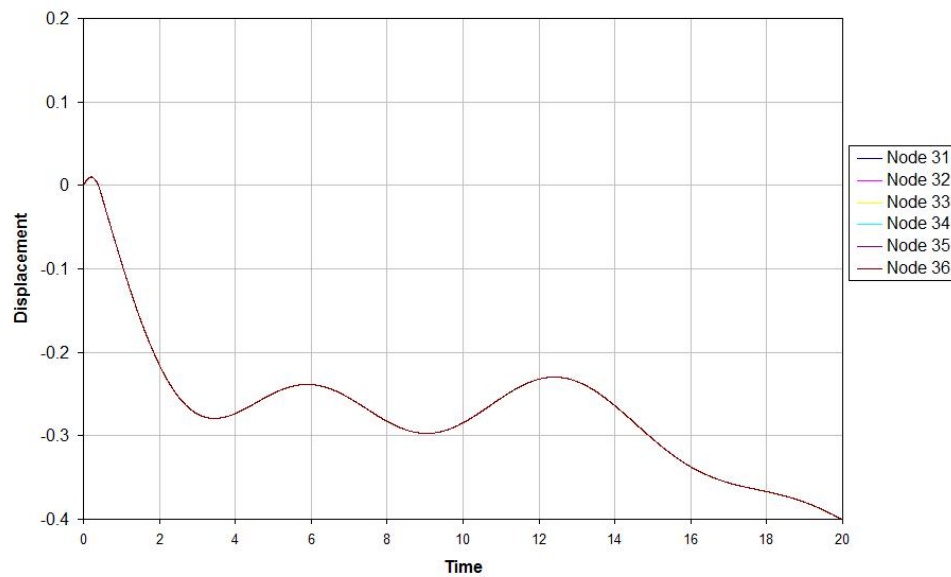


Figure 5.32 Magnified time history of displacement of top nodes in Y direction by MD/NPFEM 25 element model.

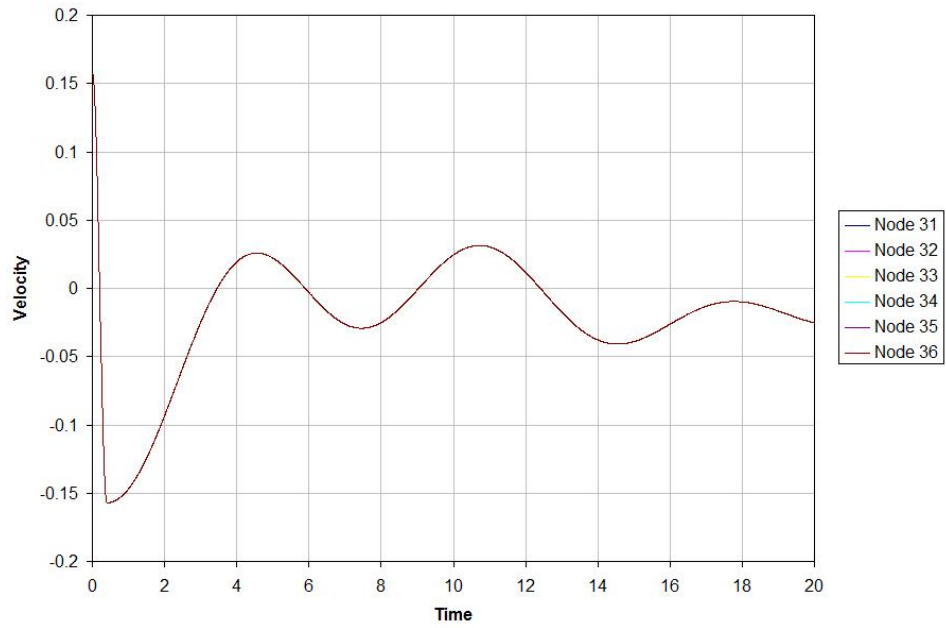


Figure 5.33 Magnified time history of velocity of top nodes in Y direction by MD/NPFEM 25 element model.

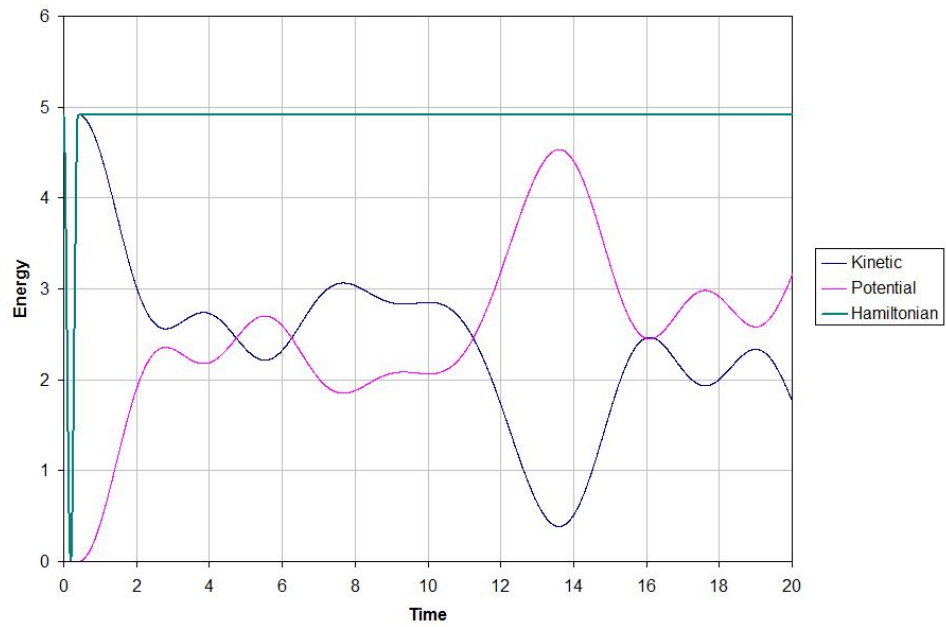


Figure 5.34 Magnified time history of system Hamiltonian by MD/NPFEM 25 element model

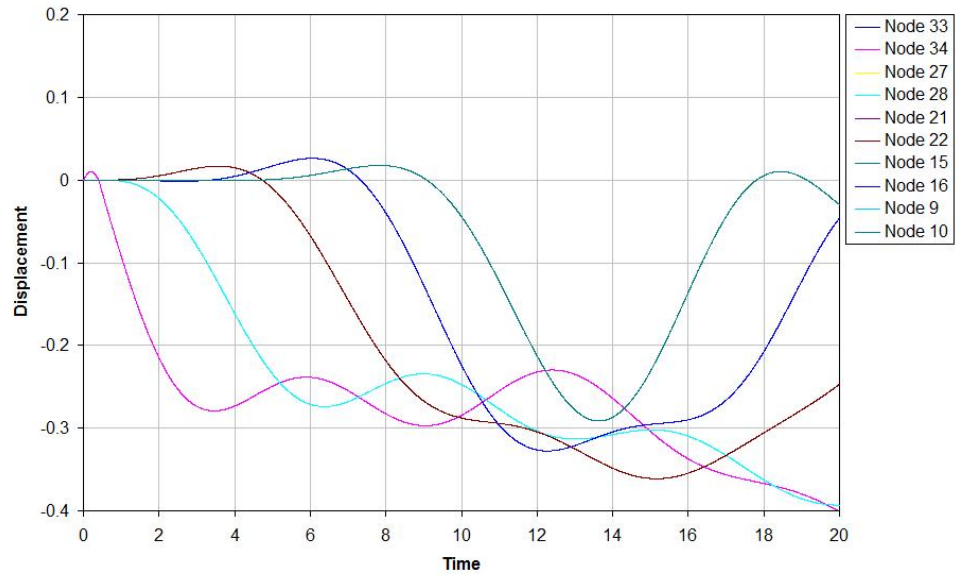


Figure 5.35 Magnified time history of displacement in different layers in Y direction by MD/NPFEM 25 element model

# Chapter 6 CONCLUSIONS AND FUTURE WORK

## 6.1 General Conclusions

In this work, we developed a multiscale modelling method to couple the molecules dynamics and continuum mechanics using bridging scale method by energy conservation. A new NPFEM has been developed and coupled with the MD for multiscale modeling. In the molecular dynamic simulation, the formulation and derivation of the mass matrix as well as interatomic force is determined based on Lennard-Jones pair potential. These two models overlap in the handshaking area and transfer information such as displacement, velocity, acceleration, force, kinetic and potential energy. In this new model, a coefficient is chosen to determine the contribution of each model in the handshaking area, which should be consistent with the structure of the region such as number of layers, nodes, and the type of mesh.

## 6.2 Thesis Accomplishments

The new model successfully passed all the information from one domain to the other without energy drift such that the sinusoidal signal, which applies on the top nodes of the structure, transferred from all the layers and reached to the bottom of the structure while the total energy of the system was constant during this process. Moreover, the newly developed method addressed the limitation of the existing models like the ghost force and the wave reflection because the formulation from the beginning starts from calculating the total Hamiltonian of the system. As we already mentioned in chapter 3, the description of

the Hamiltonian of traditional FEM is based on the nodal displacement field, while the MD describes the position of atoms/molecules using their position vectors. To overcome this inconsistency and unify the description, a new 2D Nodal Position Finite Element Method (NPFEM) is proposed here (21). Therefore, in this study two very important goals were achieved. First, from the continuum point of view, a new position based model and so called nodal position finite element method was developed to replace the conventional finite element method. The advantage of this method is that it can be coupled with the molecular dynamic more easily and efficiently. Second, from the multiscale modeling point of view, a new methodology was developed based on the conservation of energy for both regions. Therefore, the formulation starts from writing the Hamiltonian of the system, kinetic and potential energy of the two separate models in two different length scales. These two models coupled in the handshaking area and transfer information in a smooth and seamless way. In the whole process the Hamiltonian of the system was checked and showed that the total energy of the system (the sum of the kinetic energy and the potential energy) is constant. In the following subsections, we review the results achieved in the model separately and in details.

### **6.2.1 Development of Nodal Position Finite Element Method**

The dissertation developed a novel Nodal Position Finite Element Method (NPFEM) to address the limitations of conventional finite methods in the simulation of the large rigid body motion coupled with small elastic deformation. Existing approaches in this field are dominated by the finite difference method instead of the most popular and efficient engineering analysis method – the finite element method. The work demonstrated that the

simulation could be done accurately and more efficiently by the newly developed NPFEM. Since, the method is position based rather than displacement based, this is the suitable to be coupled with molecular dynamic simulation, which are also positions based.

### **6.2.2 Implementation and Validation of NPFEM**

The NPFEM have been implemented into a FORTRAN program. The numerical integration is Newmark method. Validation started from one quad-lateral element, which goes under two downwards vertical loads on the top nodes, and it is fixed on the bottom nodes. The behaviour of the model studied in terms of displacements, velocities, accelerations and total energy of the system or Hamiltonian. We observed that the Hamiltonian of the system is constant in time or the total energy of the system is conserved. Moreover, the results match with rough analytical estimation for this simple model. The model gets more complicated first with 3 and then with 25 elements and for all the cases the energy is conserved and the values are predictable and matches with the commercial software simulation based on conventional finite element method.

### **6.2.3 Molecular Dynamic Simulation in Atomic Domain**

In order to model the atomic domain, molecular dynamic is chosen. In MD modeling two critical decision should be made one is choosing the interatomic potential and the other one is the numerical integration. Lennard-Jones is chosen as interatomic potential and the Newmark method is chosen as numerical integration method. The same integration scheme has been chosen for both continuum and atomic simulations since for coupling two domains the main routine uses for both scales.

#### **6.2.4 Implementation and Validation of Molecular Dynamic**

Molecular Dynamic is implemented in FORTRAN code as well. For simulating the atomic domain with molecular dynamic, the same one element as continuum was the starting point. However, in this method we are dealing with pair atom instead of elements. Therefore, the first sample consists of four pair atom with the same element structure goes under the same vertical loads. The results show that energy is conserved and the values match with the NPFEM results. The same code was run for 3 and 25 elements and the good results achieved.

#### **6.2.5 Development of Multiscale Method Coupling NPFEM and MD**

The purpose of this study is to develop a method as well as program to simulate and study characteristics and properties of new materials with application in space and other disciplines of science and engineering. From the atomic domain, some of the atoms are chosen as representative atoms. These are the same atoms overlap with the continuum finite element nodes. In this simulation, atomic region modeled by MD is at the bottom and continuum domain modeled by NPFEM is on the top these two regions overlap in the middle of the lattice called handshaking area. The most difficult part of this research is transferring information like mechanical properties from one domain to the other smoothly such that the energy remains constant. All the formulation of this approach is based on determination of the total energy of the system or Hamiltonian.

## 6.2.6 Implementation and Validation of Multiscale Method

Both MD and NPFEM are brought in the same program. The challenging part of the problem is writing the mass matrix and the stiffness matrix in the handshaking area. The first step was considering one element and treating it like a coupled area. Therefore, the mass and stiffness matrices are written with half MD and half NPFEM force calculation and reliable results achieved. The results were totally agreed with the pure MD and pure NPFEM region and the energy was conserved. The example is the three-element structure such that it is fixed vertically at the bottom and free to move horizontally. The bottom element is modeled by MD, the top element is modeled by NPFEM and in the middle, and both methods have been coupled. As always, it goes under two vertical downward loads on the top. As we can see in this model, we have all three regions in the same structure and each region has its own simulation strategy or in other words, we have three sets of stiffness and mass matrices for this model. These three regions transfer information from one region to the next smoothly and the total energy of the system remains conserved. The last part of validation is considering a lattice of 5 by 5 elements, fixed at the bottom vertically and free to move horizontally. The first two rows from the top are modeled by NPFEM, the first two rows from the bottom are modeled by MD and one row in the middle is handshaking area and modeled by combination of both NPFEM and MD. Writing the stiffness and mass matrices for each node or atom considering all the forces with the proper weight function when two models interact is the challenging part of the implementation. The promising results achieved for this more complicated lattice as well. This model was tested in three different ways; first, loads applied on the top nodes and the behaviour of all the nodes and atoms were studied. Second, no loads applied to the lattice and only an initial displacement



applied to the first rows and the reaction of the all nodes and atoms were studied. Third, a sinusoidal wave applied to the top nodes and the propagation of the sin wave were studied through out the layers to make sure the wave pass through all the layers and reaches from the top to the bottom of the lattice. In all three cases reasonable results were achieved in addition, the energy was conserved.

### **6.3 Contributions of Thesis Work**

This dissertation proposed a novel nodal position finite element method to address the limitations of conventional finite element method. This research followed two goals; proposing an effective way first to solve the dynamic analysis of large rigid body motions when coupled with small elastic deformations and second to be coupled with another position based model like MD. The limitations of existing finite element methods in dealing with the large scale rigid body motions coupled with small elastic deformations is one of the motivation of the new formulation. On the other hand, since some of the simulation methods for atomic regions such as molecular dynamic formulation are based on position vectors rather than displacements. The existing finite element approach is prone to accumulated errors due to (a) in each time step the approximation of linearization (b) the numerical round off over the long time. This approximation and round off may result in the solution being out of balance in the end. However, by proposing the NPFEM we overcame this difficulty by deriving a position vector finite element method, in which the nodal displacements were replaced by the nodal position as basic variables this ensured that at each time step the total balance was enforced. Since the nodal position finite element method was solved for the nodal positions of each element, it can eliminate the limitation

of small rotation and it can be coupled with the molecular dynamic easily. Molecular dynamic also was modeled for the atomic region such that Lennard-Jones interatomic potential was used as well as Newmark numerical integration. The formulation of the newly proposed multi-scale modeling is such a way that it addresses the limitations of existing multiscale methods like ghost force and the wave reflection. The formulation is based on determination of the total Hamiltonian of the system. Therefore, it automatically solves the problem of the above-mentioned limitations.

## **6.4 Future Work**

From the course of thesis studies, the following areas are considered worthy of further studies:

- Developing Nonlinear Nodal Position Finite Element Method,
- Developing Molecular Dynamic with more complicated interatomic potential,
- Simulating more complicated lattice with wider handshaking area and proper weight function, and
- Choosing a material such as crosslinked silica aerogels and simulate the actual material with this model.

## Bibliography

1. *Bridging scale methods for nanomechanics and materials*. Liu, WK, et al. 13-16 , s.l. : COMPUTER METHODS IN APPLIED MECHANICS AND ENGINEERING, 2006, Vol. 195. 1.
2. *Aerogel-based thermal insulation*. D.M. Smith, A. Maskara, U. Boes. 1998, *Non-Cryst Solids*, Vol. 225, pp. 254–259.
3. *Simulating materials failure by using up to one billion atoms and the world's fastest computer: Brittle fracture*. Abraham, FF, et al. 9, s.l. : PROCEEDINGS OF THE NATIONAL ACADEMY OF SCIENCES OF THE UNITED STATES OF AMERICA, APR 30, 2002, Vol. 99, pp. 5777-5782 .
4. *A new finite-element formulation for computational fluid dynamic*.6. *Convergence analysis of the generalized SUPG formulation for linear time-dependent multi dimensional*. Hughes, TJR, Franca, LP and Mallet, M. 1, JUL 1987, COMPUTER METHODS IN APPLIED MECHANICS AND ENGINEERING, Vol. 63 , pp. 97-112 .
5. Zienkiewicz, OC and Taylor, RL.*The finite element method: Solid mechanics*. New York : McGraw Hill, 1989/1991. Vols. 1-2.
6. *A unified stability analysis of meshless particle methods*. Belytschko, T, et al. 9, JUL 30, 2000, INTERNATIONAL JOURNAL FOR NUMERICAL METHODS IN ENGINEERING, Vol. 48, pp. 1359-1400.
7. *Crack-propagation in BCC crystal studied with a combined finite element and atomistic model*. Kohlhoff, S, Gumbsch, P and Fischmeister, HF. 4, OCT 1991 ,

PHILOSOPHICAL MAGAZINE A-PHYSICS OF CONDENSED MATTER  
STRUCTURE DEFECTS AND MECHANICAL PROPERTIES, Vol. 64, pp. 851-  
878.

8. *Transformation in Regression - A robust analysis*. Carroll, RJ and Ruppert, D. 1, 1985, TECHNOMETRICS, Vol. 27, pp. 1-12.
9. *Computational nanomechanics of materials*. Liu, Wing Kam, Jun, Sukky and Qian, Dong. 5, MAY 2008, JOURNAL OF COMPUTATIONAL AND THEORETICAL NANOSCIENCE, Vol. 5, pp. 970-996 .
10. *Cellular-regulation of the iron-responsive element binding-protein - disassembly of the Cubane Iron-Sulfur cluster results in high-affinity RNA-binding*. Haile, DJ, et al. 24, DEC 15, 1992, PROCEEDINGS OF THE NATIONAL ACADEMY OF SCIENCES OF THE UNITED STATES OF AMERICA, Vol. 89, pp. 11735-11739.
11. *Observation of dynamic precursors of the isotropic-nematic transition by computer-simulation*. Allen, MP and Frenkel, D. 17, APR 27, 1987, PHYSICAL REVIEW LETTERS , Vol. 58, pp. 1748-1750.
12. *Constant-pressure equations of motion*. Hoover, WG. 3, SEP 1986, PHYSICAL REVIEW , Vol. 34, pp. 2499-2500.
13. *A synthetic peptide corresponding to a conserved heptad repeat domain is a potent inhibitor of sendai virus-cell fusion - an emerging similarity with functional domains of other viruses*. Rapaport, D, Ovadia, M and Shai, Y. 22, NOV 15, 1995, EMBO JOURNAL, Vol. 14, pp. 5524-5531.
14. *Introduction to Molecular Dynamics Simulation*. Allen, M.P. 2004, Computational Soft

- Matter: From Synthetic Polymers to Proteins, Vol. 23, pp. 1-28.
15. *Modelling the nano-scale phenomena in condensed matter physics via computer-based numerical simulations.* Rafii-Tabar, H. 6, MAR 2000, PHYSICS REPORTS-REVIEW SECTION OF PHYSICS LETTERS, Vol. 325, pp. 240-310.
  16. *On the determination of molecular fields - II From the equation of state of a gas.* Jones, JE. 738, OCT 1924, PROCEEDINGS OF THE ROYAL SOCIETY OF LONDON SERIES A-CONTAINING PAPERS OF A MATHEMATICAL AND PHYSICAL CHARACTER , Vol. 106.
  17. *Computer experiments on classical fluids .I. thermodynamical properties of Lennard-jones molecules.* Verlet, L. 1, 1967, PHYSICAL REVIEW , Vol. 159, pp. 98-+.
  18. *The potential calculation and some applications.* W., Hockney. R. 1970, METHODS IN COMPUTATIONAL PHYSICS, Vol. 9, pp. 135-211 .
  19. Allen M.P, Tildesley D.J. *Computer simulation of liquids.* s.l. : Clarendon Press, 1987. p. 385.
  20. *A Method of Computation for Structural Dynamics.* Newmark, N. M. EM3, 1959, ASCE JOURNAL OF THE ENGINEERING MECHANICS DIVISION, Vol. 85.
  21. *Nodal position finite element method for plane elastic problems.* Zhu Z.H., Pour B.H. 2, 2011, FINITE ELEMENTS IN ANALYSIS AND DESIGN, Vol. 47, pp. 73-77.
  22. *A bridging domain method for coupling continua with molecular dynamics.* Xiao, SP and Belytschko, T. 17-20, 2004, COMPUTER METHODS IN APPLIED MECHANICS AND ENGINEERING , Vol. 193, pp. 1645-1669.
  23. *Fast directional multilevel algorithms for oscillatory kernels.* Engquist, Bjoern and Ying, Lexing. 4, 2007, SIAM JOURNAL ON SCIENTIFIC COMPUTING, Vol.

- 29, pp. 1710-1737.
24. *Quasicontinuum analysis of defects in solids*. Tadmor, EB, Ortiz, M and Phillips, R. 6, JUN 1996, PHILOSOPHICAL MAGAZINE A-PHYSICS OF CONDENSED MATTER STRUCTURE DEFECTS AND MECHANICAL PROPERTIES, Vol. 73, pp. 1529-1563.
25. *Nanoindentation and incipient plasticity*. Tadmor, EB, Miller, R and Phillips, R. 6, JUN 1999, JOURNAL OF MATERIALS RESEARCH, Vol. 14, pp. 2233-2250 .
26. *Quasicontinuum models of fracture and plasticity*. Miller, R, et al. 6, JUN 1999, JOURNAL OF MATERIALS RESEARCH , Vol. 14, pp. 2233-2250.
27. *The quasicontinuum method: Overview, applications and current directions*. Miller, RE and Tadmor, EB,. 3, 2002, JOURNAL OF COMPUTER-AIDED MATERIALS DESIGN, Vol. 9, pp. 203-239.
28. *Finite-temperature quasicontinuum: Molecular dynamics without all the atoms*. Dupuy, LM, et al. 6, AUG 5, 2005, PHYSICAL REVIEW LETTERS, Vol. 95.
29. *An analysis of the quasicontinuum method*. Knap, J and Ortiz, M. 9, SEP 2001, JOURNAL OF THE MECHANICS AND PHYSICS OF SOLIDS , Vol. 49, pp. 1899-1923 .
30. *Uniform accuracy of the quasicontinuum method*. Weinan, E., Lu, Jianfeng and Yang, Jerry Z. 21, DEC 2006, PHYSICAL REVIEW, Vol. 74.
31. *Conservation properties of the bridging domain method for coupled molecular/continuum dynamics*. Xu, Mei and Belytschko, Ted,. 3, OCT 15, 2008, INTERNATIONAL JOURNAL FOR NUMERICAL METHODS IN ENGINEERING, Vol. 76, pp. 278-294 .

32. *Time history kernel functions for square lattice*. Pang, G. Tang, S. June 28, 2011, Springer-Verlag 2011.
33. *Chemistry of aerogels and their applications*. Pierre, AC and Pajonk, GM. 11, NOV 2002, CHEMICAL REVIEWS, Vol. 102, pp. 4243-4265.
34. *Concurrent coupling of length scales in solid state systems*. Rudd, RE and Broughton, JQ. 1, JAN 2000, PHYSICA STATUS SOLIDI B-BASIC RESEARCH, Vol. 217, pp. 251-291.
35. *Direct Coupling of Atomistic and Continuum Mechanics in Computational Materials Science*. Miller, Ronald E. 1, 2003, INTERNATIONAL JOURNAL FOR MULTISCALE COMPUTATIONAL ENGINEERING , Vol. 1, pp. 57-72.
36. *Atomistic/continuum coupling in computational materials science*. Curtin, WA and Miller, RE. 3, MAY 2003, MODELLING AND SIMULATION IN MATERIALS SCIENCE AND ENGINEERING , Vol. 11, pp. R33-R68.
37. *On a formulation for a multiscale atomistic-continuum homogenization method*. Chung, PW and Narnburu, RR. 10, MAY 2003, INTERNATIONAL JOURNAL OF SOLIDS AND STRUCTURES, Vol. 40, pp. 2563-2588 .
38. *Multiscale modelling of nano- and micro-mechanics of materials – Preface*. Ghoniem, NM, Busso, EP and Huang, HC,. 31-34, NOV-DEC 2003, PHILOSOPHICAL MAGAZINE , Vol. 83, pp. 3473-3473.
39. *The mechanics of machining at the microscale: Assessment of the current state of the science*. Liu, X, DeVor, RE and Kapoor, SG. 4, NOV 2004, JOURNAL OF MANUFACTURING SCIENCE AND ENGINEERING-TRANSACTIONS OF THE ASME, Vol. 126, pp. 666-678.

40. *Multiscale modelling of nanostructures.* Vvedensky, DD,. 50, DEC 22, 2004, JOURNAL OF PHYSICS-CONDENSED MATTER , Vol. 16, pp. R1537-R1576 .
41. *Hybrid continuum mechanics and atomistic methods for simulating materials deformation and failure.* Miller, Ronald E. and Tadmor, Ellad B. 11, NOV 2007, MRS BULLETIN , Vol. 32, pp. 920-926 .
42. *Coupling atomistics and continuum in solids: status,prospects, and challenges.* Wernik, J. M. and Meguid, S. A. 1, 2009, INTERNATIONAL JOURNAL OF MECHANICS AND MATERIALS IN DESIGN, Vol. 5, pp. 79-110.
43. *Multiscale methods for micro/nano flows and materials.* Kalweit, Marco and Drikakis, Dimitris. 9, SEP 2008, JOURNAL OF COMPUTATIONAL AND THEORETICAL NANOSCIENCE, Vol. 5.
44. *Hybrid atomistic simulation methods for materials systems.* Bernstein, N., Kermode, J. R. and Csanyi, G. 2, FEB 2009, REPORTS ON PROGRESS IN PHYSICS , Vol. 72.
45. *Multiscale methods for mechanical science of complex materials: Bridging from quantum to stochastic multiresolution continuum.* Liu, Wing Kam, et al. 8-9, AUG 20, 2010, INTERNATIONAL JOURNAL FOR NUMERICAL METHODS IN ENGINEERING , Vol. 83, pp. 1039-1080 .
46. *On the continuum versus atomistic descriptions of dislocation nucleation and cleavage in nickel.* Gumbsch, P and Beltz, GE. 5, SEP 1995, MODELLING AND SIMULATION IN MATERIALS SCIENCE AND ENGINEERING , Vol. 3, pp. 597-613 .
47. *Atomistic Simulation Methods and their Application on Fracture.* Eidel, Bernhard,



- Hartmaier, Alexander and Gumbsch, Peter. CISM Courses and Lectures, 2010, MULTISCALE MODELLING OF PLASTICITY AND FRACTURE BY MEANS OF DISLOCATION MECHANICS, Vol. 522, pp. 1-57.
48. *Dislocation - A new concept in continuum theory of plasticity*. Kroner, E. 1, 1963, JOURNAL OF MATHEMATICS AND PHYSICS , Vol. 42, pp. 27-+.
49. *FLIP - A method for adaptively zoned, particle-in-cell calculations of fluid-flows in 2 dimensions*. Brackbill, JU and Ruppel, HM,. 2, AUG 1986, JOURNAL OF COMPUTATIONAL PHYSICS , Vol. 65, pp. 314-343 .
50. *FLIP - A low-dissipation, particle-in-cell method for fluid-flow*. Brackbill, JU, Kothe, DB and Ruppel, HM,. 1, JAN 1988, COMPUTER PHYSICS COMMUNICATIONS , Vol. 48, pp. 25-38.
51. *Application of a particle-in-cell method to solid mechanics*. Sulsky, D, Zhou, SJ and Schreyer, HL,. 1-2, MAY 1995 , COMPUTER PHYSICS COMMUNICATIONS , Vol. 82, pp. 236-252.
52. *A particle method for history-dependent materials*. Sulsky, D, Chen, Z and Schreyer, HL,. 1-2, SEP 1994, COMPUTER METHODS IN APPLIED MECHANICS AND ENGINEERING , Vol. 118, pp. 179-196.
53. *The material point method for simulation of thin membranes*. York, AR, Sulsky, D and Schreyer, HL. 10, APR 10, 1999, INTERNATIONAL JOURNAL FOR NUMERICAL METHODS IN ENGINEERING , Vol. 44, pp. 1429-1456.
54. *Fluid-membrane interaction based on the material point method*. York, AR, Sulsky, D and Schreyer, HL,. 6, JUN 30, 2000, INTERNATIONAL JOURNAL FOR NUMERICAL METHODS IN ENGINEERING , Vol. 48, pp. 901-924 .

55. *MPM simulation of dynamic material failure with a decohesion constitutive model.* Sulsky, D and Schreyer, L. 3, MAY-JUN 2004, EUROPEAN JOURNAL OF MECHANICS A-SOLIDS, Vol. 23, pp. 423-445.
56. *Solving quasi-static equations with the material-point method.* Sanchez, J., et al. 1, JUL 2015, INTERNATIONAL JOURNAL FOR NUMERICAL METHODS IN ENGINEERING , Vol. 103, pp. 60-78 .
57. *MPM/MD handshaking method for multiscale simulation and its application to high energy cluster impacts.* Guo, Z and Yang, W. 2, FEB 2006, INTERNATIONAL JOURNAL OF MECHANICAL SCIENCES, Vol. 48, pp. 145-159.
58. *Multiscale simulation from atomistic to continuum-coupling molecular dynamics (MD) with the material point method (MPM).* Lu, H., et al. 20, JUL 11, 2006, PHILOSOPHICAL MAGAZINE, Vol. 68, pp. 2971-2994.
59. *A seamless coupling between molecular dynamics and material point method.* Chen, Huawei, Hagiwara, Ichiro and Tieu, A. K. 1, 2011, JAPAN JOURNAL OF INDUSTRIAL AND APPLIED MATHEMATICS, Vol. 28, pp. 55-67.
60. *A multiscale framework for high-velocity impact process with combined material point method and molecular dynamics.* Liu, Yan, Wang, Han-Kui and Zhang, Xiong. 2, JUN 2013, INTERNATIONAL JOURNAL OF MECHANICS AND MATERIALS IN DESIGN, Vol. 9, pp. 127-139.
61. *Hierarchical, adaptive, material point method for dynamic energy release rate calculations.* Tan, HL and Nairn, JA. 19-20, 2002, COMPUTER METHODS IN APPLIED MECHANICS AND ENGINEERING, Vol. 191, pp. 2095-2109.
62. *Coarse-grained molecular dynamics and the atomic limit of finite elements.* Rudd, RE

- and Broughton, JQ. 10, SEP 1, 1998, PHYSICAL REVIEW B, Vol. 58, pp. R5893-R5896.
63. *Coarse-grained molecular dynamics for design of nanomechanical systems.* Rudd, RE. 2003, NANOTECH 2003, Vol. 2, pp. 524-527.
64. *A general-purpose coarse-grained molecular dynamics program.* Aoyagi, T, et al. 2, MAY 15, 2002, COMPUTER PHYSICS COMMUNICATIONS, Vol. 145, pp. 267-279.
65. *Multiscale coarse graining of liquid-state systems.* Izvekov, S and Voth, GA. 13, OCT 1, 2005, JOURNAL OF CHEMICAL PHYSICS, Vol. 123.
66. *Systematic coarse-graining of nanoparticle interactions in molecular dynamics simulation.* Izvekov, S, Violi, A and Voth, GA. 36, SEP 15, 2005, JOURNAL OF PHYSICAL CHEMISTRY B, Vol. 109, pp. 17019-17024.
67. *Mixed atomistic and coarse-grained molecular dynamics: Simulation of a membrane-bound ion channel.* Shi, Qiang, Izvekov, Sergei and Voth, Gregory A. 31, AUG 10, 2006, JOURNAL OF PHYSICAL CHEMISTRY B, Vol. 110, pp. 15045-15048.
68. *Energy conservation in adaptive hybrid atomistic/coarse-grain molecular dynamics .* Ensing, Bernd, et al. 3, MAY-JUN 2007, JOURNAL OF CHEMICAL THEORY AND COMPUTATION, Vol. 3, pp. 1100-1105.
69. *Understanding ionic liquids through atomistic and coarse-grained molecular dynamics simulations.* Wang, Yanting, et al. 11, NOV 2007, ACCOUNTS OF CHEMICAL RESEARCH, Vol. 40, pp. 1193-1199.
70. *Molecular Dynamics Simulations of Polyglutamine Aggregation Using Solvent-Free Multiscale Coarse-Grained Models.* Wang, Yanting and Voth, Gregory A. 26, JUL

- 10, 2010, JOURNAL OF PHYSICAL CHEMISTRY B, Vol. 114, pp. 8735-8743.
71. *Multiscale molecular dynamics simulations of micelles: coarse-grain for self-assembly and atomic resolution for finer details.* Brocos, Pilar, et al. 34, 2012, SOFT MATTER, Vol. 8, pp. 9005-9014.
72. *Multiscale molecular dynamics simulations of sodium dodecyl sulfate micelles: from coarse-grained to all-atom resolution.* Roussel, Guillaume, Michaux, Catherine and Perpete, Eric A. 10, OCT 2010, JOURNAL OF MOLECULAR MODELING, Vol. 20, p. 2469.
73. *Multiscale plasticity modeling: coupled atomistics and discrete dislocation mechanics.* Shilkrot, LE, Miller, RE and Curtin, WA. 4, APR 2004, JOURNAL OF THE MECHANICS AND PHYSICS OF SOLIDS, Vol. 52, pp. 755-787.
74. *Analysis of nanoindentation experiments by means of atomic force.* W. H. Müller, H. Worrack, M. Zapara. 1, Dec 9, 2011, PAMM, Pro. App. Math. Mech, Vol. 11, pp. 413 – 414.
75. *EMBEDDED-ATOM METHOD - DERIVATION AND APPLICATION TO IMPURITIES, SURFACES, AND OTHER DEFECTS IN METALS.* DAW, MS and BASKES, MI. 12, 1984, PHYSICAL REVIEW B, Vol. 29, pp. 6443-6453.
76. *DISCRETE DISLOCATION PLASTICITY - A SIMPLE PLANAR MODEL.* VANDERGIESSEN, E and NEEDLEMAN, A. 5, SEP 1995, MODELLING AND SIMULATION IN MATERIALS SCIENCE AND ENGINEERING, Vol. 3, pp. 689-735.
77. *Coupled atomistic/discrete dislocation simulations of nanoindentation at finite temperature.* Shiari, B, Miller, RE and Curtin, WA. 4, OCT 2005, JOURNAL OF

ENGINEERING MATERIALS AND TECHNOLOGY-TRANSACTIONS OF  
THE ASME, Vol. 127, pp. 358-368.

78. *Analysis and minimization of dislocation interactions with atomistic/continuum interfaces.* Dewald, M. and Curtin, W. A. 3, APR 2006, MODELLING AND SIMULATION IN MATERIALS SCIENCE AND ENGINEERING, Vol. 14, pp. 497-514.
79. *Parallel algorithm for multiscale atomistic/continuum simulations using LAMMPS.* Pavia, F. and Curtin, W. A. 5, JUL 2015, MODELLING AND SIMULATION IN MATERIALS SCIENCE AND ENGINEERING, Vol. 23, p. 055002.
80. *The atomic-scale finite element method.* Liu, B, et al. 17-20, 2004, COMPUTER METHODS IN APPLIED MECHANICS AND ENGINEERING, Vol. 193, pp. 1849-1864.
81. *An Introduction to the Conjugate Gradient Method.* Shewchuk, Jonathan Richard. AUG 4, 1994, Carnegie Mellon University, pp. 1-64.
82. *Atomic-scale finite element method in multiscale computation with applications to carbon nanotubes.* Liu, B, et al. 3, JUL 2005, PHYSICAL REVIEW B, Vol. 72.
83. *Postbuckling of carbon nanotubes by atomic-scale finite element.* Leung, AYT, et al. 12, JUN 15, 2006, JOURNAL OF APPLIED PHYSICS, Vol. 99.
84. *Critical strain of carbon nanotubes: An atomic-scale finite element study.* Guo, X., et al. 2, MAR 2007, JOURNAL OF APPLIED MECHANICS-TRANSACTIONS OF THE ASME, Vol. 74, pp. 347-351.
85. *Computational modeling of the interaction of two edge cracks, and two edge cracks interacting with a nanovoid, via an atomistic finite element method.* Adelzadeh, M.,

- Shodja, H. M. and Raffi-Tabar, H. 2, APR 2008, COMPUTATIONAL MATERIALS SCIENCE, Vol. 42, pp. 186-193.
86. *An Atomic-scale Finite Element Method for Single-Walled Carbon Nanotubes*. Cecchi, M. Morandi, Rispoli, V. and Venturin, M. 2009, APPLIED AND INDUSTRIAL MATHEMATICS IN ITALY III, Vol. 82, pp. 449-460.
87. *An electromechanical atomic-scale finite element method for simulating evolutions of ferroelectric nanodomains*. Zhang, Yihui, et al. 8, AUG 2012, JOURNAL OF THE MECHANICS AND PHYSICS OF SOLIDS, Vol. 60, pp. 1383-1399.
88. *Quasicontinuum analysis of defects in solids*. Tadmor, EB, Ortiz, M and Phillips, R. 6, JUN 1996, PHILOSOPHICAL MAGAZINE A-PHYSICS OF CONDENSED MATTER STRUCTURE DEFECTS AND MECHANICAL PROPERTIES, Vol. 73, pp. 1529-1563.
89. *The quasicontinuum method: Overview, applications and current directions*. Miller, RE and Tadmor, EB. 3, 2002, JOURNAL OF COMPUTER-AIDED MATERIALS DESIGN, Vol. 9, pp. 203-239.
90. *Nanomechanics of defects in solids*. Ortiz, M and Phillips, R. 1999, ADVANCES IN APPLIED MECHANICS, Vol. 36, pp. 1-79.
91. *Mixed atomistic continuum models of material behavior: The art of transcending atomistics and informing continua*. Ortiz, M, et al. 3, MAR 2001, MRS BULLETIN, Vol. 26, pp. 216-221.
92. *Mixed atomistic/continuum methods: Static and dynamic quasicontinuum methods*. Rodney, D. 2003, THERMODYNAMICS, MICROSTRUCTURES AND PLASTICITY, Vol. 108, pp. 265-274.

93. *An analysis of the quasicontinuum method.* Knap, J and Ortiz, M. 9, SEP 2001, JOURNAL OF THE MECHANICS AND PHYSICS OF SOLIDS, Vol. 49, pp. 1899-1923.
94. *Uniform accuracy of the quasicontinuum method.* Weinan, E., Lu, Jianfeng and Yang, Jerry Z. 21, DEC 2006, PHYSICAL REVIEW B, Vol. 74.
95. *Density-functional-theory-based local quasicontinuum method: Prediction of dislocation nucleation.* Fago, M, et al. 10, SEP 2004, PHYSICAL REVIEW B, Vol. 70.
96. *An extension of the quasicontinuum treatment of multiscale solid systems to nonzero temperature.* Diestler, DJ, Wu, ZB and Zeng, XC. 19, NOV 15, 2004, JOURNAL OF CHEMICAL PHYSICS, Vol. 121, pp. 9279-9282.
97. *A NANOSCALE MESHFREE PARTICLE METHOD WITH THE IMPLEMENTATION OF THE QUASICONTINUUM METHOD.* Xiao, Shaoping and Yang, Weixuan. 3, SEP 2005, INTERNATIONAL JOURNAL OF COMPUTATIONAL METHODS, Vol. 2, pp. 293-313.
98. *Finite-temperature quasicontinuum: Molecular dynamics without all the atoms.* Dupuy, LM, et al. 6, AUG 5, 2005, PHYSICAL REVIEW LETTERS, Vol. 95.
99. *Two-grain nanoindentation using the quasicontinuum method: Two-dimensional model approach.* Iglesias, Rodrigo A. and Leiva, Ezequiel P. M. 10, JUN 2006, ACTA MATERIALIA, Vol. 54, pp. 2655-2664.
100. *Prediction of dislocation nucleation during nanoindentation of Al<sub>3</sub>Mg by the orbital-free density functional theory local quasicontinuum method.* Hayes, RL, et al. 16, JUN 1, 2006, PHILOSOPHICAL MAGAZINE, Vol. 86, pp. 2343-2358.

101. *Finite-temperature quasicontinuum method for multiscale analysis of silicon nanostructures.* Tang, Z., et al. 6, AUG 2006, PHYSICAL REVIEW B, Vol. 74.
102. *A quasicontinuum method for deformations of carbon nanotubes.* Park, JY, et al. 2, FEB 2006, CMES-COMPUTER MODELING IN ENGINEERING & SCIENCES, Vol. 11, pp. 61-72.
103. *Multiscale simulations for carbon nanotubes.* Park, Jong Youn, Kim, Sung Youb and Im, Seyoung. 2007, Mechanical Behavior of Materials X, Pts 1 and 2, Vols. 345-346, pp. 975-978.
104. *Size and microstructure effects on the mechanical behavior of FCC bicrystals by quasicontinuum method.* Sansoz, F. and Molinari, J. F. 6, FEB 12, 2007, THIN SOLID FILMS, Vol. 515, pp. 3158-3163.
105. *Adaptive nonlocal quasicontinuum for deformations of curved crystalline structures.* Park, Jong Youn and Im, Seyoung. 18, MAY 2008, PHYSICAL REVIEW B, Vol. 77.
106. *Quasicontinuum Method Simulation of Nanometric Cutting of Single Crystal Copper.* Liang, Y. C., Pen, H. M. and Bai, Q. S. 2009, ADVANCES IN MATERIALS MANUFACTURING SCIENCE AND TECHNOLOGY XIII, VOL II, Vols. 628-629, pp. 381-386.
107. *Two-dimensional quasicontinuum analysis of the strengthening and weakening effect of Cu/Ag interface on nanoindentation.* Li, Junwan, et al. 5, SEP 1, 2010, JOURNAL OF APPLIED PHYSICS, Vol. 108.
108. *Quasicontinuum simulation of crack propagation in nanocrystalline Ni.* Yu-Fei, Shao and Shao-Qing, Wang. 10, OCT 2010, ACTA PHYSICA SINICA, Vol. 59, pp.



7258-7265.

109. *Quasicontinuum simulation of crack propagation in bcc-Fe*. Vatne, Inga Ringdalen, et al. 15, JUN 15, 2011, MATERIALS SCIENCE AND ENGINEERING A-STRUCTURAL MATERIALS PROPERTIES MICROSTRUCTURE AND PROCESSING, Vol. 528, pp. 5122-5134.
110. *A local quasicontinuum method for 3D multilattice crystalline materials: Application to shape-memory alloys*. Sorkin, V., Elliott, R. S. and Tadmor, E. B. 5, JUL 2014, MODELLING AND SIMULATION IN MATERIALS SCIENCE AND ENGINEERING, Vol. 22.
111. *A multiscale quasicontinuum method for lattice models with bond failure and fiber sliding*. Beex, L. A. A., Peerlings, R. H. J. and Geers, M. G. D. FEB 1, 2014, COMPUTER METHODS IN APPLIED MECHANICS AND ENGINEERING, Vol. 269, pp. 108-122.
112. *Central summation in the quasicontinuum method*. Beex, L. A. A., Peerlings, R. H. J. and Geers, M. G. D. OCT 2014, JOURNAL OF THE MECHANICS AND PHYSICS OF SOLIDS, Vol. 70, pp. 242-261.
113. *A multiscale quasicontinuum method for dissipative lattice models and discrete networks*. Beex, L. A. A., Peerlings, R. H. J. and Geers, M. G. D. MAR 2014, JOURNAL OF THE MECHANICS AND PHYSICS OF SOLID, Vol. 64, pp. 154-169.
114. —. Beex, L. A. A., Peerlings, R. H. J. and Geers, M. G. D. JUL 2014, JOURNAL OF THE MECHANICS AND PHYSICS OF SOLIDS, Vol. 67.
115. *Quasicontinuum-based multiscale approaches for plate-like beam lattices*

- experiencing in-plane and out-of-plane deformation.* Beex, L. A. A., et al. SEP 1, 2014, COMPUTER METHODS IN APPLIED MECHANICS AND ENGINEERING, Vol. 279, pp. 348-378.
116. *The mechanical reliability of an electronic textile investigated using the virtual-power-based quasicontinuum method.* Beex, L. A. A., et al. JAN 2015, MECHANICS OF MATERIALS, Vol. 80, pp. 52-66.
117. *Coupling of atomistic and continuum simulations using a bridging scale decomposition.* Wagner, GJ and Liu, WK. 1, SEP 1, 2003, JOURNAL OF COMPUTATIONAL PHYSICS, Vol. 190, pp. 249-274.
118. *An introduction and tutorial on multiple-scale analysis in solids.* Park, HS and Liu, WK. 17-20, 2004, COMPUTER METHODS IN APPLIED MECHANICS AND ENGINEERING, Vol. 193, pp. 1733-1772.
119. *Concurrent quantum/continuum coupling analysis of nanostructures.* Qian, Dong, Liu, Wing Kam and Zheng, Qingjin. 41-42, 2008, COMPUTER METHODS IN APPLIED MECHANICS AND ENGINEERING, Vol. 197, pp. 3291-3323.
120. *Hierarchical enrichment for bridging scales and mesh-free boundary conditions.* Wagner, GJ and Liu, WK. 3, JAN 30, 2001, INTERNATIONAL JOURNAL FOR NUMERICAL METHODS IN ENGINEERING, Vol. 50, pp. 507-524.
121. *The bridging scale for two-dimensional atomistic/continuum coupling.* Park, HS, et al. 1, JAN 1, 2005, PHILOSOPHICAL MAGAZINE, Vol. 85, pp. 79-113.
122. *Mechano-kinetic coupling approach for materials with dynamic internal structure.* Karpov, Eduard G., et al. 7, 2010, PHILOSOPHICAL MAGAZINE LETTERS, Vol. 90, pp. 471-480.

123. *A multiscale modeling technique for bridging molecular dynamic with finite element method.* Lee, Y- Basaran, C. [ed.] 253. JUL 12, 2013, Journal of Computational Physics, pp. 64-85.
124. K.J., Bathe. *Finite Element Procedures.* s.l. : Prentice-Hall, 2007.